BIOFUELS AND BIOCHEMICALS PRODUCTION FROM MICROALGAE OVER SOLID CATALYSTS

A Thesis Submitted to
the Graduate School of Engineering and Sciences of
İzmir Institute of Technology
in Partial Fulfillment of the Requirements for the Degree of

DOCTOR OF PHILOSOPHY

in Chemical Engineering

by
Özgün DELİİSMAİL

July 2020
İZMİR

ACKNOWLEDGMENTS

Firstly, it is with immense gratitude that I acknowledge the supervision, encouragements, guide and academic supports of my supervisor, also my role model, Prof. Dr. Erol Şeker. Besides, I would like to express my deep and sincere gratitude to my committee members, Prof. Dr. Sedat Akkurt, and Assist Prof. Dr. A. Can Kızılkaya.

I would like to thank to research specialists, Filiz Kurucaovalı, Esra Tuzcuoglu Yücel for their help. I warmly express my special thanks to my co-workers, Bertan Özdoğru, Berk Türkkul and Oğuzhan Akın for their help and supports. They are not just a co-worker but also my companions. I am also grateful to my friend Okan Akın.

My deepest gratefulness goes to my wife, Elif Güngörmüş Deliismail for her help, motivation, endless support, understanding, and priceless advices throughout my life. Finally, special thanks goes to my mother, Esin Deliismail for supporting me during all my educational life. This thesis would never have been concluded without their never-ending love, support and encouragement.

ABSTRACT

BIOFUELS AND BIOCHEMICALS PRODUCTION FROM MICROALGAE OVER SOLID CATALYSTS

The target of this study was the investigation of biofuel and/or biochemical production from microalgae in growth medium or its lipids over heterogenous catalyst. The primary aim was to study the conversion of 6 wt. % *N. Oculata* into biofuels without harvesting and dewatering over Ni-Al_2O_3-SiO_2 catalyst at 80^oC and 1 atm for 24 h. The catalysts were synthesized via modified sol-gel method in which the acids of H_2SO_4, HCl, and HNO_3 were used to investigate the effect of acid type on activity. The catalyst prepared with H_2SO_4 yielded the highest conversion. The treatment of the catalyst prepared by H_2SO_4, with NaCl increased the conversion from 74 % to 91.5 % under same reaction conditions. The products included poly- or monosaccharides, esters and fatty acids. To achieve this conversion, Ni presence was significant beside total acidity of 25 μmol per gram of catalyst, and acidic strength ranging between 130-380^oC. A new industrial application was proposed for direct conversion of 6 wt. % *N. Oculata* into biofuels at 80^oC and 1 atm. The capacity of the plant was 1669 liters biofuel per year from 1064 liters microalgae solution per hour. The catalyst prepared with H_2SO_4 was used to coat either inner surface of tubes or 1-meter pluggable monoliths in tubular reactor having 20 m length and 1000 tubes each of which had 4 cm diameter. The microalgae solution was heated with Therminol®66 heated via parabolic troughs. For operation continuity, ~46000 kg of oil was stored in the tank at 120 ^{o} C for 12 h.

The production of ethyl ester biodiesel from *Spirulina sp.* and *N. Oculata* lipids over 60 % CaO/Al_2O_3 was studied at 50^oC and 1 atm. Ethanol: lipid molar ratio, catalyst amount and reaction time were investigated parameters to identify their effects on catalytic activity. The study showed that ~59 % yield was obtained in the presence of the catalyst amount of 6 wt. % of lipids, in 30 min. at ethanol: lipid molar ratio of 12 while 90 %-99 % yield was acquired at ethanol: lipid molar ratios of 24 and 48. To achieve these yields, weak basic strength in the form of bicarbonate was necessary while high basicity was not essential. Commercial alumina and CaO did not yield any lipid conversion. Glycerolysis of triacylglycerol took place in series with reverse transesterification of triacylglycerol at catalyst amount which was 6 wt. % of lipids, ethanol: lipid molar ratio of 24 and 48, and reaction time of 60 minutes.

ÖZET

MİKROALGLERDEN KATI KATALİZÖRLER ÜZERİNDE BİYOYAKIT VE BİYOKİMYASAL ÜRETİMİ

Bu çalışmanın amacı mikroalglerden katı katalizörler üzerinde biyoyakıt ve biyokimyasalların elde edilmesidir. Yapılan çalışmada mikroalglerin biyoyakıta dönüştürülmesi üç ayrı kısımda incelenmiştir. İlk bölümde büyüme ortamında kütlece 6% olan *N.Oculata* mikroalginin hasatlama ve kurutma olmadan katı katalizör üzerinde direkt biyoyakıt ve biyokimyasallara dönüştürülmesi 80^{o}C ve 1 atm çalışma koşullarında ve 24 saat reaksiyon süresinde gerçekleştirilmiştir. Bu amaçla katalizörlerin asitlik ve asit bölgelerinin kuvvetlerinin reaksiyon üzerindeki etkilerini incelemek amacıyla sol-jel yöntemi kullanılarak farklı asitler (H_2SO_4, HCl ve HNO_3) ile alümina-silika destekli nikel katalizörleri sentezlenmiştir. Yapılan reaksiyon çalışmaları sonucunda en yüksek mikroalg dönüşümü sülfürik asit ile sentezlenen katalizör üzerinde elde edilmiştir. Ayrıca bu katalizör NaCl ile muamele edilmiş ve elde edilen katalizör kullanılarak aynı koşullarda gerçekleştirilen reaksiyonların sonucunda mikroalg dönüşümünün %74 'den %91,5'e yükseldiği gözlemlenmiştir. Reaksiyon sonucunda elde edilen ürün dağılımının içerisinde yağ asidi, polisakkarit, monosakkarit ve esterlerin olduğu görülmüştür. Yüksek mikroalg dönüşümünün elde edilmesi için nikel varlığının yanı sıra toplam katalizör asitliğinin gram katalizör başına 25 μmol olması ve asitlik kuvvetinin 130-380^{o}C arasında olması gerektiği bulunmuştur. Bunun yanı sıra, büyüme ortamındaki *N.Oculata* mikroalginin hasatlama ve kurutma olmadan direkt olarak biyoyakıtlara çevrilmesinin endüstriyel uygulanma yöntemi ile ilgili bir öneri sunulmuştur. Bu önerinin temelinde reaktörde bulunan tüplerin veya monolitlerin sentezlenen katalizörler ile kaplanması prensibi yatmaktadır.

Bir diğer yapılan çalışmada ise *Spirulina sp.* ve *N.Oculata* mikroalg lipitlerinden % 60 CaO/Al_2O_3 katalizörü üzerinde etil ester biyodizel üretimi gerçekleştirilmiştir. Yapılan çalışmalarda 12 etanol: lipit oranında ve lipidin kütlece % 6'sı kadar katalizör miktarında, %59 biyodizel verimi 30 dakikalık reaksiyon sonucunda elde edilirken % 90-99 biyodizel verimi 24 ve 48 etanol: lipit oranlarında elde edilmiştir. Yüksek verimleri elde edebilmek için katalizör üzerinde bikarbonat fazında düşük bazik kuvvetinin olması gerektiği bulunmuştur. Ayrıca saf alümina ve ticari kalsiyum oksit katalizörleri üzerinde herhangi bir lipit dönüşümü elde edilmemiştir.

TABLE OF CONTENTS

LIST OF FIGURES

Figure **Page**

LIST OF TABLES

CHAPTER 1

INTRODUCTION

The fuels and their derivatives based on crude oil have been used for decades in industrial, transportation and residential operations but as known, greenhouse gases are the major problem in the fossil fuels' usage due to the increment of air pollutant emissions year by year. The major contribution to air pollution originated mainly from transportation such that Zachariadis and Kouvaritakis (2003) reported that CO_2 emissions from transport would be 70 % higher in 2030 compared to 2000. Thus, the transition into CO_2 neutral biofuels from fossil fuels become more of an issue to decrease environmental disruption in near future. However, major drawback in the production of biofuels is the high operating cost. For example, operating cost in biodiesel production from oil crops constitutes ~80 % of total costs. On the other hand, it is not desired to use oil crops in biodiesel production owing to rising demand of oil crops for human consumption (Chisti 2008); thus, the key challenge is to find economically applicable biomass source. Among many biomass sources, high lipid content of aqua biomass makes them one of the strongest contenders for proceeding of sustainable evolution in every point of daily life. Microalgae is viable aqua biomass source due not to require any fresh water or agriculture and CO_2 can be fixed via photosynthesis by microalgae (Chen et al. 2015). For instance, salty or wastewater and atmospheric or flue gas could be used to grow microalgae (Schenk et al. 2008). Also, microalgae have higher potential compared to macroalgae due to the other reasons of: (i) Microalgae have high growth rate (Rittmann 2008); (ii) Oil production, 15-300 times more compared to conventional crops, is doable (Chisti 2007); (iii) The lipid content can also be modified by altering composition of growth medium (Meher et al. 2006); (iv) Microalgae harvesting can be applied for multiple times in a year (Schenk et al. 2008). Moreover, the production of biofuels and/or biochemicals from microalgae has a disadvantage factor related to harvesting cost because the weight percentage of microalgae in growth medium alters between 3 wt. % and 10 wt. % which make essential to rise its concentration to ~20 wt. % for further downstream process in biofuel production. Batan et al. (2016) stated that dewatering and lipid extractions steps

constitute ~33 % and 32 % of total direct installed capital cost in the production of biofuels from microalgae, respectively.

This study investigated the microalgae conversion into biofuels over solid catalysts to develop new method for economically viable biofuel production from microalgae and as well as improving currently available solutions from microalgal lipids. Fundamentally, the core of this study is the catalyst synthesis procedure and the catalyst formulation. This study investigated the biofuels and/or biochemicals production from microalgae in three chapters as given in the following: (i) Biofuel production from marine microalgae without harvesting and dewatering (ii) Ethyl ester biodiesel production from microalgal lipids over alumina-calcium oxide catalyst (iii) The industrial implementation proposal for direct microalgae conversion into biofuels/biochemicals.

CHAPTER 2

BIOFUEL PRODUCTION FROM MARINE MICROALGAE WITHOUT HARVESTING AND DEWATERING

Environmental concerns to reduce greenhouse gas emissions and uncertainties in petroleum-based economy prompt the society to produce alternative fuels instead fossil fuels. Renewable biofuels are unarguably the best candidate to replace fossil fuels for continuous sustainable energy such that the European Union stated in the Renewable Energy Directive (2009/29/EC) that renewable biofuels must be at least 10 % in the transport fuel by 2020 (EU 2009). Therefore, the key challenge is to develop catalysts and processes for sustainable energy generation and conversion achievement to reduce greenhouse gas emission with proper biomass. Among many biomasses, it is worthy to selecting microalgal biomass growing in the salty water medium as biomass source to produce carbon neutral biofuels. It is unfortunate that the biggest issue in microalgae usage is the cost of harvesting, because microalgae in growth medium in which mainly water exists, has the weight percentage of 3-10 wt.% and there is a necessity to increase this percentage to minimum 20 wt. % for the further biofuel production processes using wet microalgae. In despite of costly harvesting and oil extraction, the usage of microalgae in biofuel production seems valuable due to the reasons given below;

- No requirement to any agriculture or fresh water (Chen et al. 2015).
- Having high growth rates (Rittmann 2008).
- Harvesting more than once in a year (Schenk et al. 2008); thus, it means that large amount of microalgae can be produced per hectare per year.
- Salty or wastewater growing medium; thus, elimination of freshwater necessity (Schenk et al. 2008).
- Capability to modify the lipid, protein and carbohydrate content by altering growth conditions (Meher et al. 2006)
- Carbon dioxide in air or power plants' flue gas could be fed as carbon source to microalgae growth medium (Schenk et al. 2008).

- For all species, it is tolerable to NOx, but not SO_2. (i.e. *Tetraselmis* sp. can tolerate SO_2)

Microalgae harvesting means the removal of microalgae from its growth medium and it is divided into one or more steps as chemical, physical and biological steps. In fact, the microalgae are grown in huge amounts of water, and have roughly comparable specific gravity to water; retaining a stable, dispersed state owing to its negatively charged membrane, so microalgae harvesting and/or dewatering is challenging task to handle the feasible biofuel production from microalgal biomass. The common methods in microalgae harvesting are the centrifugation, coagulation or flocculation, and filtration. These methods can be applied independently or in combination, whereas they demonstrate economic and technological cons as high energy requirements (centrifugation), contamination with addition of electrolyte/cationic polymers (coagulation,flocculation) or non-feasible scale-up (Heimann and Huerlimann 2015).

There have been many studies dealing with harvesting and dewatering steps and the conversion of 20 wt. % wet or dry microalgae into biochemicals and biofuels (see Figure 2.1). As seen in Figure 2.1, thermochemical and biochemical processes are the common methods to convert microalgae into value-added products. Among thermochemical conversion methods, pyrolysis commonly works with dry algae at 400-600 ^{o} C under atmospheric pressure in the absence of oxygen. Meanwhile, sub- or supercritical water is necessary in the liquefaction method to convert 20 wt. % wet microalgae to bio-oil. Thus, the cost and energy intensive necessities make these thermal methods unviable for continuous large-scale biofuel production from microalgal biomass. On the other hand, biochemical methods such as anaerobic digestion and fermentation, need long time and high-water content to produce methane or ethanol since these methods are not feasible as well for continuous industrial processes. In the literature, there have been some alternative studies in which enzymatic and chemical pretreatments were applied on microalgae, to release the carbohydrates from algal cell. Harun and Danquah (2011) and Ho et al. (2013) studied the disruption of algal cell walls and hydrolysis carbohydrates to monosaccharides in acidic medium for which sulfuric acid was used but it is homogeneous process and this leads to another economic disadvantage factor in which the acidic reaction medium has to be washed to remove sulfuric acid and adjust pH.

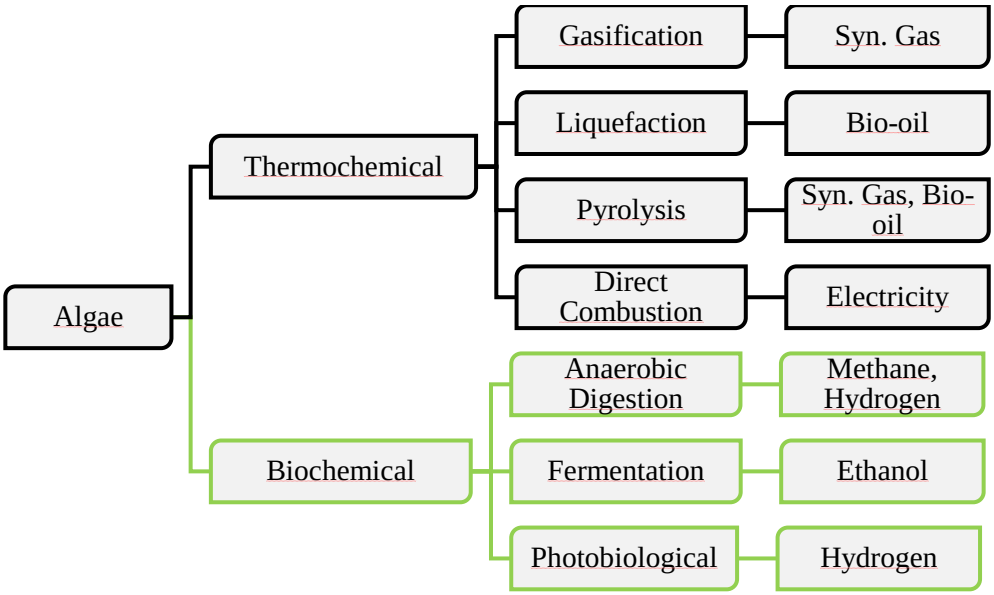

Figure 2.1. Biofuel production methods from microalgae biomass (Source: adapted from Tsukahara and Sawayama (2005))

In the literature, Batan et al. (2016) studied the techno-economic evaluation of biofuel production from microalgal biomass. The authors stated that microalgae cultivation, harvesting and algal oil extraction constituted the 96 % of the operating cost. On the other hand, the dewatering and lipid extraction processes constituted approximately 33 % and 32 % of total direct installed capital cost of the biofuel production processes which need the usage of dry microalgae; thus, the conversion of 6 wt. % wet microalgae in sea water into biofuels and biochemicals over heterogeneous catalysts under relatively mild conditions, at 80 ^{o}C under atmospheric pressure without harvesting and dewatering would be precious solution to the problems observed in harvesting and dewatering techniques and also, in present thermochemical methods and homogeneous/enzymatic catalytic processes.

2.1. Nannochloropsis oculata

Nannochloropsis oculata is a marine-water microalga from the class of *Eustigmatophyceae*. The content of algal cells of *Nannochloropsis oculata* offers great potential as promising feedstock for biofuel and biochemical production so it has been widely considered in literature. Volkman et al. (1993) reported the biochemical composition of *Nannochloropsis oculata* and Table 2.1 demonstrated the biochemical

analysis of *Nannochloropsis oculata* which consists of various carbohydrates, proteins and, lipids in its cell physiology.

(a)

(b)

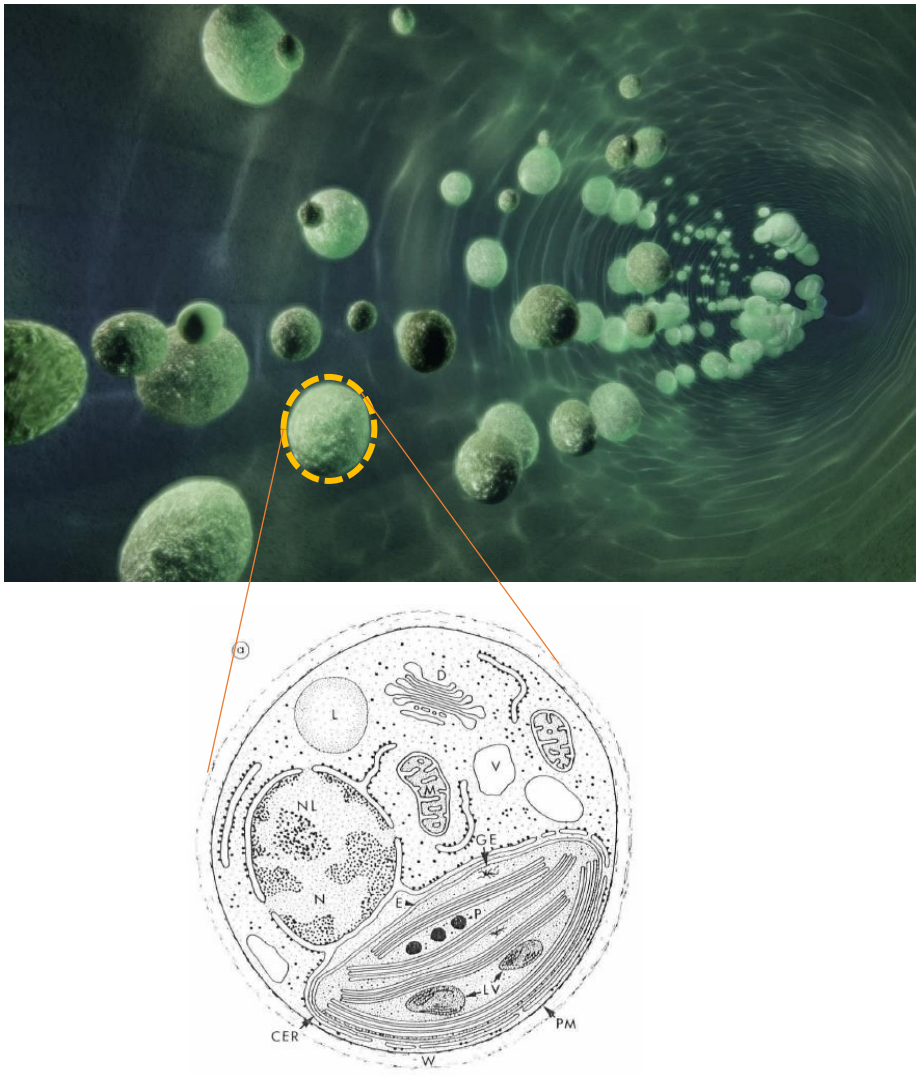

Figure 02.2. (a) Conceptual view of microalgae (b) Schematic view of cytological features of *Nannochloropsis Oculata* (Source: adapted from Antia et al. (1975))

Protein is the major constituent in *Nannochloropsis oculata* (20 wt. % of dry microalgae) while it is followed by lipids (11 wt. % of dry microalgae), and then carbohydrate (5.2 wt. % of dry microalgae) under the growth conditions used in the study. Carbohydrates is generally stored at the outer and inner layer of cell wall (i.e., cellulose, hemicellulose), and inside the cell (i.e., starch). It was reported that polysaccharides had the highest portion in total carbohydrate amount (Volkman et al. 1993). The cell wall structure of *N.Oculata* was constituted by only cellulose (Arnold et al. 2015).

Table 2.1. Total carbohydrate, protein, lipids, and chlorophyll content of the *Nannochloropsis oculata* (Source: adapted from Volkman et al. (1993))

Weight of constituent (pg.cell^{-1})	***Nannochloropsis oculata***
Total carbohydrate	0.16
Mono- and oligosaccharides	0.027
Polysaccharide	0.13
Total protein	0.62
Total lipids	0.34
Polar lipids	0.32
Triacylglycerols	0.006
Sterols	0.019
Chlorophyll	0.051

Table 2.2 shows the sugar compositions of the polysaccharide isolated from *Nannochloropsis oculata.* As seen from Table 2.2, glucose which represented 60.6 % of the total sugars, was the principal polysaccharide. Fucose, galactose, mannose, rhamnose, ribose, and xylose were much less abundant, and arabinose was rarely present in the microalgae. Therefore, it demonstrates the potential to yield fermentable sugars as a result of cell fractionation via hydrolysis.

Table 2.2. Sugar compositions of polysaccharide isolated from *N. oculata* (Source: adapted from Volkman et al. (1993))

	Nannochloropsis oculata
Arabinose	0.7
Fucose	7.0
Galactose	6.3
Glucose	60.6
Mannose	3.7
Rhamnose	10.4
Ribose	6.4
Xylose	4.8

Apart from carbohydrate, microalgae can accumulate lipids within its cell structure. Lipids can be separated into two main groups: (i) Storage lipid (neutral or nonpolar lipid) and (ii) Structural (membrane or polar lipid). The storage lipid is constituted by triacylyglycerols (TAGs), steryl esters, and wax esters (Prabandono and Amin 2015). As known from literature that triacylglycerols, TAGs which can be extracted via solvent extraction and converted into biodiesel via transesterification reaction route, are the energy storage point in the microalgae. Neutral lipids are based on the general structure of a triple ester in which three-long chain fatty acids are coupled to glycerol molecule, while structural lipids contain high amount of polyunsaturated fatty acids

(PUFAs) and present in cell membranes in the form of glycerol-based phospholipids and glycolipids. As tabulated in Table 2.1, polar lipids were predominant in total lipid amount of *Nannochloropsis oculata*. Moreover, Table 2.3 tabulates the total fatty acid compositions of *Nannochloropsis oculata* with respect to Bligh Dyer extraction. C16 is the main fatty acid in saturated fatty acids with C14 as secondary saturated fatty acid while palmitoleic acid (C16:1(n-7)) and oleic acid are the major fatty acids among monounsaturated fatty acids. C20:5(n-3) is the major polyunsaturated fatty acids existing in the *Nannochloropsis oculata*.

Table 2.3. Total fatty acid compositions of *Nannochloropsis oculata*
(Source: adapted from Volkman et al. (1993))

Saturated fatty acids	
14:0	4.6
15:0	0.5
16:0	14.2
18:0	0.6
Subtotal	20.0
Monounsaturated fatty acids	
16:1(n-9)	0.1
16:1(n-7)	29.4
16:1(n-5)	0.2
16:1(n-13)	0.4
17:1(n-8)	0.8
18:1(n-9)	6.3
18:1(n-7)	0.3
Subtotal	37.4
Polyunsaturated fatty acids	
16:2(n-7)	0.8
16:2(n-4)	0.1
16:3(n-4)	0.2
18:2(n-9)	0.3
18:2(n-6)	2.0
18:3(n-6)	0.3
18:3(n-3)	0.1
20:3(n-6)	0.4
20:3(n-3)	0.1
20:4(n-6)	8.8
20:5(n-3)	28.8
22:6(n-3)	-
Subtotal	42.2
Others	0.8
Concentrations	
pg fatty acid.cell^{-1}	0.27
mg fatty acid.g^{-1} dry wt	88

2.2. Sol-gel chemistry

In this study, solid catalysts were synthesized via single step sol-gel method which serves the advantages of “bottom-up” approach. This method is selected to synthesize desired catalysts since the reasons for the value of and interest in sol-gel prepared materials become clear:

- Apart from densification, required temperatures for all stages are low, and generally close to room temperature, since sol-gel provides the mixing of materials in atomic level. Therefore, thermal degradation of material is minimized, and high can be succeeded.
- Precursors as metal alkoxides and mixed alkyl/alkoxides in sol-gel method are generally volatile and, these can easily be purified to very high levels.
- Homogeneous controlled doping is relatively simple, because organometallic precursors including different metals are generally miscible.
- When it is not possible to produce thermally and thermodynamically instable materials using conventional methods such as impregnation method, sol-gel process could be an alternative method to produce such materials.
- The necessary conditions are frequently mild. Hydrolysis and condensation steps are catalyzed by acid and bases, and severe pH values can be avoided.
- High porous and nano-scaled crystalline materials can be prepared.
- It is possible to cast ceramic materials in a range of complex shapes and to produce thin films or monoliths without the necessity of melting due to the usage of liquid precursors.
- Control might be succeeded over hydrolysis and condensation rates, and over colloid particle and pore size, porosity, and pore wall chemistry of the final material by chemical modifications on precursors.
- Covalent attachment of organic species to porous silicate glass structures is probable by using functionalized precursors.
- The temperature is below the crystallization temperature of oxide materials; which permits to produce unusual amorphous materials.
- The mechanical strength and pore size can be controlled by manipulating ageing and drying steps.

- The usage of precursors including polymerizable organic ligands is available, the materials including both organic and inorganic polymer networks can be produced (Wright and Sommerdijk 2001).

2.3. Theory

It has been known that Al_2O_3-SiO_2 has widespread application in petroleum industry as hydrocracking catalyst due to its acidity, and herein, several questions can be addressed regarding alumina-silicate supported metal catalyst usage in the conversion of *Nannochloropsis oculata* to biofuel and biochemicals. The usage of silica-alumina can be attributed to its surface area, strong metal interaction, and acidic nature. To straighten out the reasons behind the usage of the supported metal catalyst, the acid site structure of the catalyst should initially be investigated. As mentioned previously, silica-alumina shows acidic behavior within its nature, although its strength is extremely dependent on the modifications and preparation method. In our study, it is expected that distinct acidity and acidic strengths would be obtained with the addition of different acid types; sulfuric acid, hydrochloric acid and nitric acid. To understand the acidic site structure of silica-alumina, I would like to summarize the several proposals in the literature regarding acidic structure of silica—alumina. The acid site structure of silica-alumina was proposed by Ward and Hansford (1969) as given below;

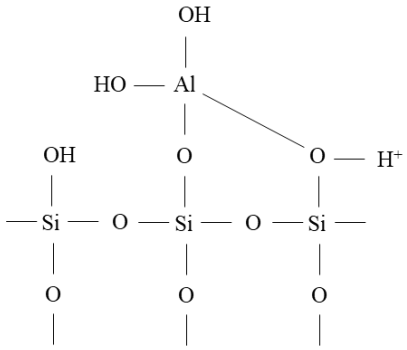

Figure 2.3. Acid site structure of the silica-alumina proposed by Ward and Hansford (1969)

As shown in Figure 2.3, –OH groups in which strong binding power of oxygen to hydrogen exists, constitute the silica gel surface. Aluminum hydroxide react to split out of water between the aluminum hydrate and –OH groups of the silica gel surface with the surface hydroxyl groups. As a result, the binding power of oxygen becomes weak by the

coordination with aluminum of the hydroxyl oxygen, and hydrogen behaves as an acid. Thomas (1949) made another proposal to define the acid site structure of silica-alumina. Figure 2.4 shows the acid site structure of silica-alumina with respect to Thomas' proposal.

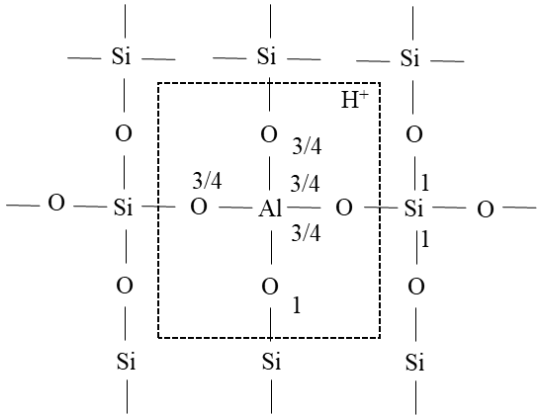

Figure 2.4. Acid site structure of the silica-alumina proposed by Thomas (1949)

In the structure of silica, a tetrahedral aluminum atom is placed instead the silicone atom as showed with dashed line in Figure 2.4. AlO_4 is unsatisfied by a whole valence unit. To balance the electrostatic neutrality, hydrogen ion must be associated with four oxygen atoms. This hydrogen atom acts as acid.

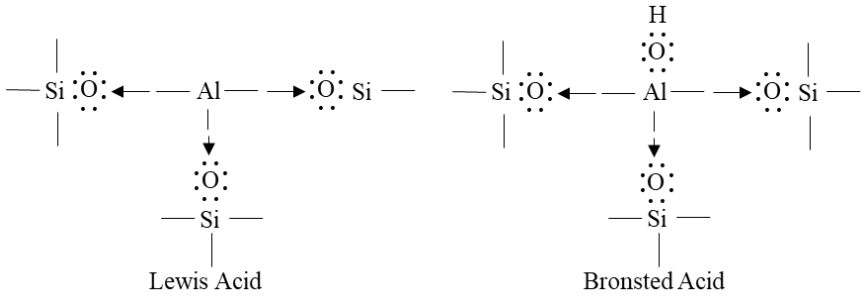

Figure 2.5. Acid site structure of the silica-alumina proposed by Tamele (1950)

Moreover, the proposal of Tamele (1950) is demonstrated in Figure 2.5. Al atoms coordination which have three positive charges with oxygen atoms, attached to Si which has four positive charges show the displacement of electrons by the proximity of Si ions (as shown by the arrows). In the hydrated state, the electron pair was denoted by water with weak hydrogen held by electrostatic attraction. Simultaneously, the hydroxyl group growth into the solid structure (The dehydrated state becomes Lewis acid).

All in all, to generalize the acid site generation on alumina-silicate, the condensation of Si-OH with Al-OH initially occurs for the formation of Si-O-Al linkage. Then, hexacoordinated Al is converted into tetracoordinated Al on heating by liberation of

water. High temperature heating results in the decomposition of NH_4^+ into H^+ and NH_3. Later, desorption of NH_3 from the surface happens and H^+ remains on the surface. At this position, H^+ acts as Bronsted acid while further heat treatment causes dihydroxylation forming Lewis acid site. That's why, shortly, it can be said that Bronsted acid site is proton donor while Lewis acid is electron acceptor (Chu et al. 2011). Acid site generation on Al_2O_3-SiO_2 was schematically represented at Figure 2.6.

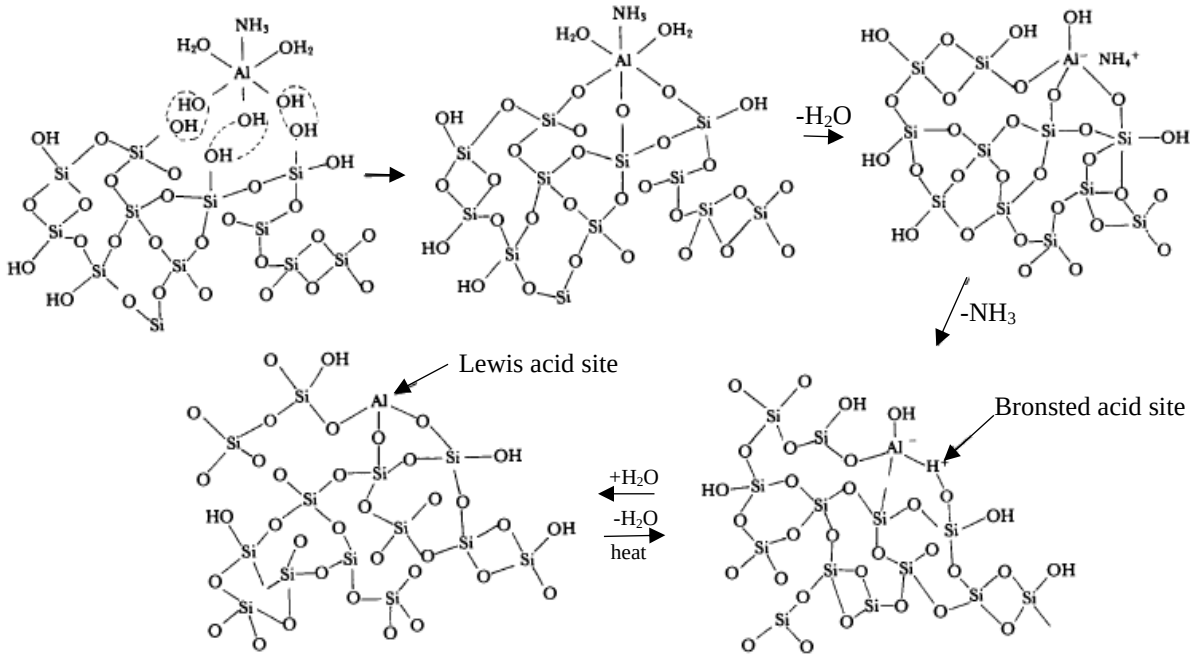

Figure 2.6. Generation of acid sites on alumina-silicate
(Source: Tanabe (1989))

The acid site generation could follow different pathway with respect to preparation method of the catalyst, acid type and precursor. For example, sol-gel technique follows hydrolysis, condensation, and polymerization. Feng et al. (2010) synthesized the strong water-repellent alumina by using sol-gel method, and they proposed a formation of alumina structure by sol-gel method that illustrated in Figure 2.7.

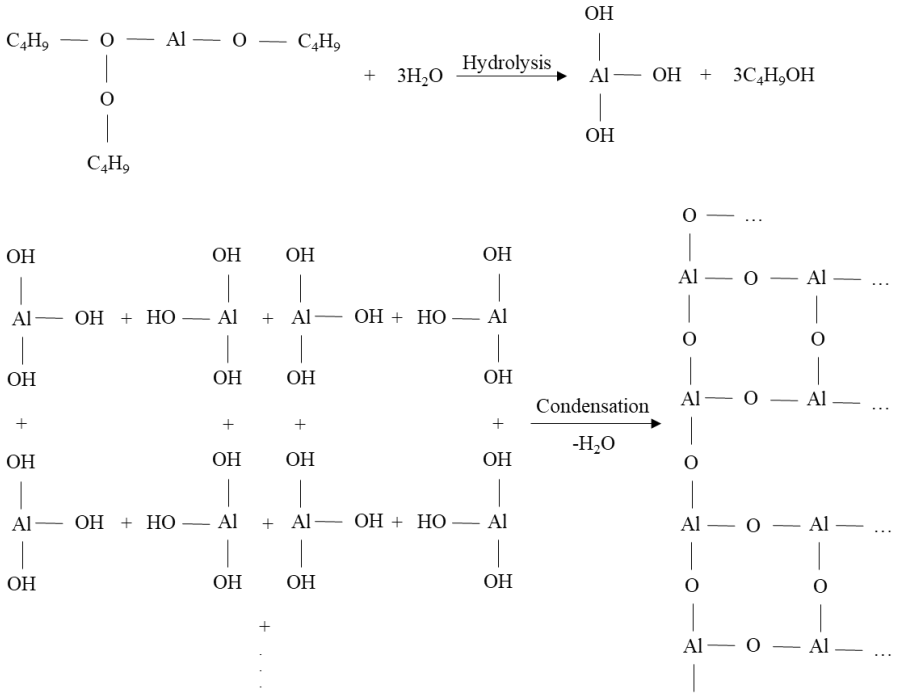

Figure 2.7. The formation of alumina by sol-gel method
(Source: adapted from Feng et al. (2010))

Bourne et al. (1970) studied the silica-alumina to identify the acid sites in its structure. They synthesized two types of silica-alumina with low concentrations of aluminum atoms on (i) the surface of silica gel (aluminum on silica) and (ii) within the silica lattice (aluminum in silica). They performed pyridine chemisorption to define the acid sites in the synthesized silica-alumina, and they concluded that aluminum on silica includes only Lewis acid sites while aluminum in silica includes only Bronsted acid sites. Another study was performed by Ballivet et al. (1972). They performed infrared and thermogravimetric analysis of pyridine which was chemisorbed on a silica-alumina having different alumina contents. Initially, the silica-alumina containing 14 wt. % alumina exposed to hydrochloric acid solutions until the contents of 9.4, 2.4 and 0.1 wt. % alumina was obtained. As a result of dealumination, neither Bronsted nor Lewis sites were observed in the sample containing 0.1 wt. % alumina. Moreover, the other samples contained fewer acid sites when compared to sample having 14 wt. % alumina. Hence, it can be said that alumina populously establishes the acidic structure of the silica-alumina while silica is generally used as support due to its high surface area which will directly affect the activity of the reaction. Acidity and acidic strength of catalyst can act important role to disrupt the cellulosic cell wall of *Nannochloropsis Oculata*. Hence, acidity and its strength will be dependent on the type and amount of acid introduced on the carrier,

although the nature of the oxide carrier is important as well, whereas properties of oxide carrier and support was fixed in the study. Marczewski et al. (2004) studied the acidic properties of different oxide/SO_4^{-2} super acids. The authors found that acid strength of the Al_2O_3/SO_4^{-2} changed significantly with sulfuric acid amount as following; $-7.05<H_0<-10$ (%1), $-10<H_0<-14$ (2-3%), $H_0<-14$ (4-9%). On the other hand, SiO_2/SO_4^{-2} had acidic strength between $-0.75<H_0<-3.50$ (1-9%). Thus, it is important to define the phase formation of the acid introduced to Al_2O_3 if surface sulfate (change with respect acid introduced) phase will be formed or how introduced acid will attach to carrier. It would directly affect the acidic strength of the catalyst that will be synthesized. Additionally, various modifications can be applied to arrange the attachment of acid phase to desired position on carrier. It is not expected for SiO_2 to form this type of phases due to the electronegativity of Si than Al. On the other hand, the acid type is another factor affecting the acidic strength. Two full positive charges on sulfur are available on sulfuric acid. This has pulling electrons effect from the attached oxygen atoms making increment in the apparent electronegativity of the O atoms, thus hydrogen atom has more positive character for sulfuric acid when compared to nitric acid, whereas as indicated previously, it is not the sole reason to decide on the acid strength of catalyst.

Moreover, transition metal has high surface free energies; thus, it would tend to agglomerate to decrease its surface area. Therefore, it is necessary to stabilize the metal particles on the surface of the support material, whereas this stabilization of metal particles on support would affect the morphology due to the smaller the particle the more its physical properties. That's why, nature of the support material would affect catalytic properties of metal. It is expected that strong metal-support interaction would be obtained between transition metal and silica-alumina due to favorable spreading of metal having lower surface free energies when compared to parent metals, on silica-alumina at suitable conditions.

The utilization of heterogeneous metal supported catalysts has been serving great potential for hydrolysis reaction to transform cellulose to glucose. It is very crucial to achieve cellulose conversion over the catalysts because only cellulose constitutes the cell wall of *Nannochloropsis Oculata*. Simultaneously, achievement of cellulose transformation to glucose, in other words, disintegration of cell wall of *Nannochloropsis Oculata*, means the release of valuable components as lipids and other polysaccharides in algal cellular structure, and transformation of these into linear alkane, fatty acids, and

other constituents. At this point, acidity and acidic strength of the catalysts have great significance in acid hydrolysis, therefore directly in cellulose conversion which would take place via hydrolysis reaction such that proton donating compound would catalyze the reaction. One part of the cleaved product receives H^+, and the other a –OH moiety of a water molecule which is available in reaction medium consisting of mostly sea water.

Various studies were performed in the literature to inspect the effect of acidic strength of metal oxide, supported metal catalyst and liquid acid catalysts on cellulose conversion, whereas the usage of heterogeneous catalysts has some advantages as easy separation, recyclability, and less harm to the reactor. Tagusagawa et al. (2010) used mesoporous Nb-W oxide as solid acid catalyst for sucrose and cellobiose hydrolysis. The study showed that the rate of glucose production and the turnover frequency (TOF) for sucrose hydrolysis reaction were obtained higher when compared to others as Amberlyst-15, $Nb_2O_5.mH_2O$, resins, and zeolites. The acid strength increased with the help of W, and mesoporous Nb_3W_7 oxide provided the highest reaction rate. The high catalytic performance of the catalyst could be attributed to strong acid sites and high surface area on which the reactant, sucrose, would firstly adsorbed. On the other hand, Nb-W oxide catalyst showed lower activity in cellobiose hydrolysis owing to low Bronsted acid sites. Same authors proposed another transition metal oxide, $HNbMoO_6$ to hydrolyze sucrose, cellobiose, cellulose and starch. $HNbMoO_6$ showed higher sucrose and cellobiose hydrolysis activity as twice the Amberlyst-15 due to acidity, water-tolerance and intercalation ability, whereas low product yield in cellulose hydrolysis was obtained for this catalyst. This showed that increment in the acidic strength, and surface area is necessity to convert cellulose to sugars. Hence, the usage of different acids as sulfuric acid, hydrochloric acid and nitric acid would change the acidic behavior; acidity and acidic strength of the alumina-silica supported metal catalyst and it would affect the performance of the cellulose and lipid hydrolysis reaction.

Kobayashi et al. (2010) used supported Ru catalyst to transform cellulose to glucose. The authors used various support materials as mesoporous carbon materials (CMKs), carbon black, activated carbon, and C_{60}. CMK supported Ru catalyst showed better performance when compared to other catalysts. Also, the amount of Ru loading on the catalyst was investigated and they found that Ru loading amount had an apparent effect especially on the product distribution. The glucose yield showed increment from 28 % to 34 % when Ru loading was changed from 2% to 10%. The yield of total reducing

sugars including glucose and oligosaccharides, was calculated as 40 %. On the other hand, CMK itself showed %21 glucose yield with 43 % total reducing sugars at 503 K, therefore it could be said that CMK was able to transform cellulose to oligosaccharide, and Ru acted a role to convert oligosaccharides into glucose. Moreover, cellobiose conversion to glucose was investigated on CMK and Ru/CMK by the authors. Ru/CMK gave 25 % glucose yield, while CMK itself showed very low yield as blank samples which were performed in the absence of any catalyst. Hence, it could be said that support material did not affect the hydrolysis reaction, and Ru acted significant role to hydrolyze β-1,4-glycosidic bonds. Further study demonstrated that the active phase of $RuO_2.H_2O$ desorbed the hydrated water to give Lewis acid site which could convert cellulose to glucose. The other reason could be that Ru worked as a Bronsted acid. Acidic strength of the catalyst is very crucial to convert carbohydrates to monosaccharides, therefore it is expected that mixed oxide, alumina-silicate which shows acidity within its nature, supported metal catalysts prepared with different acids as sulfuric acid, hydrochloric acid and nitric acid would yield different acidic strengths and in direct different product distributions. Nickel was used as metal site of the catalyst, so alumina-silicate supported nickel catalysts were synthesized with different acid types. Also, it has been known from the literature that nickel has inarguably significant effect in carbon-carbon bond cleavage especially in catalytic cracking (Shrotri et al. 2012, Santillan-Jimenez et al. 2013), and bi-functional catalyst effect could be observed for proposed catalyst because carbon-carbon bonds in lipids of microalgae which extracted as a result of cell wall hydrolysis would be broken during the reaction.

In this study, direct conversion of 6 wt. % *Nannochloropsis Oculata* in sea water to biofuel and biochemicals without harvesting and dewatering was studied over single-step sol gel made alumina-silicate supported nickel catalyst at 80^{o}C under atmospheric pressure. To the best of our knowledge, this study is the only in the literature dealing with the conversion of marine 3-10 wt. % *N. Oculata* into hydrocarbons, saccharides and esters over heterogeneous catalysts without harvesting and dewatering.

Figure 2.8. The summary of direct conversion of 6 wt. % *Nannochloropsis Oculata* to biofuel and biochemicals over alumina-silicate supported nickel catalysts

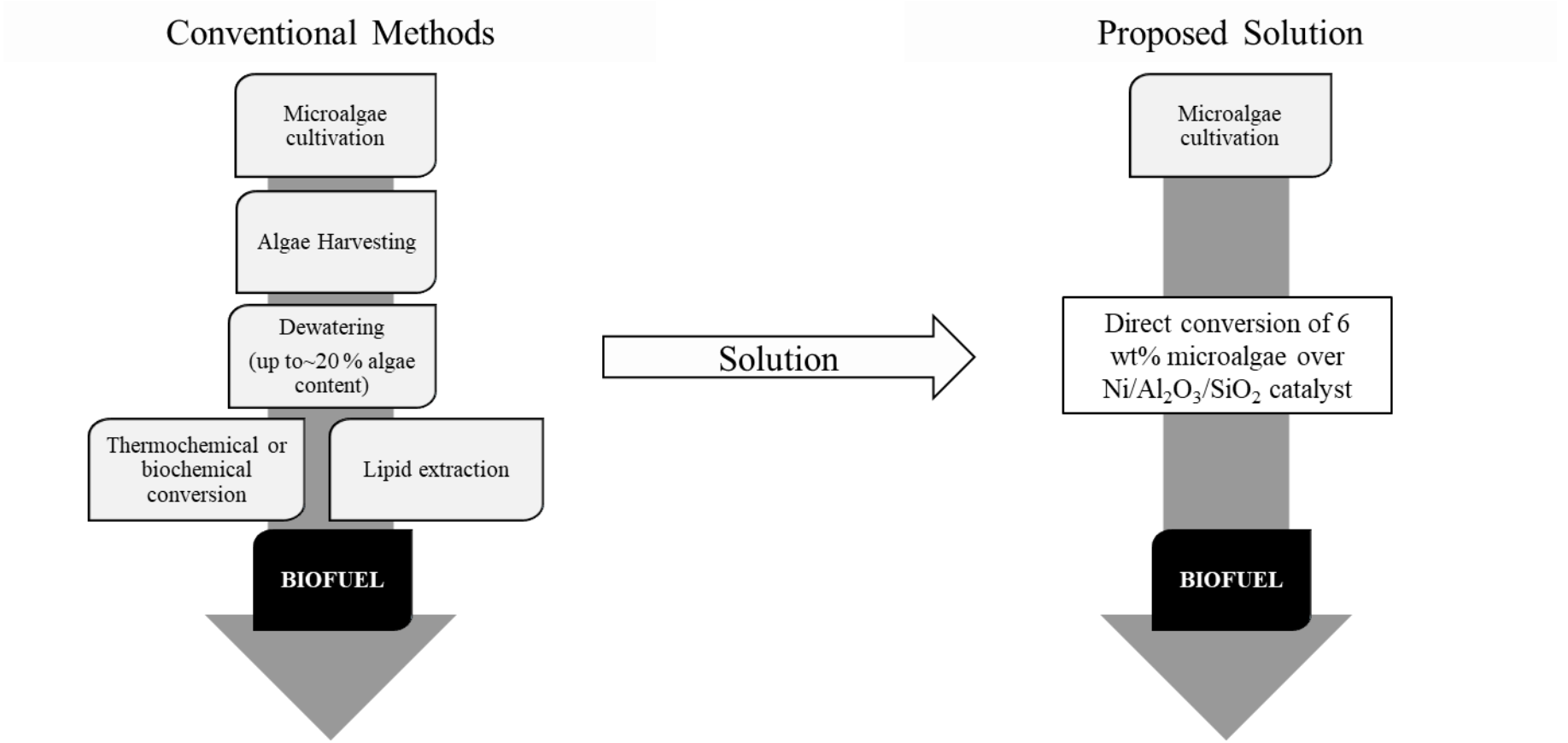

2.4. Experimental

2.4.1. Catalyst preparation

Modified single step sol-gel method was used to synthesize alumina-silicate supported nickel catalysts as given in the study of Umdu (2008). The prepared catalysts contained 70 % Al_2O_3, 30 % SiO_2 and 10 % Ni. Briefly, silica sol and alumina sol were prepared individually, and then, they were mixed to each other. To prepare silica sol, the precursor of tetraethyl-orthosilicate (≥ 98 purity, Fluka), ethanol (≥99.8 % purity, Sigma-Aldrich), and deionized water were mixed with 1 M hydrochloric acid (HCl, 36.5-38 wt. %, Sigma-Aldrich) at 80 ^{o} C for 2 hours. Hydrolysis reaction to synthesize alumina sol was carried out by mixing precursor of aluminum isopropoxide (≥ 98 % purity, Aldrich), deionized water and intended acids e.g. sulfuric acid (≥98 purity, Aldrich), hydrochloric acid, and nitric acid (68 wt. %, VWR Chemicals) at 85 ^{o} C. These sols were mixed to each other and, then nickel (II) acetate hydrate (> 99 % purity, Alfa Aesar) was added to sol mixture. Ultimately, excess solvent was evaporated at 70^{o}C to obtain gel. Thereafter, gel was dried at 120 ^{o} C for 12 h, and calcined at 900 ^{o} C for 6 h with 10^{o}C /min heating rate. After calcination, the catalysts were ground and sieved to 100-200 mesh size for further characterization and catalytic reactions.

Finally, the prepared catalysts with distinct acids were denoted as following: 10 % Ni-30 % Al_2O_3- 70 % SiO_2-H_2SO_4, 10 % Ni- 30 % Al_2O_3- 70 % SiO_2-HCl, 10 % Ni- 30 % Al_2O_3-70 % SiO_2-HNO_3. The catalyst of 10 % Ni- 30 % Al_2O_3- 70 % SiO_2-HNO_3 means that alumina-silicate supported nickel catalyst was prepared by using nitric acid via single step sol-gel method.

2.4.2. Catalyst activity determination

In this study, 6 wt. % *Nannochloropsis oculata* in sea water was used as microalgal biomass source due to its availability. 6 wt. % *Nannochloropsis Oculata* of which properties and growth medium conditions was like given in literature (Durmaz 2007), was supplied from Dr. Durmaz in Ege University.

Catalytic conversion of 6 wt. % *N. Oculata* without harvesting and dewatering were performed in batch reactor with algal solution:catalyst ratio of 100. For instance, 25 ml of salty aqueous algal solution consisting of 6 wt. % *N. Oculata* with 0.25 g of dry catalysts were reacted

in batch reactor at 80 °C and 1 atm for 24 hours with constant stirring rate of 330 rpm to avoid mass transfer limitations. Also, to comprehend the effect of sodium chloride in sea water on catalytic activity, the treatment of fresh 10 % Ni- 30 % Al_2O_3- 70 % SiO_2-H_2SO_4 catalyst with 35 g of NaCl per kg of water was applied at 80°C and 1 atm for 24 h. Then, this catalyst was denoted as 10 % Ni- 30 % Al_2O_3- 70 % SiO_2-H_2SO_4-SW.

To evaluate conversion at the end of reaction, initial amount of microalgae (g) in sea water and final amount of microalgae must be determined. Initial amount of microalgae (g) was established in a way that firstly, water was evaporated in the initial solution and then microalgae paste washed with deionized water to remove salts and other ions. Finally, washed microalgae paste was dried and weighted to find initial amount of microalgae in the solution. The final amount of microalgae (g) after reaction was determined by initially washed with recovered catalyst and microalgae paste with deionized water to remove salts and other ions and then, dried at 55 °C under vacuum for 48 h. After subtracting catalyst amount from final paste yielded final amount of microalgae (g) at the end of the reaction. The microalgae conversion over solid catalysts were calculated by using given formula:

$$\text{Microalgae Conversion}(\%) = \frac{\text{Initial amount of microalgae (g) in sea water - Final amount of microalgae (g) after reaction}}{\text{Initial amount of microalgae (g) in sea water}} \times 100 \quad (2.1)$$

2.4.3. Product Analysis

At the end of the reaction, final reaction medium was centrifuged at 4000 rpm for 5 minutes to separate the catalyst and unreacted microalgae paste from liquid phase products. Then, liquid-liquid extraction was performed by the addition of 2.5 ml of hexane onto liquid phase products to collect hexane soluble components at room temperature for 24 h at constant stirring rate of 660 rpm. Phase separation was observed after liquid-liquid extraction, and the products solved in hexane phase was analyzed by using gas chromatography-mass spectrometry (GC/MS, Agilent 6890 N / 5973 N Network GC/MSD) which was equipped with DB-5 column. Remained polar liquid phase products as poly- and monosaccharides which were insoluble in hexane, was diluted with deionized water, and then filtered. The qualitative and quantitative analysis of the products in this phase were performed via high performance liquid chromatogram (HPLC, Agilent 1100) equipped with RI detector, and HyperREZ XP

Carbohydrate H^+ column (8 μm, 300 mm × 7.7 mm). The operating temperature was 65 ^{o}C and mobile phase was pure water with 0.4 ml/min flow rate.

2.4.4. Catalyst Characterization

Crystalline structures formed in the catalysts were investigated via Philips X'Pert Pro Diffractometer with Ni-filtered CuKα radiation (λ=1.54056 Å, operated at 40 kV and 45 mA) in the range of 5-80^{o} 2θ values. The crystal size of catalysts was calculated by Scherrer equation:

$$d=\frac{K\times\lambda}{\beta\times\cos(\theta)} \tag{2.2}$$

where K was shape factor and it was approximately 0.9, β was peak broadening effect using the Full-Width Half Maximum (FWHM), θ was the main diffraction angle in degree, and λ was 1.54056 Å which was the wavelength of X-ray.

Textural properties of the catalysts based on Brunauer, Emmet and Teller (BET) method, were determined by N_2 adsorption isotherms at 77 K with volumetric adsorption device Micromeritics Gemini V. Degassing of samples was applied under vacuum condition (10^{-6} Torr) at 300^{o}C for 24 h.

To identify the number of acidic sites on the catalysts and their acidic strengths, chemisorption analysis was performed by using temperature programmed desorption (TPD) technique with Micromeritics AutoChem II 2920. Ammonia (NH_3) was used as basic probe molecule to measure the acidities and acidic strengths of all catalysts. Irreversibly adsorbed ammonia amount yielded the total amount of acidic sites available on the surface of the catalyst while desorption temperature of ammonia gave the acidic strengths of these acidic sites. Figure 2.9 represents temperature programmed desorption method for adsorption and desorption of ammonia on the catalysts.

As seen in Figure 2.9, firstly, the catalysts were cleaned at 900^{o}C which was the calcination temperature, for 30 min. and then cooled to room temperature under helium flow. Later, ammonia adsorption was applied at room temperature for an hour, followed by helium gas purge to remove gas phase and weakly adsorbed ammonia. Further, ammonia desorption was performed under helium gas flow with increasing temperature from room temperature to 900^{o}C with 10^{o}C/min ramping rate.

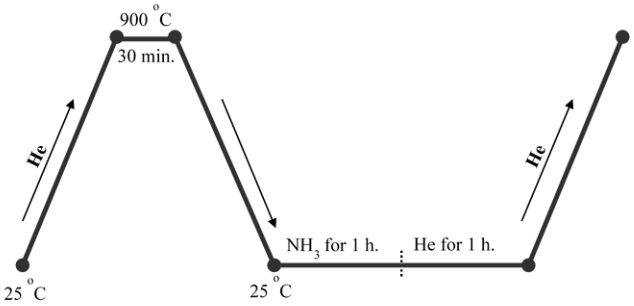

Figure 2.9. Temperature programmed desorption method for ammonia adsorption and desorption

All in all, Figure 2.10 summarizes hierarchy of experimental studies in the direct conversion of 6 wt. % *Nannochloropsis Oculata* into biofuels and biochemicals over alumina-silicate supported nickel catalyst prepared with different acids.

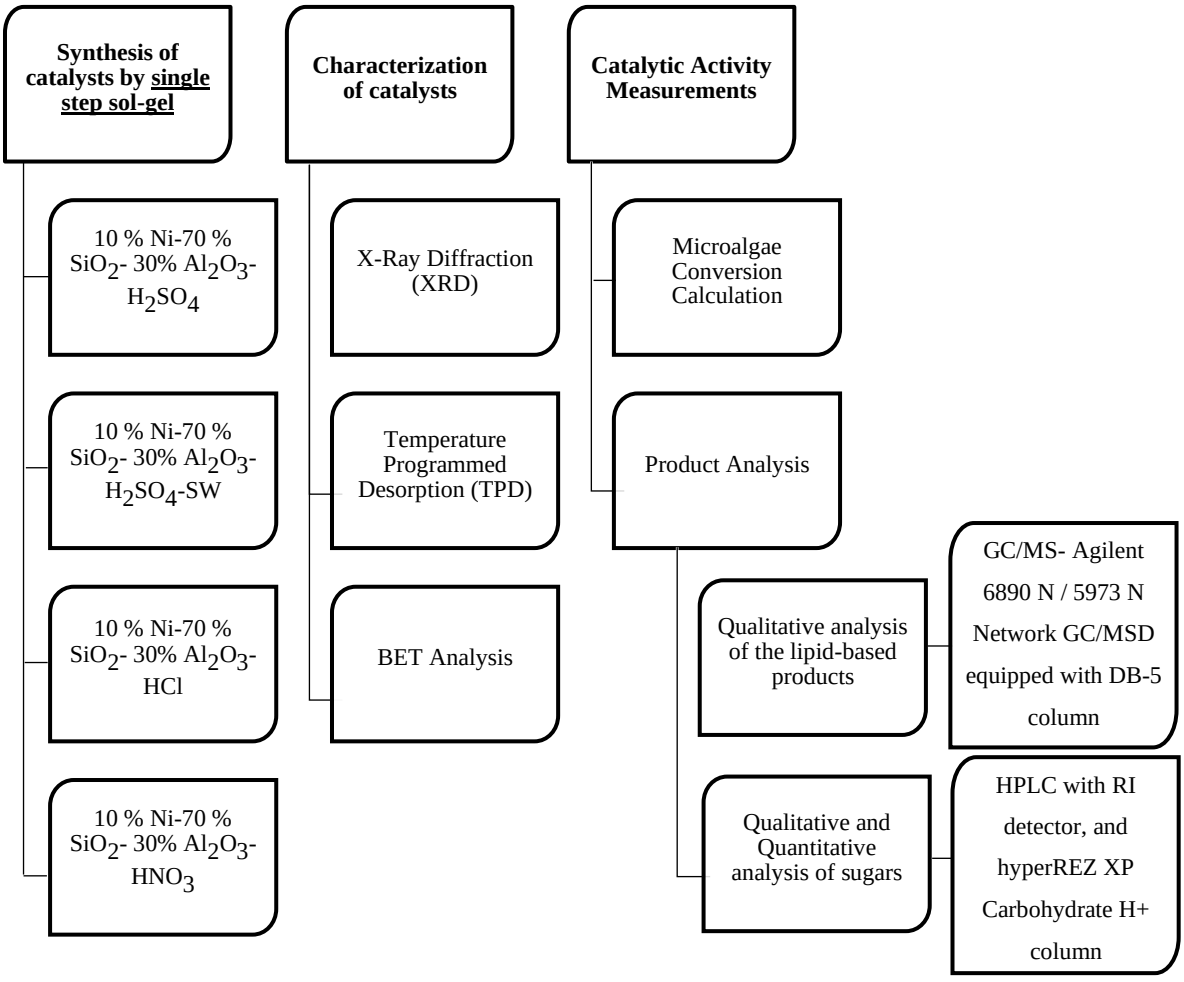

Figure 2.10. The summary of experimental study hierarchy in direct conversion of 6 wt. % *Nannochloropsis Oculata* microalgae into biofuels and biochemicals

2.5. Results and Discussion

The crystalline phases and average sizes of the catalysts were determined by X-Ray Diffractometer to comprehend the reasons behind the distinct conversions on the catalysts prepared with different acids; sulfuric acid, hydrochloric acid, and nitric acid. Figure 2.11 represents the XRD spectra of the catalysts. The crystalline phases in the catalysts were identified by Powder Diffraction File of International Centre for Diffraction Data (JCPDS-ICDD 2000).

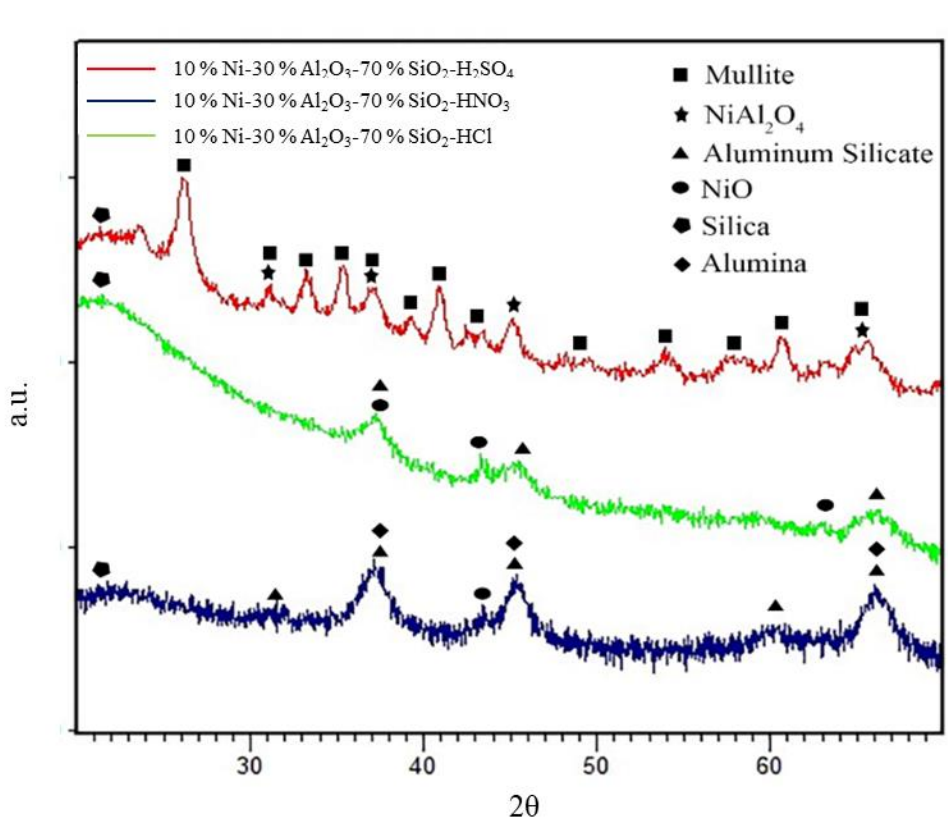

Figure 2.11. X-Ray Diffraction spectra of the catalysts

As seen from Figure 2.11, 10 % Ni-30 % Al_2O_3-70 % SiO_2-H_2SO_4 consisted of mullite, and nickel aluminate crystalline phases while for 10 % Ni- 30 % Al_2O_3- 70 % SiO_2-HCl, aluminum silicate and nickel oxide crystalline phases were observed. Contrary to this, 10 % Ni-30 % Al_2O_3- 70 % SiO_2-HNO_3 had only alumina, NiO and aluminum silicate crystalline phases in its structure. On the other hand, alumina and aluminum silicate crystalline phases were overlapped to each other in 10 % Ni- 30 % Al_2O_3- 70 % SiO_2-HNO_3; so, it is not possible to calculate the crystal size of these crystalline phases. Moreover, XRD spectrum of 10 % Ni- 30

% Al_2O_3- 70 % SiO_2-H_2SO_4 which prepared in the absence of nickel, showed no peaks belonging to mullite, and alumina-silicate crystal phases; only silica phase was existed.

The crystallite sizes in the catalysts which were calculated via Scherrer equation, were tabulated at Table 2.4.

Table 2.4. Crystalline phases and crystallite sizes for all the catalysts

	Crystalline phases and crystallite sizes (nm)				
Catalyst ID	**$NiAl_2O_4$**	**Mullite**	**NiO**	**Al_2O_3**	**Aluminum Silicate**
10% Ni-70% SiO_2-30% Al_2O_3-H_2SO_4	11.2	15.9	-	-	-
10% Ni-70% SiO_2-30% Al_2O_3-H_2SO_4-SW	10.9	15.7	-	-	-
10% Ni-70% SiO_2-30% Al_2O_3-HCl	-	-	49.9	-	4
10% Ni-70% SiO_2-30% Al_2O_3-HNO_3	-	-	<3	6	-

As tabulated in Table 2.4, the crystallite size of nickel aluminate and mullite were calculated as roughly 11 nm and 16 nm in 10 % Ni- 30 % Al_2O_3- 70 % SiO_2-H_2SO_4 and 10 % Ni- 30 % Al_2O_3- 70 % SiO_2-SW, respectively. This shows that treatment 10 % Ni- 30 % Al_2O_3- 70 % SiO_2-H_2SO_4 catalyst with sodium chloride did not yield formation of new crystalline phases and change in sizes within the detection limits of wide-angle X-Ray Diffractometer. Moreover, the crystallite sizes of alumina-silicate phases in 10 % Ni- 30 % Al_2O_3- 70 % SiO_2-HCl and 10 % Ni- 30 % Al_2O_3- 70 % SiO_2-HNO_3 were calculated as 4 and 6 nm, respectively. Also, the size of nickel oxide crystallite was found as approximately 50 nm for 10 % Ni- 30 % Al_2O_3- 70 % SiO_2-HCl; while it was found as value less than 3 nm for 10 % Ni- 30 % Al_2O_3- 70 % SiO_2-HNO_3 because the diffraction peak of nickel oxide was too small ($2\theta=43^o$) to calculate the crystallite size (Cullity 1978).

Total acidity and acidic strength of the catalysts were determined via Temperature Programmed Desorption with probe molecule of ammonia. The amount of adsorbed ammonia yields acidic sites' amounts available on catalyst while desorption temperature of ammonia yields the strength of the acidic sites on the catalysts (Tanabe 1989). Table 2.5 represents the acidity and acidic strength of catalysts and their BET surface areas.

Table 2.5. Acidity/Acidic strength and BET surface areas of all catalysts

Catalysts ID	BET Surface Area (m^2/g)	Acidity (µmole NH_3/ g of catalyst)	Maximum Desorption Peak Temperature (^oC)
1	130	16.96	134 181 376 622 733
2	309	85.98	151
3	325	62.63	147
4	97	25.14	130 183 300 387

In Table 2.5, the numbers (1-4) were corresponded to the followings: (1) 10 % Ni- 30 % Al_2O_3- 70 % SiO_2-H_2SO_4 (2) 10 % Ni- 30 % Al_2O_3- 70 % SiO_2-HCl (3) 10 % Ni- 30 % Al_2O_3- 70 % SiO_2-HNO_3 (4) 10 % Ni- 30 % Al_2O_3- 70 % SiO_2-H_2SO_4-SW. As seen in Table 2.5, total acidity was calculated as the highest for 10 % Ni- 30 % Al_2O_3- 70 % SiO_2-HCl as 85.98 µmole/g while the lowest total acidity, 16.96 µmole/g, was calculated for 10 % Ni- 30 % Al_2O_3- 70 % SiO_2-H_2SO_4. Acidic strength could be separated into two section: Weak and strong. Desorption peak temperature between 100^{o}C – 350^{o}C could be dedicated to weak acidic strength while between 350^{o}C -500^{o}C desorption peak temperatures were assigned to strong acidic strength. For 10 % Ni- 30 % Al_2O_3- 70 % SiO_2-H_2SO_4 and 10 % Ni- 30 % Al_2O_3- 70 % SiO_2-H_2SO_4-SW catalysts, there were more than one desorption peak temperatures ranging from 134^{o}C-733^o C. Indeed, high desorption peak temperatures (622^{o}C, and 733^{o}C) were vanished after the treatment of 10 % Ni- 30 % Al_2O_3- 70 % SiO_2-H_2SO_4 with NaCl which has desorption peak temperatures ranging from 130^{o}C-387^o C. Inversely, on 10 % Ni- 30 % Al_2O_3- 70 % SiO_2-HCl and 10 % Ni- 30 % Al_2O_3- 70 % SiO_2-HNO_3 catalysts, there was only desorption peak temperature located at 151^{o}C and 147^{o}C, respectively and, thus; these catalysts had weak acidic strengths when compared to other catalysts.

The catalytic activities of prepared catalysts in the conversion of 6 wt. % *Nannchloropsis Oculata* in sea water at 80^{o}C and 1 atm for 24 h. were illustrated in Figure 2.10. There were no *N. Oculata* conversion observed at same reaction conditions in the absence of catalyst and in the presence of 30 % Al_2O_3- 70 % SiO_2-H_2SO_4 catalyst which did not have any

nickel in its structure. The microalgae conversion over the catalysts given in Figure 2.12 were tabulated within experimental uncertainty of ±4.54%.

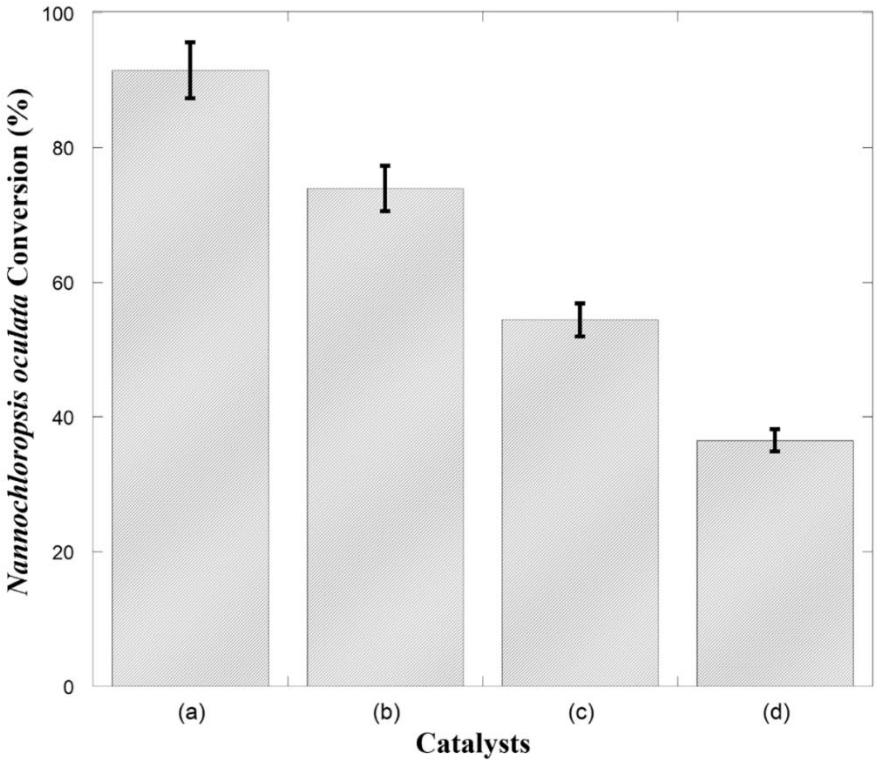

Figure 2.12. The conversion of *Nannochloropsis oculata* (a) 10% Ni - 30% Al_2O_3--70% SiO_2-H_2SO_4-SW, (b) 10% Ni-30% Al_2O_3-70% SiO_2-H_2SO_4, (c) 10% Ni-30% Al_2O_3-70% SiO_2-HNO_3, (d) 10% Ni-30% Al_2O_3-70% SiO_2-HCl

As seen in Figure 2.12, on 10% Ni- 30% Al_2O_3-70% SiO_2-HCl and 10% Ni- 30% Al_2O_3-70% SiO_2-HNO_3 catalysts, microalgae conversion at 80 ^{o}C under atmospheric pressure was obtained as 37 % and 54 %, respectively. The conversion of microalgae increased to 74 % over 10% Ni- 30% Al_2O_3-70% SiO_2-H_2SO_4 catalyst. Surprisingly, the highest conversion, 91.5 % was obtained over 10% Ni- 30% Al_2O_3-70% SiO_2-H_2SO_4-SW catalyst. This study is the first of its kind that handling the microalgae conversion over heterogeneous catalysts without harvesting and dewatering at mild conditions, whereas there were some studies regarding microalgae conversion to acids or sugars over homogenous catalysts as sulfuric acid, hydrochloric acid, and enzymes and also, some thermochemical studies to convert microalgal biomass to value-added products. However, there had been no studies in the literature directly related to this study. For instance, Choi et al. (2014) and Park et al. (2016) studied microalgae conversion over homogenous catalysts. Park et al. (2016) studied *C.vulgaris* conversion into galactose and glucose at 121^{o}C over several acids as sulfuric acid, hydrochloric acid, nitric acid, peracetic acid and phosphoric acid of which concentrations varied from 1 to 4% (w/w). The

authors reported that highest microalgae conversion, 8-11 % (w/w) to glucose and galactose observed in the presence of hydrochloric acid. Also, Choi et al. (2014) studied the hydrolysis of *Golenkinia sp*. in the presence of sulfuric acid and enzyme. They found that algae conversion into glucose in 120 min was 72.6 % in the presence of 2 wt. % sulfuric acid at 120 ^{o} C. On the other hand, Duan and Savage (2011) studied the hydrothermal liquefaction of *N.Oculata* paste into bio-oil over Pd/C catalyst and they found 57 % conversion of microalgal paste into bio-oil in autoclave reactor at 350 ^{o} C in 60 min., whereas roughly 35 % bio-oil yield was also observed in the absence of catalyst within same reaction conditions. In other study, Xu et al. (2014) investigated the *Chlorella pyrenoidosa* conversion at 300^{o}C in autoclave reactor over Ce/HZSM-5 and HZSM-5. The authors found % 49.9 and % 34 bio-oil yields from algal biomass at given reaction conditions over Ce/HZSM-5 and HZSM-5, respectively. Also, in the absence of catalyst, they calculated same bio-oil yield value as in the presence of HZMS-5. Therefore, generally, homogeneous acid catalysts or thermochemical conversion methods were used in the literature to convert microalgal biomass into biofuels or biochemicals, whereas, there were some problems in these methods such that in homogenous catalyst usage, there would be catalyst recovery problem and purification steps (e.g. washing step) would be necessary or in liquefaction of microalgal biomass into crude bio-oil, beside the high temperature or pressure requirement, harvesting and dewatering which were the most energy and cost intensive processes in microalgal biomass conversion into biofuel and biochemicals, were required. Hence, in our study, there were no necessity for the cost and energy intensive steps like in thermochemical methods to convert microalgal biomass into biofuels and biochemicals. Moreover, in this study, there was no problem in catalyst recovery because heterogeneous catalyst, alumina-silicate supported nickel catalyst was used. Also, reusability tests of these catalysts were investigated and found that these catalysts could be used more than twice and there was no activity loss observed during reusability tests. Another major concern for hydrothermal liquefaction studies that the catalysts could lose their activities due to the leaching of active components under hydrothermal conditions; i.e. high temperature and water requirement. As seen in Figure 2.12, comparable or better results were obtained even in the presence of high salinity, low temperature and pressure by using alumina-silicate supported nickel catalysts when compared to reported studies in the literature.

Table 2.6 tabulates the product distribution after conversion of 6 wt. % *N. Oculata* microalgae over alumina-silicate supported nickel catalysts at 80^{o}C under atmospheric pressure for 24 h. It was known that the cell wall and structure of *N.oculata* consist of various lipids, glycolipids, carbohydrates, and protein (Volkman et al. 1993). Therefore, it was founded that

the microalgal biomass was converted over alumina-silicate supported nickel catalysts to esters, triglycerides, monosaccharides, polyols, and alkanes. In fact, there were two phases in product analysis: Hexane-soluble products and non-soluble products. As seen in Table 2.6, however, there were some undefinable products which could be phospholipids and carbohydrates, aqueous phase which was non-soluble in hexane, mainly consists of glucose, arabinose, and glycerol as main products for all catalyst except for 10% Ni- 30% Al_2O_3-70% SiO_2-H_2SO_4-SW catalyst on which glucose and glycerol were the aqueous phase products and there were no arabinose detected for this catalyst. The reason not to observe arabinose could be due to that arabinose could be dehydrated to furfural (Hongsiri et al. 2015). The observation of glycerol was not surprising because triglyceride hydrolysis yields glycerol, carbohydrates as glucose, esters and fatty acids (Ozdogru 2017). In hexane soluble phase analysis, the presence of FA and their esters (i.e. hexadecenoic acid and 9-Octadecanoic acid, Methyl ester) confirmed the hydrolysis of triglycerides which were extracted from microalgal cell structure as a result of hydrolysis of cell wall. Also, it was conceivable to observe glucose in the aqueous phase products due to the hydrolysis of cellulose in the cell wall of microalgae. The products as esters and fatty acids showed similarity to the products studied in the literature as a results of microalgae conversion in the presence of homogeneous acid catalyst, sulfuric acid and hydrothermal liquefaction (Duan and Savage 2011, Choi et al. 2014, Park et al. 2016). Moreover, it is not rational to compare the product distribution of all catalysts to each other so as not to have iso-conversion condition for all catalysts. Unfortunately, it is difficult to quantify all the products produced during the conversion of 6 wt.% *N. oculata* over the catalysts due to inadequate reference materials; thereby, it sounded reasonable to tabulate the list of the products in hexane phase and their GC peak area percentages.

Table 2.6. Product Distribution

Catalysts	**Products in Aqueous Phase**	**Products in Hexane Phase**	**Peak Area (%)**
10% Ni- 30% Al_2O_3-70% SiO_2- H_2SO_4	Glucose (69 mg/L) Arabinose (71 mg/L) Glycerol (97 mg/L)	$C_9H_{10}O$, Benzaldehyde 2,5-dimethyl- $C_{14}H_{30}$ (Tetradecane) $C_{12}H_{26}O$ (1-Dodecanol) $C_{10}H_{12}Cl_2O$(2,6-dichloro-4-(1,1-dimethylethyl)phenol) $C_{16}H_{34}$ (hexadecane) $C_{19}H_{38}O_2$ (Isopropylpamitate) $C_{21}H_{42}O_2$ (Isopropylstearate)	33.3 4.6 9.1 12.5 7.2 14.3 19.0
10% Ni- 30% Al_2O_3-70% SiO_2-HCl	Glucose (88 mg/L) Arabinose (58 mg/L) Glycerol (95 mg/L)	C_9H_{12} (Benzene,1,3,5-trimethyl) $C_{19}H_{36}O_2$ (9-Octadecanoic Acid, Methyl Ester)	81.4 18.6
10% Ni- 30% Al_2O_3-70% SiO_2-HNO_3	Glucose (145 mg/L) Arabinose (36 mg/L) Glycerol (81 mg/L)	C_9H_{12} (Benzene,1,3,5-trimethyl) $C_{14}H_{30}$ (Tetradecane) $C_{16}H_{34}$ (Hexadecane) $C_{20}H_{42}$ (Eicosane) $C_{18}H_{38}$ (Octadecane) $C_{18}H_{36}O_2$ (Hexadecanoic acid, ethyl ester) $C_{20}H_{40}O_2$ (Octadecanoic acid, ethyl ester)	30.1 5.5 13.3 10.2 12.7 16.5 11.8
10% Ni-30% Al_2O_3-70% SiO_2-H_2SO_4-SW	Glucose (86 mg/L) Glycerol (103 mg/L)	C_9H_{12} (Benzene,1,3,5-trimethyl) $C_{10}H_{22}$ (Hexane,2,2,3,3-tetramethyl) $C_{20}H_{42}$ (Eicosane) $C_{16}H_{32}O_2$ (Hexadecanoic acid) $C_{18}H_{36}O_2$ (Hexadecanoic acid, ethyl ester) $C_{15}H_{28}O_2$ (Dodecylacyrlate) $C_{20}H_{39}ClO_2$ (3-Chloropropionic acid, heptadecyl ester) $C_{30}H_{50}$ (Squalene)	10.4 3.4 4.1 12.4 11.4 11.7 22.6 24.0

It was reported that the hydrolysis of saccharides and triglycerides occurs rapid in the presence of acid catalyst when compared to base catalyst (Ozdogru 2017, Umdu 2012). Volcano curve (see Figure 2.13) was plotted to illustrate the calculated conversion as a function of total acidity to comprehend the correlation between acidity of catalyst & acidic strength and the observed conversion of microalgae into biofuels and biochemicals (Thomas and Thomas 2015).

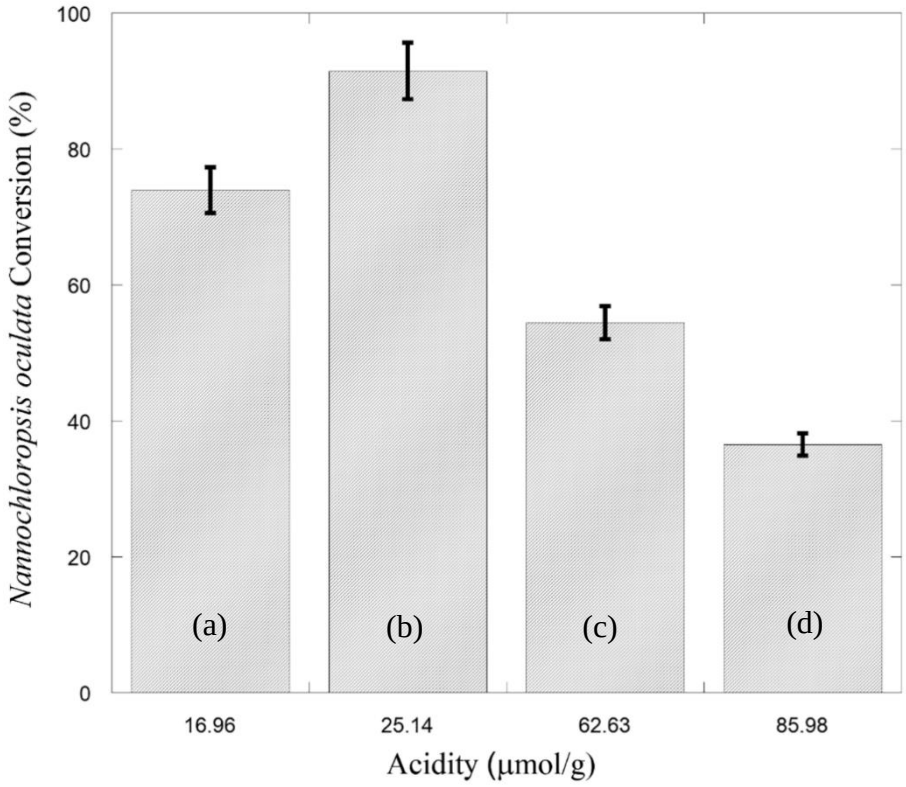

Figure 2.13. Volcano curve for *Nannochloropsis oculata* conversion (%) as a function of acidity (μmol/g) (a) 10% Ni-30% Al_2O_3-70% SiO_2-H_2SO_4, (b) 10% Ni-30% Al_2O_3-70% SiO_2-SW, (c) 10% Ni-30% Al_2O_3-70% SiO_2-HNO_3, (d) 10% Ni-30% Al_2O_3-70% SiO_2-HCl

As seen in Figure 2.13, the highest microalgae conversions, higher than 70 % were obtained at relatively low acidity, 15-25 μmol/g. In contrast to this behavior, lower microalgae conversions were observed at total acidity higher than 60 μmol/g. Indeed, the highest microalgae conversion was obtained over 10% Ni-30% Al_2O_3-70% SiO_2-SW catalyst which had total acidity of 25.14 μmol/g while the lowest microalgae conversion was observed over 10% Ni-30% Al_2O_3-70% SiO_2-HCl catalyst which had total acidity of 85.98 μmol/g; thus, it could be said that low total acidity was necessary to obtain high microalgae conversion, whereas one could ask how acidic strength was effective on

conversion or if there was any specific crystalline phases/crystallite size for direct conversion of microalgae into biofuel and biochemicals.

As tabulated in Table 2.5, the desorption peak temperatures of 10% Ni-30% Al_2O_3-70% SiO_2-H_2SO_4 catalyst altered between 130°C-730°C, whereas the acidic strengths at 600-730°C were vanished after the treatment of the catalyst with NaCl and the acidic strength distribution shifted to range of 130-380°C. That's why, it could be said that high microalgae conversion was observed over the catalysts which had low total acidity and acidic strength altering between the range of 130-380°C. Also, to prove the exigency of nickel presence on catalyst, TPD-NH_3 analysis performed for 70% SiO_2-30% Al_2O_3-H_2SO_4 catalyst which did not have any nickel, it was founded that it had total acidity of 19.48 μmol/g and acidic strength at roughly 165°C and as mentioned previously, it did not yield any microalgae conversion even if TPD results were very close to the results of 10% Ni-30% Al_2O_3-70% SiO_2-SW. This means that not only total acidity and acidic strength was effective but also nickel must be present to increase the catalytic activity. Benbenek et al. (1993) studied the acidity of Ni/Al_2O_3 and Ni/Al_2O_3/SiO_2 catalysts to investigate the effect of nickel on the acidity of the catalysts. The authors found that the addition of nickel onto alumina and silica-alumina substantially improved the acidity of the catalysts. After addition of nickel onto alumina, the quantity and strength of Lewis acid sites increased. This result confirmed the findings of Stanislaus et al. (1989). As seen in Table 2.4, $NiAl_2O_4$ crystalline phase formed by the reaction of nickel oxide and alumina and also resistive when compared to others, existed in only 10% Ni-70% SiO_2-30% Al_2O_3-H_2SO_4 catalyst which showed the best performance when compared to other catalysts because for $NiAl_2O_4$ crystalline phase, the net positive charge of the surface might be higher than the pure alumina. This resulted in the high strength of Lewis acid sites, in other words, the positive charge on Al^{+3} surface cations. In the study of Benbenek et al. (1993), the strength of Lewis acid centers did not alter when Ni^{2+} ions were incorporated onto the surface of alumina-silicate, whereas the addition of nickel onto silica-alumina increased the Bronsted acidity. This increment could be explained by the phenomenon that coordinatively unsaturated Ni^{2+} ions showed an ability to interact with oxygen atoms of the surface OH groups. In this case, the electron density on these oxygen atoms decreased and this provided more acidic protons attached to the oxygen. In fact, these explain why 10% Ni-30% Al_2O_3-70% SiO_2-HCl and 10% Ni-30% Al_2O_3-70% SiO_2-HNO_3 catalysts showed lower activity and higher acidity when compared to the catalysts of 10% Ni-30% Al_2O_3-70% SiO_2-H_2SO_4 and 10% Ni-30% Al_2O_3-70% SiO_2-

H_2SO_4-SW. However, the strength of Bronsted acid sites could be higher for the catalysts of 10% Ni-30% Al_2O_3-70% SiO_2-HCl and 10% Ni-30% Al_2O_3-70% SiO_2-HNO_3, it was thought that relatively medium strength Lewis acid centers may improve the catalytic performance of catalysts on microalgae conversion even if they showed higher total acidity. Also, Bronsted acid site should be available on the surface of the catalysts, whereas medium strength of Lewis acid site was mainly responsible for the cell wall degradation of *N. Oculata*; cellulose hydrolysis of cell wall. Beside Lewis acidity, the catalytic performance of 10% Ni-30% Al_2O_3-70% SiO_2-H_2SO_4 could also be attributed to $NiAl_2O_4$ crystalline phase because by the formation of this crystalline phase (Mohammad et al. 2010). Also, the calcination temperature of the catalysts was 900^oC. This would also lead to increase the Lewis acid sites while Bronsted acid sites would decrease because dehydroxylation could be occurred at this temperature (Brunner et al. 2008).

As known that metal oxides are the solid catalysts with many Lewis acid sites. These metal oxides can be used for hydrolysis of sucrose, cellobiose, and cellulose (Huang and Fu 2013). Shimizu et al. (2009) studied the hydrolysis of cellobiose and cellulose on heteropoly acid and metal salt. The authors found that maximum TOFs for cellulose conversion and TRS formation were achieved with moderate Lewis acidity and high Bronsted acid. Also, Kobayashi et al. (2010) studied the cellulose conversion to glucose on supported Ru catalyst. They found that the active Ru species was $RuO_2.H_2O$ desorbing the hydrated water to give a Lewis acid site which can depolymerize cellulose to glucose. Moreover, Chambon et al. (2011) studied the hydrolysis of cellulose over zirconia-based catalyst and found that Lewis acid promoted the cellulose depolymerization while Bronsted acid enhanced the product selectivity; thus, it can be said that not only Bronsted acid site was adequate for cellulose hydrolysis. On the other hand, the acidity of 10% Ni-30% Al_2O_3-70% SiO_2-HNO_3 catalyst was obtained as lower when compared to 10% Ni-30% Al_2O_3-70% SiO_2-HCl catalyst due to formation of NiO crystalline phase reducing acidity as it was described in the study of Viswanathan and Yeddanapalli (1974).

As given in Figure 2.13, the highest microalgae conversion was obtained for 10% Ni-30% Al_2O_3-70% SiO_2-H_2SO_4-SW catalyst as 94.8 %. Hereby, besides the acidity measurements to explain this catalytic activity, the catalytic activity of this catalyst could also be attributed to Na^+ ions available on the surface of the catalyst. Szczepanska (1975) studied the effect of Na^+ ion on methanol dehydration for which alumina-silicate gels

containing various amounts of Na^+, were prepared. Also, TPD-NH_3 adsorption was carried out to estimate the total acidity of catalysts. Up to 300°C, ammonia adsorption was at maximum as 0.54 μmol Na^+ $.m^{-2}$ which corresponds to an activity maximum for methanol dehydration. Also, total acidity showed increment again with increasing Na^+ ion for Na^+>0.8-1.0 μmole$.m^{-2}$. As a result of this, it was proposed that at low Na^+ ion content, the exchange of mobile protons in OH surface groups occurred for sodium ions which results in activity and acidity decrease, e.g. adsorption bands of OH groups were also vanished, whereas further Na^+ ion doping exerted a polarizing effect which leaded to surface structure and charge change on various atoms of alumina-silicate. That's why, the treatment with 35 wt. % NaCl might be high enough to cause a change in surface structure and charge of 10% Ni-70% SiO_2-30% Al_2O_3-H_2SO_4-SW due to existence of Na^+ ions exchanging with mobile protons being available on catalyst surface. Moreover, Na^+ ions on the catalyst surface might behave as strong Lewis acid centers which increased *N. oculata* conversion when compared to the others. Moreover, in the study of Grabowski and Malinows.S (1973), the authors used the quantum mechanical calculations to show that Na^+ ions in silicate were strong Lewis acid centers in Si-O-Na surface groups. A similar behavior was also observed for alumina-silicate surface. The maximum acidity and activity functions were obtained at ratio of Na/Al which equals to 1 due to the interactions between the latter pair being a maximum for equal numbers of the two species. In their study, infrared spectra confirmed that Lewis and Bronsted acid centers at medium strength increased after Na^+ ion addition. When Na/Al ratio was higher than 1 in the surface, the concentration of acidic sites decreased, and the gel surface was ruined at high Na^+ ion content. The acidity increased again ultimately with Na^+ ions which formed Lewis acid centers. This probably happened because alumina-silicate gel became like a sodium impregnated SiO_2 gel. In this study, 10% Ni-30% Al_2O_3-70% SiO_2-H_2SO_4 had a wide range acidic strength from 130°C to 730°C but acidic strengths at 600-730°C was vanished and shifted to 130-380°C for 10% Ni-30% Al_2O_3-70% SiO_2-H_2SO_4-SW which gave the highest conversion. This situation confirmed the results of Grabowski and Malinows.S (1973) that medium acidic strength tended to behave as strong Lewis acid centers for 10% Ni-30% Al_2O_3-70% SiO_2-H_2SO_4-SW catalyst, and enhancement in catalytic activity was achieved after NaCl treatment. In fact, initial algae solution consisted of 35 % NaCl for all experiments conducted for each catalyst, whereas the treatment with NaCl increased the Na^+ ions in the solution and increment in activity for

10% Ni-30% Al_2O_3-70% SiO_2-H_2SO_4-SW confirmed the results of the studies in the literature.

The reusability test of 10% Ni-30% Al_2O_3-70% SiO_2--H_2SO_4 catalyst was also performed to observe if there were any activity loss due to leaching of active component at operating conditions and the effects of any poisoner components as phospholipids coming from algal biomass. This catalyst was selected for reusability test because it gave the highest microalgae conversion among the other catalysts. In reusability test, after 24 hours reaction time, fresh microalgae in seawater was added to reaction medium without separating the catalyst and then reactor remained at same temperature for additional 24 h. Microalgae conversion was again calculated and liquid products were analyzed after 48 hours reaction time, and it was found that the microalgae conversion was improved. This means that there were no adverse effects of possible poisoner from microalgal biomass and salinity on catalytic activity. Also, it could be said that there was no coke formation on the catalyst surface on which all reactions, i.e. hydrolysis of cellulose and lipid, occurred due to high size differences between catalysts' pores and microalgae not in the pores of catalysts. In fact, this was the main reason why we treated 10% Ni-30% Al_2O_3-70% SiO_2-H_2SO_4 catalyst with NaCl. Even if the catalyst could be used more than twice, in fact, long-term usage performance tests of the catalysts should be carried on.

CHAPTER 3

ETHYL ESTER BIODIESEL PRODUCTION FROM MICROALGAL LIPIDS OVER ALUMINA-CALCIUM OXIDE CATALYST

Biodiesel can be produced via esterification or transesterification of vegetable oils or algal lipids and alcohol with base or acid catalyst depending on the process. The reaction steps observed in reversible transesterification at which base catalyst is used, were given below (Yusoff et al. 2014).

Triacylglycerol (TAG) + alcohol = Diglyceride + fatty acid alkyl or ethyl ester (3.1)

Diacylglycerol (DAG) + alcohol = Monoacylglycerol (MAG) + fatty acid alkyl or ethyl ester (3.2)

Monoacylglycerol (MAG) + alcohol = Glycerol + fatty acid alkyl or ethyl ester (3.3)

The use of homogeneous catalysts as metal hydroxides (sodium hydroxide and/or potassium hydroxide) and sulfuric acid are the common methods for the transesterification of triglyceride to biodiesel by reason of their high activity at low temperature. Miao and Wu (2006) studied methyl ester biodiesel (FAME) production form *Chlorella protothecoides* microalgae in the presence of sulfuric acid at relatively low temperature 30^{o}C while Li et al. (2007) reported 98.2 % *Chlorella protothecoides* microalgae conversion to biodiesel on lipase for 12 hours. Moreover, Hossain et al. (2008) produced methyl ester biodiesel from *Oedigonium and Spirogyra* macroalgae by using NaOH as catalyst. There have not been many studies regarding methyl ester biodiesel production from algal oils over heterogeneous catalyst. The study of Umdu et al. (2009) is the first of its kind that the authors reported microalgal oil transesterification at 50^{o}C over magnesium oxide and alumina supported calcium oxide which were carried out via modified single step sol-gel method. In addition, Guldhe et al. (2017) obtained approximately 98 % conversion in transesterification of algal lipid of *Scenedesmus obliquus* into methyl ester biodiesel over chromium-aluminum mixed oxide catalyst at

80^{o}C for 4 hours. Moreover, Teo et al. (2014) studied *Nannochloropsis Oculata* microalgal lipid transesterification to methyl ester biodiesel over heterogeneous catalyst. The authors tabulated 92 % algal lipid conversion to methyl ester biodiesel over calcium methoxide catalyst at 60^{o}C in 30-240 min.

In the homogeneous transesterification of oils, it is technically hard to separate the products and base catalysts from medium and large amount wastewater is produced after purification process i.e. neutralization, washing steps. Therefore, replacement of homogeneous catalysts with heterogeneous catalyst will serve the ease of separation of the reaction mixture, elimination of washing steps and lower downstream processing and total production cost. Also, the usage of heterogeneous catalyst will give another benefit that reusability of heterogeneous catalysts hinders the loss of catalyst (Bart et al. 2010). Solid catalyst can be separated from the product via physical methods as centrifuge. Bart et al. (2010) stated that there were no commercially available heterogeneous catalysts operating in the range of 318-338 K. Also, some of catalysts could be available in the range of 373-423 K operating temperature whereas excess of 4 hours was necessary in reactor residence times and large amounts of catalyst were required to obtain relatively high conversion. Also, in this temperature range, high pressure was necessary to hold the alcohol in liquid phase; thus, main challenging task is to prepare a solid catalyst, that can be used at low operating conditionsin the transesterification reactions.

Contrary to the use of methanol in transesterification of vegetable or algal oil, ethanol usage gave promising solution to obtain greener biodiesel because ethanol could be obtained from biological sources and processes (e.g. fermentation); thus, it can be said that biodiesel production would be completely renewable with the usage of ethanol. Additionally, the biggest issue for methyl ester biodiesel is the poor cold properties compared to crude-oil based diesel fuel so ethanol usage as alcohol in transesterification yields enhancement in the cold properties of biodiesel as cloud point. Leggieri et al. (2018) compared the cloud points of fatty acid methyl ester and fatty acid ethyl ester and found that cloud point of fatty acid ethyl ester with different carbon numbers and saturation was always lower compared to fatty acid methyl ester. Moreover, there have been few studies regarding the usage of ethanol in transesterification of vegetable oils over both homogeneous and heterogeneous catalysts to obtain ethyl ester biodiesel. Alamu et al. (2008) studied palm kernel oil transesterification with ethanol in the presence of 1 % potassium hydroxide. The reactions were carried out at distinct alcohol: lipid ratios at 60^{o}C for 120 min. The highest palm kernel oil conversion, 96 % was obtained with

0.15 alcohol: lipid ratio. Additionally, Li et al. (2009) studied canola oil and ethanol transesterification over mixed oxide catalysts derived from layered double hydroxide of Mg-Co-Al-La. The performance of catalysts prepared with different compositions, were tested at 473 K for 5 h. Lam and Lee (2011) reported the biodiesel production from waste cooking oil reacting with ethanol-methanol mixture over heterogeneous acid catalyst, SO_4^{-2} /SnO_2-SiO_2. The authors found that 81.4 % biodiesel yield was achieved at MeOH: EtOH: lipid ratio of 9:6:1 in the presence of 6 wt. % catalyst at 150 ^{o} C for 1 h. In this study, novel alumina-calcium oxide catalyst was prepared for transesterification of algal oil into ethyl ester biodiesel at 50 ^{o} C under atmospheric pressure.

Butanol is another alcohol which can be used in the transesterification of microalgal lipids. However, fatty acid butyl ester production has rarely been studied in the literature compared to esters produced from methanol and ethanol and in most of the studies, homogeneous catalyst was used rather than heterogeneous catalysts (Hájek et al. 2017, Leadbeater et al. 2008, Lee et al. 1995, Nimcevic et al. 2000). Like ethanol, butanol can also be produced via biological sources and processes as fermentation (Kumar and Gayen 2011). Thus, the production of fatty acid butyl ester would follow completely renewable route as in the usage of ethanol whereas the usage of butanol as alcohol in transesterification serves another advantage that cold properties of biodiesel is improved compared to biodiesels which are produced from methanol and ethanol. Lee et al. (1995) made a comparison about the cloud properties of biodiesels which were produced from soybean oil and different alcohols. The authors found that the cloud point of butyl ester biodiesel was approximately 10^{o}C lower than both methyl and ethyl ester biodiesels. Moreover, the caloric value of butyl ester is higher than both methyl and ethyl ester (Nimcevic et al. 2000). Table 3.1 tabulated the combustion values for ethyl, methyl and butyl esters.

Table 3.1. Combustion values of ethyl, methyl and butyl esters (Source: adapted from Nimcevic et al. (2000))

Esters	Combustion value (MJ/kg)	Molar fraction of alcohol in ester molecule (%)
Ethyl ester	40.03	12.2
Methyl ester	39.83	8.7
Butyl ester	40.52	18.4

Moreover, butanol is miscible with its ester and lipids, so it can react with fatty acids faster compared to methanol, and this miscibility yields better glycerol separation which is formed as by-product. Also, the separation of excess amount of butanol is not essential (Kótai et al. 2011). Therefore, in this study, fatty acid butyl ester biodiesel production from *Spirulina sp.* microalgal lipid was studied over alumina-calcium oxide catalyst at 50^{o}C and 1 atm due to these advantages.

Theoretically, the catalyst used in biodiesel production is initially activated in the presence of alcohol under elevated temperature and stirring. In the activation of catalyst, deprotonation of alcohol occurs and metal-alkoxide formation is observed. The alkoxide part stays attached to the metal oxide catalyst and behave as transesterification catalyst; thus, initial activation of catalyst becomes more of an issue in the transesterification reactions. After primary activation of catalyst, the triglyceride source which algal oil is added to solution and metal-alkoxide serves as an initiator for nucleophilic attack on the electrophilic carbonyl group of triacylglycerol, TAG (also called as triglyceride). This leads to tetrahedral intermediate formation, subsequently rearranged to yield alkyl or ethyl ester and diacylglycerol (DAG) anion which taking proton from catalyst surface to stabilize itself. Then, DAG produces monoacylglycerol (MAG) which reacting to produce glycerol and biodiesel. Ultimately, biodiesel is produced with one mole glycerol which is by-product (Kumar et al. 2018). In algal oil conversion into ethyl ester biodiesel production over alumina-calcium oxide catalyst, calcium ethoxide would initially be formed by basic site of the catalyst abstracting H^{+} proton from alcohol. Therefore, the formation of calcium ethoxide serving as transesterification catalyst, depends on the basic properties of the catalyst and transesterification of algal oil is strongly dependent on the basic nature of the catalyst.

In this study, the production of ethyl ester biodiesel by using *Spirulina sp.* and *Nannochloropsis Oculata* algal lipids and ethanol over alumina-calcium oxide catalyst was studied at 50^{o}C and 1 atm with respect to distinct amount of catalyst, ethanol: lipid ratios, and reaction time. Also, transesterification of microalgal lipid of *Spirulina sp.* to fatty acid butyl ester in the presence of butanol over 60 wt. % CaO on alumina catalyst was studied. To the best of our knowledge, this is the first of its kind dealing with the production of ethyl ester and butyl ester biodiesel from algal lipids and ethanol/ butanol at such a mild condition over heterogeneous catalyst. Moreover, this study was studied with my co-worker, Berk Türkkul who helped to collect the data in the production of ethyl ester biodiesel.

3.1. Experimental

3.1.1. Catalyst Preparation

In this study, alumina-calcium oxide catalyst was synthesized via modified single step sol-gel method as described in the study of Umdu (2008). To prepare alumina sol, aluminum isopropoxide (≥ 98 % purity, Aldrich) which was precursor of alumina, initially mixed with deionized water at 85^{o}C for 1 hour, then nitric acid (68 wt. %, VWR Chemicals) was added and mixed for additional 1 hour. Separately, calcium nitrate tetrahydrate was solved in water and then, added to alumina sol and mixed for extra 1 hour. Ultimately, excess solvent was evaporated at 70^{o}C to get gel which was further dried at 120^{o}C for 12 h and then calcined at 700^{o}C for 6 h with 10^{o}C / min heating rate. To use catalyst in activity measurements, calcined catalyst was sieved and ground under 400 mesh size.

3.1.2. Algal lipid extraction

Spirulina sp. marine microalgae powder which was freeze dried was supplied from Optimally Organic Inc. Freeze dried *Spirulina sp.* microalgae powder was formed in organic way and free of irradiation and additives. *Nannochloropsis Oculata* marine microalgae paste was supplied from Prof. Dr. Durmaz, Ege University. The growth conditions and properties of *Nannochloropsis Oculata* paste were given in the study of Durmaz (2007). To extract algal lipids from *Nannochloropsis Oculata* paste and freeze dried *Spirulina sp.* marine microalgae powder, partial extraction method was used by using Soxhlet extractor. In Soxhlet extraction, hexane was used solvent because it is non-polar solvent which made able to eliminate the extraction of polar-lipid compounds (e.g. phospholipids) and non-lipid compounds; thus, it was called partial extraction. Soxhlet extraction was performed at roughly 73 ^{o} C for 10-24 h until the color of circulating solvent became completely transparent. After extraction, to collect algal lipids, hexane was evaporated from hexane-algal lipid mixture by using rotary evaporator at 50 ^{o} C under vacuum.

3.1.3. Catalytic activity tests

It was decided to calcine the catalysts at 700 º C for 6 hours because in the one of the study of Seker's group (Yalman 2012). Same catalyst composition, 60 wt. % CaO/ Al_2O_3, was used in the transesterification of canola oil with ethanol at distinct calcination temperature. Approximately 100 % yield of the ethyl ester biodiesel was detectedin less than 1 hour. In Yalman (2012) study, the reactions were carried out at 50 º C under the reaction conditions of that ethanol: canola oil molar ratio was 9:1 with catalyst amount of 6 wt.% of lipid amount. Therefore, 60 wt.% CaO on alumina catalyst calcined at 700 º C was used in transesterification of microalgal lipids (*Spirulina sp.* and *Nannochloropsis Oculata*) with ethanol at 50 º C and 1 atm in batch reactor with given parameters in Table 3.2.

Table 3.2. Reaction conditions in transesterification of *Spirulina sp.* and *Nannochloropsis Oculata* algal lipids

Ethanol: Lipid Molar Ratio	12:1 - 24:1 - 48:1
Catalyst Amount (wt. % of algal lipid)	6 - 12 - 48
Reaction Time (min.)	30 - 60 – 120
Temperature (ºC)	50

Transesterification of *Spirulina sp.* and *Nannochloropsis Oculata* algal lipids were carried out at 50ºC in the presence of ethanol over alumina-calcium oxide catalyst, 60 wt. % CaO/ Al_2O_3. At the end of the reaction, single phase product was obtained because ethanol: lipid molar ratio was in excess of the stoichiometric molar ratio; thus, biodiesel had to be separated from glycerol rich phases. For this aim, catalyst initially separated from reaction medium by using centrifuge which was operated at 5000 rpm for 10 min. After removal of catalyst, equal volume of glycerol was added to single liquid phase and centrifuged at same conditions. Then, two-phase liquid formation was observed and biodiesel rich phase in upper phase including biodiesel and unconverted algal lipids, was collected. To separate unconverted lipids and biodiesel, equal volume of ethanol was added to this phase because ethanol was miscible with ethyl ester biodiesels and not with algal lipids (Liu et al. 2008, Machado et al. 2011). Again, centrifuge was used to collect ethanol-biodiesel ethyl esters mixture from unconverted algal lipids.

In the butyl ester biodiesel production, transesterification reaction was carried out at 50°C and 1 atm over 60 wt. % CaO on alumina catalyst as in ethyl ester biodiesel production. Butanol-catalyst mixture was initially heated to 50°C and held for 10 minutes to obtain butoxide groups and then, algal oil at 50°C was added to the mixture. To separate the products, different method than the separation of ethyl ester biodiesel was performed due to the liquid-liquid equilibrium. Ternary phase diagram for glycerol- stearic acid butyl ester- 1-butanol was shown in Figure 3.1.

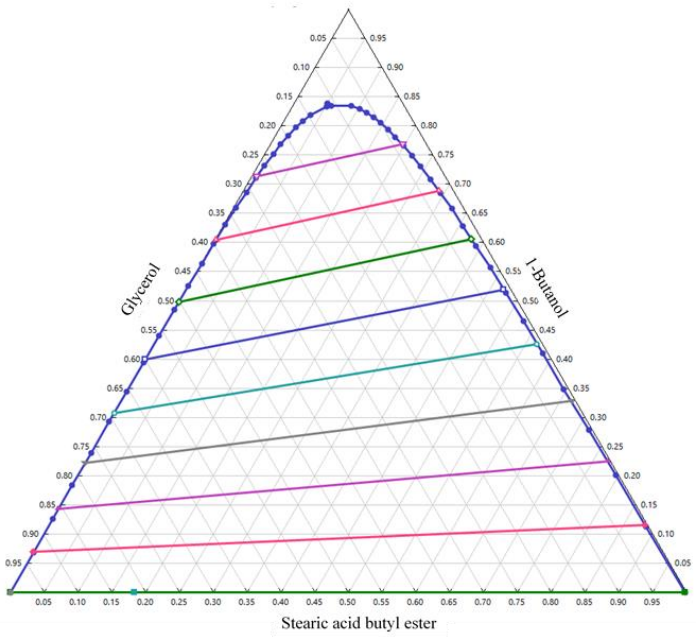

Figure 3.1. Ternary phase diagram for glycerol-stearic acid butyl ester-1-butanol

At the end of the reaction, firstly, centrifuge method was used at 6000 rpm for 10 min. to separate catalyst from the products. Subsequently, due to existence of one phase, the products were washed with 3 vol. % HCl solution at room temperature for 1 hours and at the end of washing and centrifuge, three phases were obtained and upper phase containing butanol and butyl ester biodiesel was collected.

3.1.4. Product analysis and catalyst characterization

To obtain the amount of ethyl esters biodiesel content in the ethanol-biodiesel mixture, gas chromatography (Agilent 6890 N Ga Chromatograph) equipped with FID detector and DB-WAX 122-7032 column having 60 m column length, 0.25 mm column diameter and 0.25 μm film thickness was used. The column was operated at 225 °C while

injection port and detector were operated at 250 ^{o}C. Helium flow and split ratio were 32 cm/s and 150, respectively. In the quantification of butyl ester biodiesel amount, same procedure with same equipment was followed as in ethyl ester biodiesel determination.

At the end of the analysis, ethyl/ butyl esters biodiesel amount was calculated by using given formula:

$$\text{Biodiesel yield (\%)} = \frac{\text{Amount of ethyl/butyl ester biodiesel in upper phase (g)}}{\text{Initial amount of microalgal lipid (g)}} \quad (3.4)$$

Crystalline structures formed in alumina-calcium oxide catalyst was determined by using Philips X'Pert Pro Diffractometer with Ni-filtered CuKα radiation (λ=1.54056 Å, operated at 40 kV and 45 mA) in the range of 5-80^{o} 2θ values. The crystal size of catalyst was calculated by using Scherrer equation given below:

$$d = \frac{K \times \lambda}{B \times \cos(\theta)} \quad (3.5)$$

where K was shape factor and it was approximately 0.9, B was peak broadening effect using the Full-Width Half Maximum (FWHM), θ was the main diffraction angle in degree, and λ was 1.54056 Å which was the wavelength of X-ray.

Basicity and basic strength of the catalyst could not be determined by using Temperature Programmed Desorption method due to its relatively low surface area (~1 m^2/g). Hence, FTIR Spectroscopy was used to determine basic properties of the catalyst. In FTIR analysis, irreversibly adsorbed carbon dioxide peaks gave total basicity; in other words, the amount of total basic site available on the catalyst while its absorption band and wavelength yielded strength of these basic sites. For FTIR analysis, acidic probe molecule, carbon dioxide was adsorbed on the catalyst with given procedure in Figure 3.2.

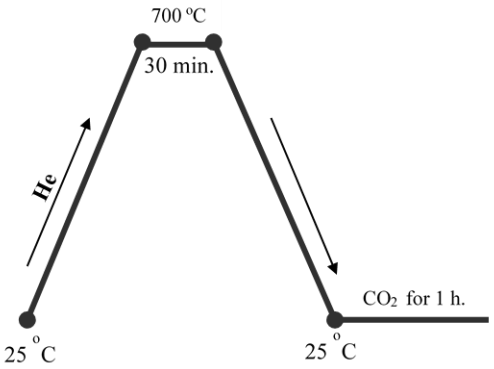

Figure 3.2. Temperature programmed desorption method for carbon dioxide adsorption

As seen in Figure 3.2, initially, alumina-calcium oxide catalyst was cleaned at its calcination temperature, 700ºC, for 30 min. and then the temperature was decreased to room temperature under helium flow. Carbon dioxide adsorption was applied at room temperature for an hour. 60 wt. % CaO on alumina catalyst could adsorb water even at high temperatures so after carbon dioxide adsorption, catalysts pellets for FTIR analysis was immediately prepared in glove box which was dehumidified by silica and zeolite X, to eliminate the overlapping of water peaks and main peaks in FTIR analysis.

3.2. Results and Discussion

Ethyl ester biodiesel manufacture from *Spirulina sp.* and *Nannochloropsis oculata* microalgal lipids on 60 wt. % CaO on alumina catalyst at 50 º C under atmospheric pressure was studied in this study. As shown in Table 3.2, catalyst amount, ethanol: lipid mol ratio, and reaction time were altered to find the optimal catalytic activity in transesterification of microalgal oils.

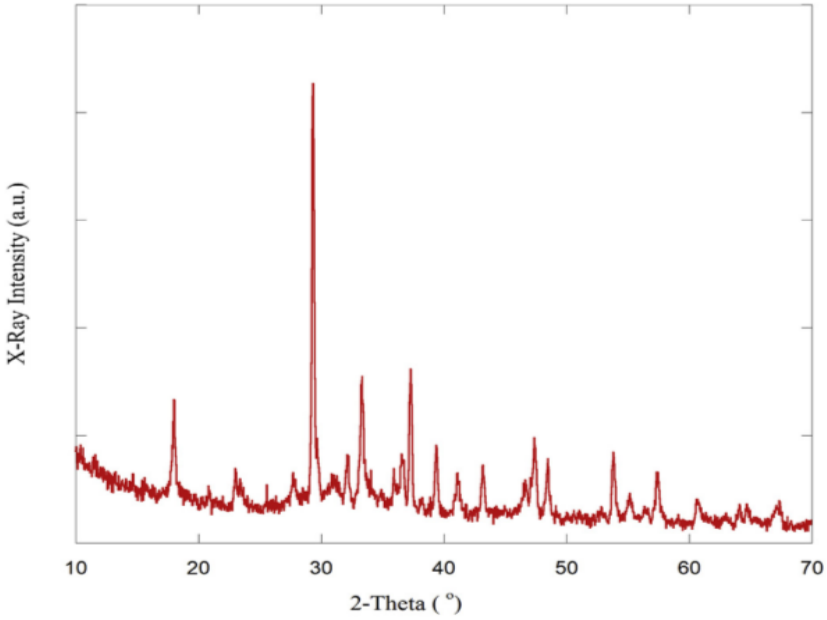

Figure 3.3. XRD pattern of 60 wt.% CaO on alumina

Figure 3.3 represents the XRD patterns of 60 wt.% CaO on alumina catalyst prepared via modified single step sol-gel method and calcined at 700 º C for 6 hours. As seen in Figure 3.3, observed diffraction patterns were corresponded to calcium oxide (CaO), calcium hydroxide ($Ca(OH)_2$), calcium calcite ($CaCO_3$), and alumina (Al_2O_3) crystalline phases and also, the hydrated form of them as $2CaO.Al_2O_3.8H_2O$ and

$3CaO.Al_2O_3.3CaCO_3.3H_2O$ were observed. Table 3.3 tabulates the diffraction angles and standard reference card numbers of crystalline phases observed in 60 wt. % CaO on alumina catalyst.

Table 3.3. Observed crystalline phases with their standard reference card numbers

Diffraction angles	**Crystalline phases**	**Reference card numbers**
18.03, 36.67, 47.09	$Ca(OH)_2$	00-044-148
23.02, 29.41, 35.97, 39.40, 43.15, 47.12, 47.49, 48.51, 57.40, 60.68, 64.68	$CaCO_3$	00-005-0586
32.20, 37.34, 53.86, 67.38	CaO	00-037-1497
27.77, 29.70, 32.09, 36.54, 39.49, 46.51, 47.65, 53.85, 57.48, 67.20, 67.25	Al_2O_3	00-046-1215
33.20, 35.89, 37.38, 43.09, 57.71	$2CaO.Al_2O_3.8H_2O$	00-045-0564
22.97, 23.42, 32.97, 33.17, 34.06, 35.79, 36.69, 37.17, 43.05, 46.94, 47.22, 47.47, 48.35, 55.00, 57.19	$3CaO.Al_2O_3.3CaCO_3.3H_2O$	00-041-0215

The average crystal sizes of these observed peaks were also calculated via Scherrer equation and given in Table 3.4. It was not doable to calculate the crystal sizes of hydrated form of the crystalline phases and alumina because their diffraction peaks were overlapped on other peaks.

Table 3.4. The average crystallite size of crystalline phases observed in 60 wt. % CaO

Crystalline phase	Crystallite size (nm)
CaO	44
$Ca(OH)_2$	27
$CaCO_3$	40

Moreover, Figure 3.4 illustrates XRD patterns of commercial $CaCO_3$, $Ca(OH)_2$ and CaO and alumina which was prepared via single step sol-gel method without calcium oxide.

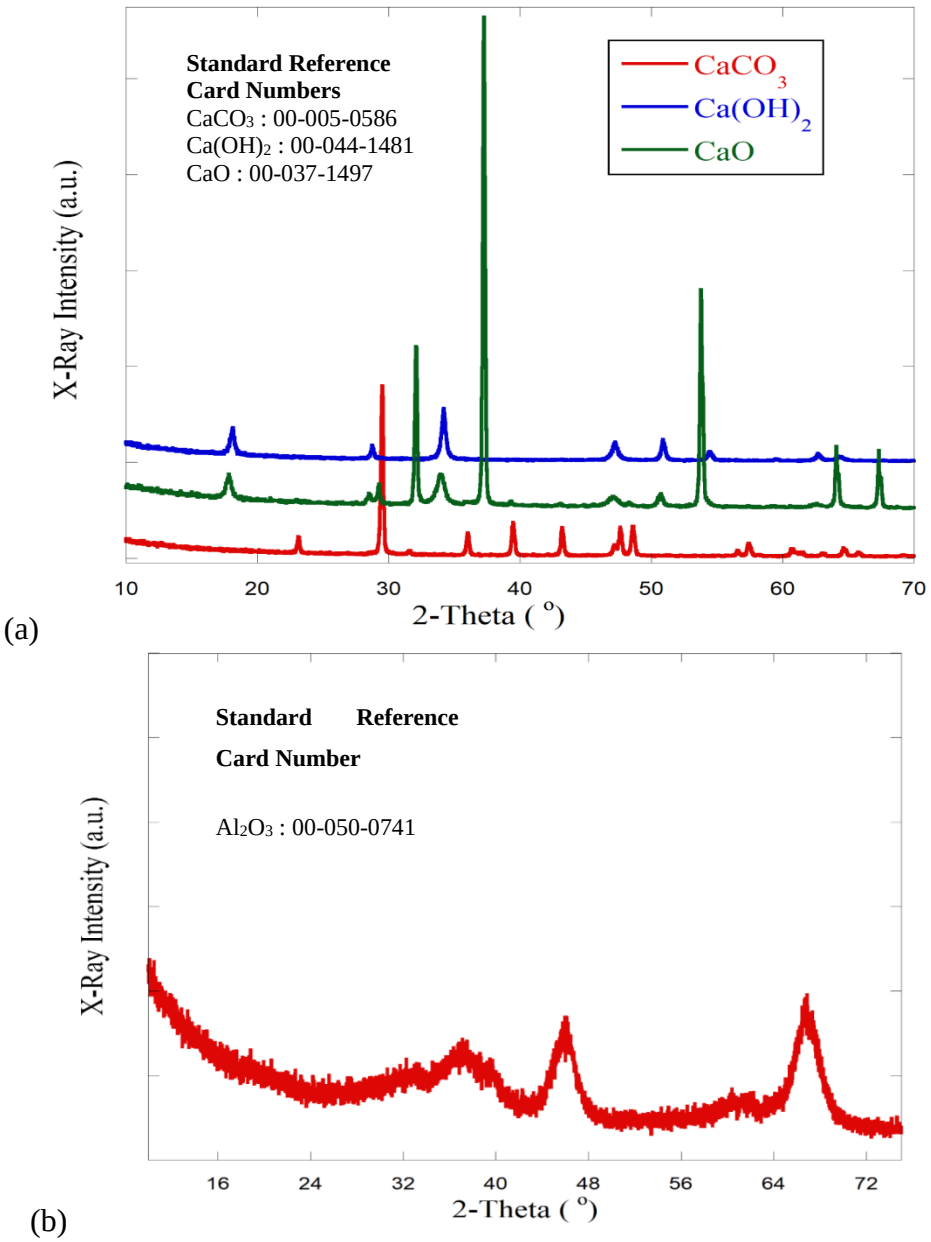

Figure 3.4. XRD patterns of (a) commercial $CaCO_3$, Ca $(OH)_2$ and CaO catalysts (b) alumina prepared via single step sol-gel method

As seen in Figure 3.4., commercial CaO had Ca $(OH)_2$ crystalline phase in its structure owing to water adsorption in air throughout XRD analysis. After exposure CaO catalyst to air, following reactions occurs due to adsorption of water and carbon dioxide from air by basic site of calcium oxide (Kesic et al. 2016);

$$CaO + H_2O \rightarrow Ca(OH)_2 \quad (3.6)$$

$$CaO + CO_2 \rightarrow CaCO_3 \quad (3.7)$$

$$Ca(OH)_2 + CO_2 \rightarrow CaCO_3 + H_2O \quad (3.8)$$

The average crystallite size of commercial CaO was calculated as 77 nm while average crystallite size of gamma alumina in prepared alumina without calcium oxide, was calculated as 82 nm.

Table 3.5 listed the total basicity of 60 wt. % CaO on alumina and pure components which were determined by using FTIR. As seen in Table 3.5, the basicity of 60 wt. % CaO on alumina catalyst was calculated as 41 μmol CO_2 per gram of catalyst while the basicity of pure alumina and CaO were determined as 47.1 and 192.6 μmol CO_2 per g catalyst. Even if the basicity of pure components were much higher than 60 wt. % CaO on alumina catalyst, there was no algal lipid conversion in the presence of pure components while in the presence 60 wt. % CaO on alumina catalyst, minimum 58 % algal lipid conversion which was dependent on the reaction conditions, was observed. Therefore, it showed that alone basicity did not answer the high conversion of algal lipid over 60 wt. % CaO on alumina catalyst. High algal lipid conversion could be attributed to the basic strengths of 60 wt. % CaO/Al_2O_3 catalyst and pure components.

Table 3.5. Total basicity of catalyst and pure components

Catalysts calcined at 700ºC	**Total Basicity (μmol CO_2/g of catalyst)**	**FTIR CO_2 adsorption maximum wavenumber (cm^{-1})**
60 wt % CaO on alumina	41	1266 1333 1432 1635 1798 2513
Pure CaO	192.6	1074 1424 1484 1653 1794 2564
Pure Alumina	47.1	1404 1533 1637

The absorption band wavenumber of carbon dioxide on the catalysts given in Table 3.5 gives the information regarding the basic site strength. As listed in Table 3.5, for pure CaO, Two weak absorption bands were detected at 1074 and 1794 cm^{-1}. In addition, one strong absorption band centered at 1454 cm^{-1} with a band splitting at 1424 and 1484 cm^{-1} with a weak shoulder at 1653 cm^{-1} was also attributed. There was also a

weak band at 2564 cm^{-1}. These results of pure calcium oxide confirmed IR results of pure CaO tabulated in the literature. The bands observed at 1630, 1460 and 1213 cm^{-1} were attributed to bicarbonate, and the bands at 1560, 1390 and 1069 cm^{-1} were defined as unidentate carbonate in the study conducted by Gruene et al. (2011). Zaki et al. (2006) yielded similar results; thus,stretching band of C-O bond and symmetric/ asymmetric stretching bands of O-C-O bonds in unidentate carbonate could be defined with the bands at 1074 cm^{-1} and the band with the splitting at 1424 and 1484 cm^{-1} with a weak shoulder at 1653 cm^{-1} found in this study.. Also, the weak band observed at 1794 cm^{-1} was attributed to the bridging carbonate species, whilethe band at 2564 cm^{-1} were appointed to the linearly adsorbed CO_2 at a cation site.. These proved the dominant presence of the unidentate carbonate species in pure CaO. There were two weak bands at 1266 and 1798 cm^{-1} and a strong band located at 1432 cm^{-1} which had shoulders at 1333 and 1635 cm^{-1} and no band splitting in 60 wt. % CaO on alumina catalyst. Therefore, the band located at 1266 cm^{-1} belonged to C-OH bending and the bands located at 1333, 1432, and 1635 cm^{-1} were corresponded to the symmetric/asymmetric stretching of O-C-O bonds of bicarbonate species. The bridging carbonate species stretching was specified with the band at 1798 cm^{-1}. Additionally, there was also a weak band at 2513 cm^{-1} due to the linearly adsorbed CO_2 at cation site as observed in pure CaO. As comprehended, bicarbonate species had domination in 60 wt. % CaO on alumina catalyst instead the unbidentate and identate carbonate species, which showed that 60 wt. % CaO on alumina catalyst had different basic strength compared to pure CaO due to distinct chemical environment of basic sites. The absorption band was observed at weaker absorption band energy for the 60 wt. % CaO on alumina catalyst, compared to the band energy of pure CaO so it could be said that basic site strength of 60 wt. % CaO on alumina catalyst was weaker compared to pure CaO. This could be attributed to the domination of bicarbonate species which could yield higher microalgal lipid conversion into fatty acid ethyl ester biodiesel (FAEE).

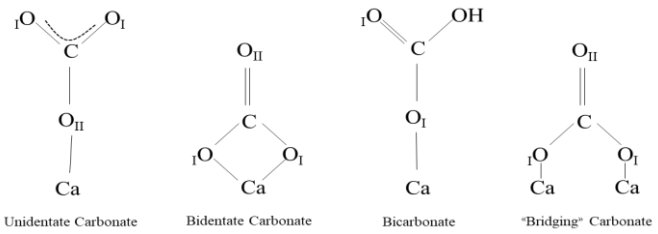

Figure 3.5. The formation of surface carbonates by CO_2 adsorption on CaO (Source: adapted from Philipp and Fujimoto (1992))

Figure 3.6 illustrates gas chromatograms of pure ethanol and ethyl ester biodiesel produced via *Spirulina sp.* microalgal lipid transesterification under the reaction conditions given in following: Ethanol: lipid molar ratio=24; catalyst amount= 6 wt. %; reaction time= 30 min.

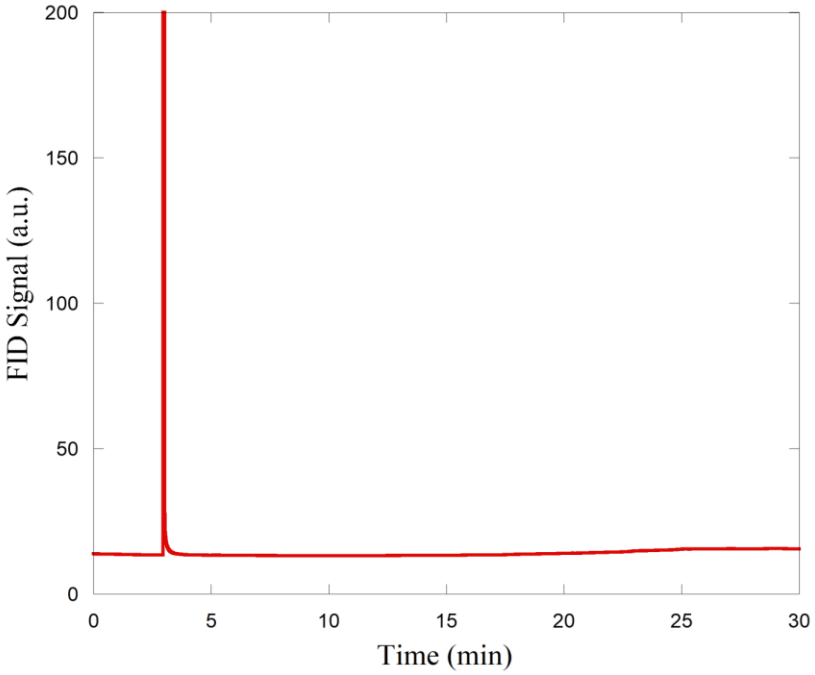

(a)

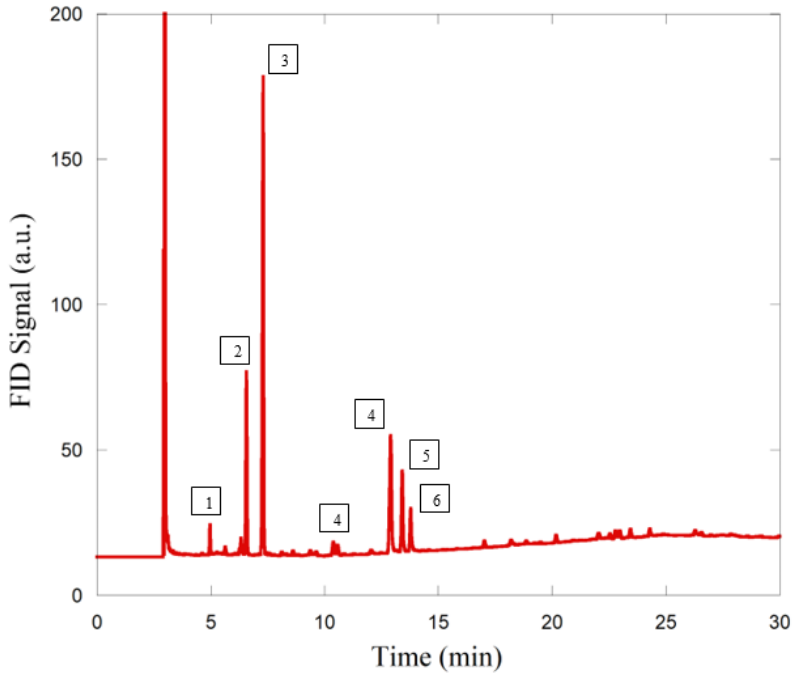

(b)

Figure 3.6. Gas chromatograms of (a) pure ethanol (b) fatty acid ethyl esters biodiesel produced from *Spirulina sp.* microalgal lipid

Figure 3.6.b illustrated the fatty acid ethyl esters biodiesel produced from *Spirulina sp.* microalgal lipid. As seen in Figure 3.6, ethyl ester biodiesel included (1)

C14:0 (Myristic acid ethyl ester), (2) C16:0 (Palmitic acid ethyl ester), (3) C18:0 (Stearic acid ethyl ester), (4) C18:1-C18:2 (Oleic acid ethyl ester and Linoleic acid ethyl ester), (5) C20:0 (Arachidic acid ethyl ester), (6) C22:0 (Behenic acid methyl ester). In the study of Al-Dhabi and Valan Arasu (2016), the fatty acid content of *Spirulina sp.* was analyzed via a gas chromatography havingflame-ionization detector and their results confirmed the obtained fatty acid contents in fatty acid ethyl ester biodiesel.

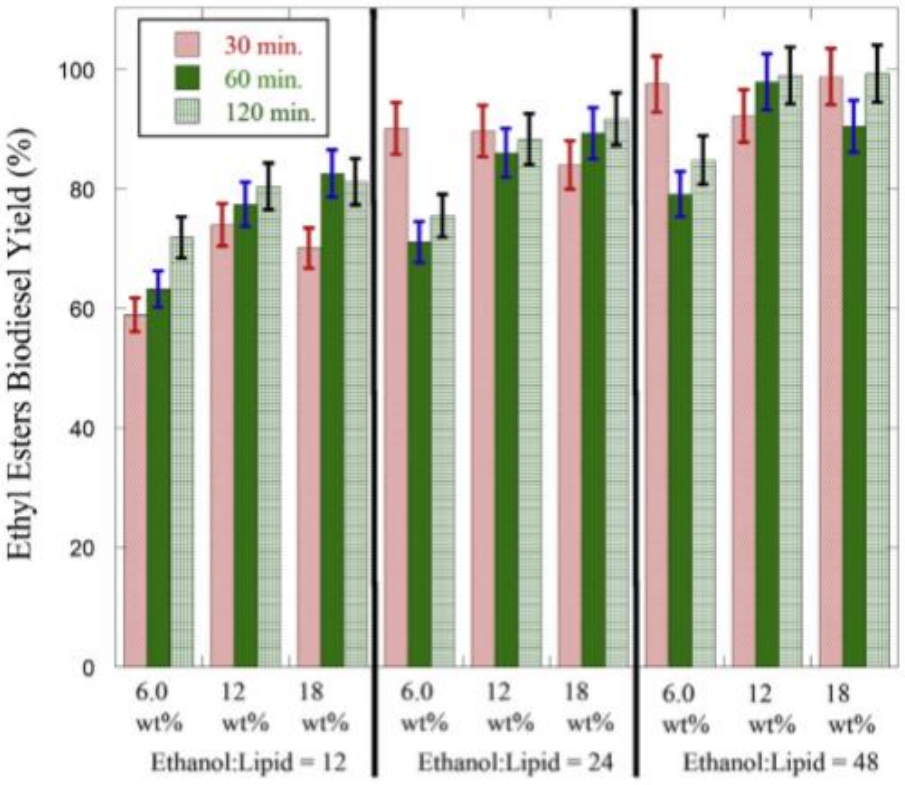

Figure 3.7. Fatty acid ethyl esters (FAEE) biodiesel yield with respect to ethanol: oil molar ratio, the catalyst amount and reaction time

Figure 3.7 represents the ethyl ester biodiesel yields over 60 wt.% CaO on alumina catalyst at 50 ^{o} C and 1 atm for distinct operating parameters of catalyst amount, ethanol: lipid ratio, and reaction time. Fatty acid ethyl ester biodiesel yield showed increment as the catalyst amount was changed from 6 wt.% to 12 wt.%. When the catalyst amount increased from 6 wt. % to 12 wt. % of lipid amounts, yield showed increment from roughly 59 % to 74 % at constant ethanol: lipid molar ratio of 12 in 30 minutes of reaction time. Contrary to this, biodiesel yield did not alter as a function of the reaction time at ethanol: lipid molar ratios of 24 and 48 when the catalyst amounts were 12 wt. % and 18 wt. %. The yield of biodiesel raised with reaction time when ethanol: lipid ratio was kept at 12 and the catalyst amount was 6 wt. %. With reaction time increment, it was not

surprising to observe increment in biodiesel yield for reversible reactions because it was not close to the equilibrium conversion whereas when the equilibrium conversion had been reached, conversion had to stay constant with increment in reaction time. Additionally, forward transesterification reaction rate was accelerated with an increase of the ethanol: lipid molar ratio.

Ethanol: lipid molar ratio was 4, 8, and 16 times greater than the stoichiometric ethanol: lipid molar ratio of 3, in this study. Therefore, at higher ethanol: lipid molar ratio, 100 % of equilibrium conversion was expected. Figure 3.8 shows the ethyl esters biodiesel yield with respect to time, ethanol: lipid molar ratio for 6 wt. % catalyst amounts of algal lipid. For the ratios as 24 and 48 , ethyl ester biodiesel yields were obtained as greater than 90 % at 30 minutes, then declined at 60 minutes and after that it was constant at 120 minutes.

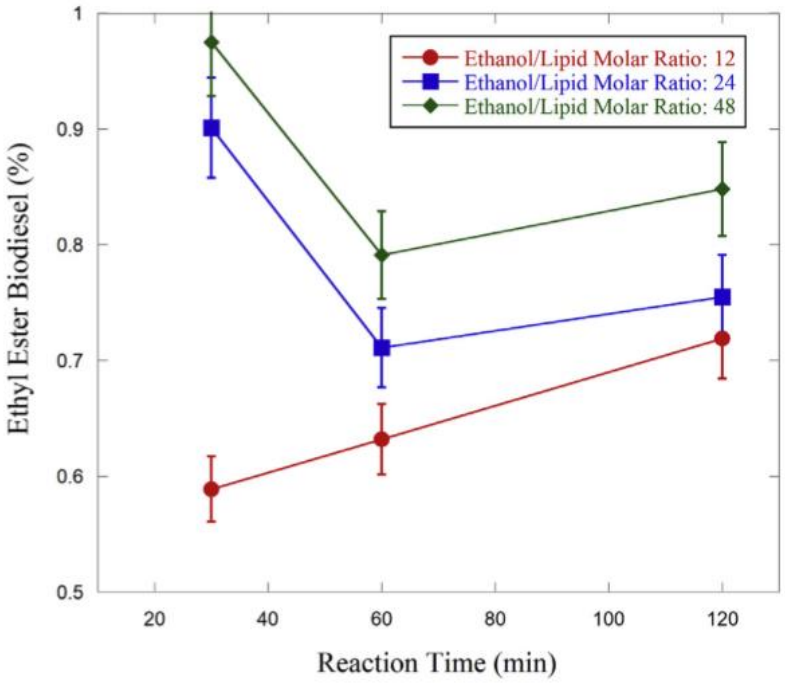

Figure 3.8. Fatty acid ethyl esters biodiesel yield with respect to reaction time, ethanol: lipid molar ratio for catalyst amount of 6 wt.% of lipid

For ethanol: lipid molar ratio of 24, the yield of biodiesel was approximately 90 % at 30 minutes in 6 wt. % catalyst amount of algal lipid, and then it showed decrement to 71 % at 69 minutes and stayed constant at 120 minutes. Same behavior was also observed for ethanol: lipid molar ratio of 48 so it could be said that the equilibrium yield was reached. This kind of behavior observed for ethanol: lipid molar ratios of 24 and 48, could be

assigned to glycerolysis of lipids taking place in series with transesterification of triacylglycerol (equations 1-3). Glycerolysis of triacylglycerol was given below;

Triacylglycerol + 2Glycerol = 3 Monoacylglycerol (3.9)

Triacylglycerol + Glycerol = Monoacylglycerol + Diacylglycerol (3.10)

Diacylglycerol + Glycerol = 2 Monoacylglycerol (3.11)

As presented in Figure 3.8, the microalgal lipids' conversion to fatty acid ethyl ester biodiesel for 30 minutes had been already obtained as greater than 90 %. This means there was adequate glycerol formation occurred over the reactions 1-3. Therefore, glycerolysis of triacylglycerol took place through the reactions 4-6 with an increase in the reaction time to 60 minutes. Fatty acid ethyl ester was consumed as a result of the reverse reactions of 1 and 2 and this leaded to decrement in biodiesel yield at 60 minutes. During GC analysis, triacylglycerol, monoacylglycerol, diacylglycerol and glycerol could not be measured due to column used for this study whereas confirmation of triacylglycerol glycerolysis was performed by measuring the fatty acid ethyl ester formation with respect to reaction time.

Fatty acid ethyl ester biodiesel production from *Nannochloropsis Oculata* algal lipid was also investigated over 60 wt. % CaO on alumina catalyst at 50 ^{o}C and 1 atm for the selected reaction time, ethanol: lipid molar ratios, and catalyst amounts. Fatty acid ethyl ester biodiesel production from *Nannochloropsis Oculata* algal lipid had similar trend as *Spirulina sp.* algal lipid. Table 3.6 tabulates the fatty acid ethyl ester biodiesel yield from *N.Oculata* algal lipid with respect to ethanol: lipid molar ratio, catalyst amount and reaction time. The parameters were selected as in tabulated in Table 3.6 because of the reasons of (i) having similar fatty acid compositions of *N. Oculata* and *Spirulina sp.* algal lipids; (ii) limiting supply of *N.Oculata* microalgal lipid or paste.

Table 3.6. Fatty acid ethyl ester biodiesel yields as a result of *N.Oculata* transesterification

Catalyst amount wt. % of algal lipid	**Ethanol: lipid molar ratio**	**Reaction time (in minutes)**	**Fatty acid ethyl ester biodiesel yield (%)**
6	24	30	82.1
12	24	30	96.2

(Cont. on next page)

Table 3.6. (Cont.)

Catalyst amount wt. % of algal lipid	Ethanol: lipid molar ratio	Reaction time (in minutes)	Fatty acid ethyl ester biodiesel yield (%)
12	12	120	62.0
12	24	120	95.5
12	48	120	99.0

As the catalyst amount was rised from 6 wt. % to 12 wt. %, the yield of ethyl ester biodiesel showed increment from 82.1 % to 96.2 % at constant ethanol: lipid molar ratio of 24 and 30-minutes reaction time. Moreover, ethyl ester biodiesel yield increased from 62 % to 99 % when ethanol: lipid ratio was raised from 12 to 48 at 12 wt. % of catalyst amount and 120-minutes reaction time. These results were closer to the results obtained for *Spirulina sp.* algal oil conversion in this study and it is not surprising because fatty acid compositions of these algal oils were similar. As in *Spirulina sp.* algal oil conversion, at same reaction conditions, commercial calcium oxide and pure alumina did not yield any ethyl ester biodiesel during transesterification of *N.Oculata* algal oil at any ethanol: lipid molar ratio and any catalyst amounts.

Moreover, ICP-MS was carried out to find the amount of calcium cation dissolved in ethyl ester biodiesel produced from algal lipids. It was found that ethyl ester biodiesel had less than 12 ppm calcium cation. Additionally, it was determined that 12 ppm calcium cations did not contribute to the homogeneous transesterification of algal lipids in the presence of ethanol at 50^{o}C and no ethyl ester formation was observed due to the leaching within experimental uncertainty.

CHAPTER 4

IMPLEMENTATION OF DIRECT MICROALGAE CONVERSION INTO BIOFUELS AND BIOCHEMICALS

The production of biofuels or biochemicals using microalgae have many advantages over conventional production methods using vegetable oils or biomasses; for instance, 1) high production rate of microalgae per hectare per year; 2) salty or waste water usage instead of using fresh water; 3) usage of coal/natural gas power plant's flue gas as carbon source; 4) usage of non-agricultural lands. Despite of these advantages, the cost of the harvesting and dewatering of microalgae biomass from growth medium accounts for 80-90% of the total production cost. Even if this is in fact the major roadblock for microalgae based industrial applications, microalgal based biofuels would still be the strong contender to the next generation fuel. For instance, the target of ExxonMobil is the production of 10,000 BBPD from microalgae by 2025 (ExxonMobil 2018). Figure 3.1 illustrates the OPEX of biofuel production from microalgae biomass for different cases which includes conventional harvesting and dewatering techniques to reach the primary target of ExxonMobil. The data used in Figure 4.1 were adapted from the study of Fasaei et al. (2018).

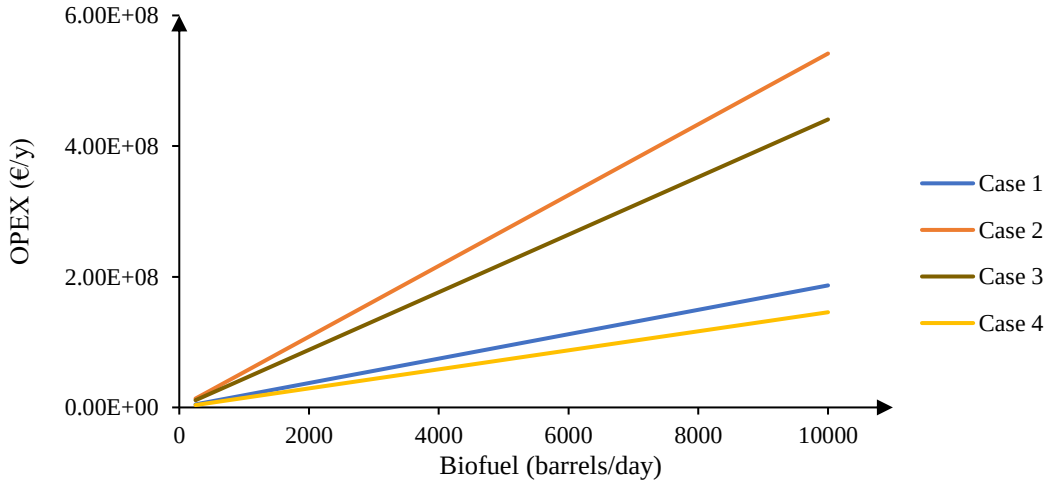

Figure 4.1. OPEX for biofuel production for microalgae with conventional techniques

In Figure 4.1, the cases were corresponded to microalgae harvesting and dewatering techniques, and they were given as: Case 1= Pressure Filter/ Centrifuge; Case 2= Membrane Filter/ Centrifuge; Case 3= Cationic Flocculation/ Centrifuge; Case 4= Chitosan Flocculation/ Centrifuge. As shown in Figure 3.1, microalgae harvesting, and dewatering processes are extremely cost and energy intensive processes to produce 10,000 barrels biofuels per day from microalgal biomass. Even if there are several research or prototype level solutions available for dewatering/harvesting of the microalgal culture media (e.g. centrifugal separation, capillary or ultrasound harvesting techniques or the hydrothermal liquefaction of microalgal medium in high pressure and temperature reactors operating at 200-350^{o}C and 50-200 atm) after dewatering to increase microalgal mass to 20%, one of the most significant step is to develop new approaches which includes the elimination of harvesting and dewatering steps to decrease OPEX in the manufacture of biofuels from microalgae. As indicated in Chapter 1, our approach differs from the current solutions available in two-aspects: 1) microalgae biomass catalytic conversion to biochemicals and biofuels is achieved in the growth medium of microalgae without harvesting and dewatering at 80^{o}C and 1 atm; 2) low pressure and temperature continuous process can be employed without using centrifugal or any other harvesting and dewatering techniques or hydrothermal liquefaction reactors. Thus, the study on direct conversion of 6 wt. % *Nannochloropsis Oculata* marine microalgae into biofuels and biochemicals without harvesting and dewatering at 80^{o}C and 1 atm was the first of its kind in the literature. Therefore, this study has great benefits to overcome especially economic disadvantage factor of microalgal biomass conversion into products. The elimination of cost and energy intensive processes as harvesting and dewatering makes this study more attractive. Therefore, to improve our approach further, we proposed a conceptual continuous process without harvesting and dewatering microalgae based on our lab scale tests to current solutions.

4.1. Industrial Application Proposal: Direct Conversion of 6 wt. % *Nannochloropsis Oculata* into biofuel and biochemicals over heterogeneous catalyst

The proposed plant was planned to be constructed in Imperial Valley, California because ExxonMobil has its algae facility (e.g. open pond system to grow microalgae) in

Imperial Valley, Ca. The proposed plant had roughly 1669 liters biofuel per year production capacity from 1064 liters algae solution per hour which had 6 wt. % *Nannochloropsis Oculata* in sea water without harvesting and dewatering.

In this process, our catalyst formulation, alumina-silicate supported nickel catalyst ($Ni/Al_2O_3/SiO_2$) was used to coat inner surface of tubes to make structured reactors, such as a tubular reactor. For this conceptual design, the best catalyst formulation which was highly active and achieved the highest microalgal biomass conversion in sea water to a extensive range of biofuels and biochemicals likehydrocarbons, triglycerides, esters and sugars among the others was selected to coat the inner surface of tubes inside the reactor. That's why, 91.5 ± 4 % microalgae conversion obtained over 10% Ni-30% Al_2O_3-70% SiO_2-H_2SO_4-SW catalyst at 80^{o}C and 1 atm in 24 h. was used in the calculation of reactor properties; e.g. size of the reactor. Also, the coating of the surface of inner tubes with this catalyst leaded to another benefit that there would be no necessity to separate or filter sodium chloride inside sea water because the presence of large amount of sodium chloride in sea water did not hinder activity/selectivity of our catalyst under our operating conditions. Besides, sodium chloride presence improved the catalytic activity in the conversion of microalgal biomass.

Moreover, solar parabolic reflectors were also used to heat thermal fluid, Therminol® 66 from 25^{o}C to 120 ^{o}C to supply necessary heat to tubular reactors to directly convert microalgae to the mixture of biofuels and biochemicals at 80^{o}C and 1 atm. All in all, to reach desired capacity, in proposed solution, approximately 108 parabolic troughs to heat Therminol® 66, 3 storage tanks, one of them was for algae storage and the others were for hot and cold Therminol® 66 storage, and 1 coated reactor to convert microalgae into biochemicals/biofuels were necessary.

Figure 4.2 represents the conceptual view of our proposed plant and production flow diagram for the conversion of *Nannochloropsis Oculata* into biofuels and biochemicals without harvesting and dewatering at 80^{o}C and 1 atm.

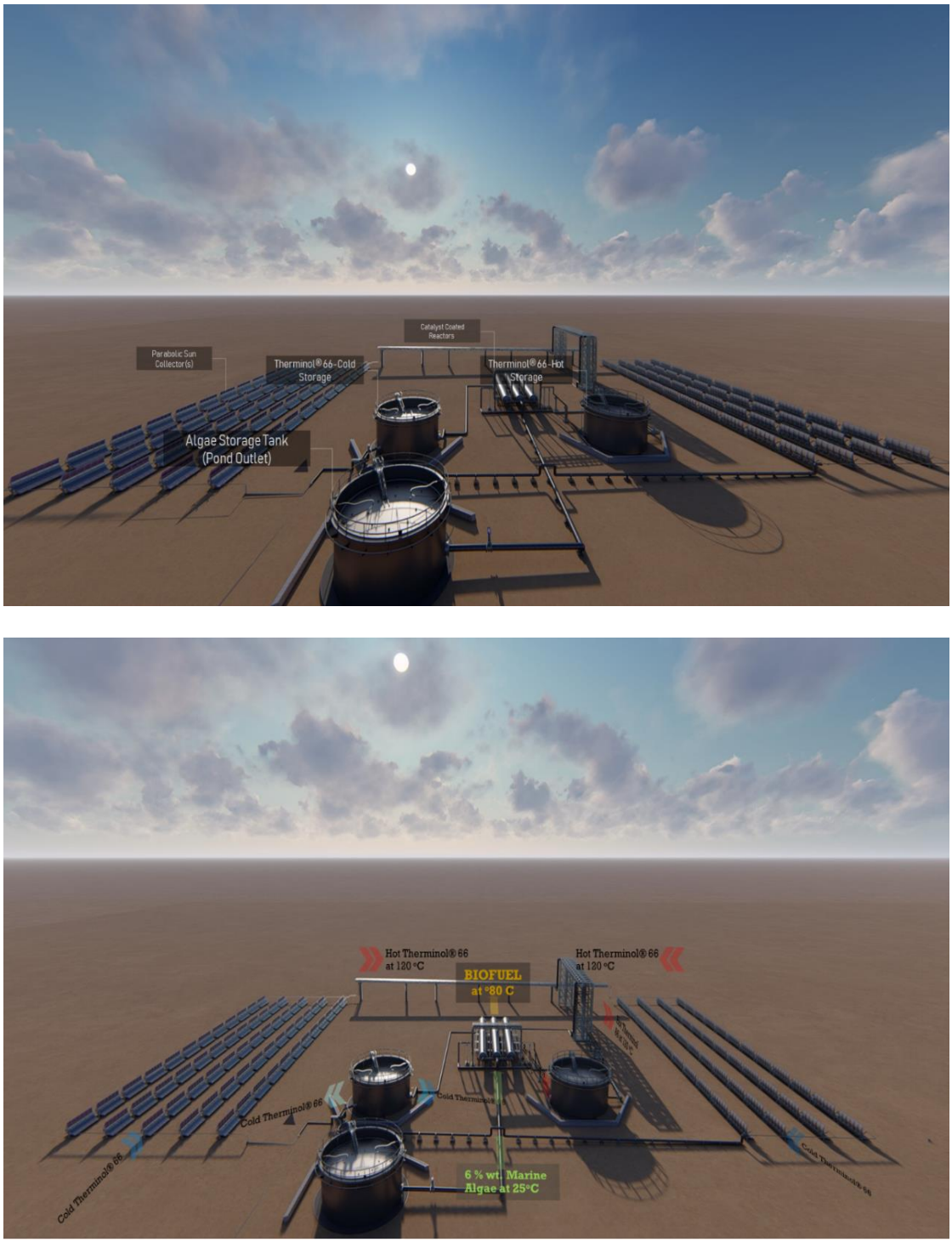

Figure 4.2. Conceptual plant lay-out of our proposal for direct conversion of microalgae into biofuels

In the proposed study, parabolic sun collectors was used to heat thermal fluid, Therminol® 66 which was used as heating medium in the tubular reactor to heat microalgae solution coming from algae storage tank at 25ºC, to 80ºC. National Renewable Energy Laboratory System Advisor Model (NREL-SAM) was used for

physical design of parabolic sun collectors. The meteorological data of Imperial Valley, CA was imported and used in the sun collector design.

Figure 4.3 illustrates the parabolic sun collectors and assembly designed via NREL SAM. The number of loops and SCA/HCA assemblies per loop were found as 9 and 12, respectively.

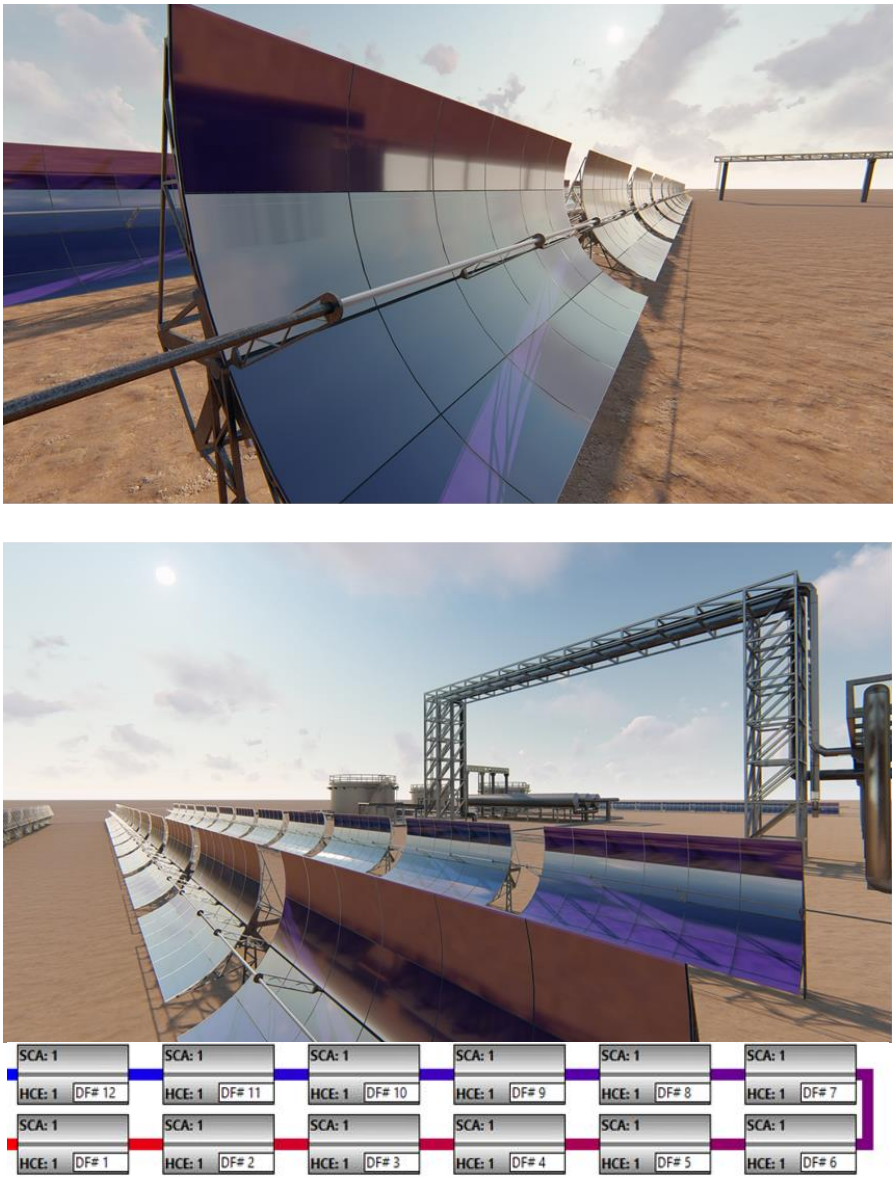

Figure 4.3. Parabolic sun collectors and assembly designed via NREL SAM

As seen in Figure 4.3, a parabolic sun collector consists of mainly two components called collector and receiver. For proposed solution, the collector was selected as SkyFuel SkyTrough while the receiver was selected as Solel UVAC 3. Default characteristics of these commercial collector and receiver defined in NREL-SAM were used in the

simulation of parabolic sun collectors. The characteristics of SkyFuel SkyTrough collector and SOLEL UVAC 3 receiver were tabulated at Table 4.1.

Table 4.1. The characteristics of receiver and collector used in parabolic sun collector design

SOLEL UVAC 3 Receiver		SkyFuel SkyTrough Collector	
Inner diameter of absorber tube (m)	0.066	Reflective aperture Area (m^2)	656
Outer diameter of absorber tube (m)	0.07	Aperture width, total structure (m)	6
Glass envelope inner diameter (m)	0.115	Length of collector assembly (m)	115
Glass envelope outer diameter (m)	0.121	Average surface -to-focus path length (m)	2.15
Absorber flow pattern/material type	Tube flow/ 304L	Piping distance between assemblies (m)	1

The main problem in the usage of parabolic sun collectors could be the continuity of the operation in every month of year and, also night period in a day. That's why, the design of parabolic sun collector and storage tanks for thermal fluid must be made to provide continuity of microalgal biomass conversion operation without being affected from change in ambient temperature in a year. Simultaneously, tubular reactor was designed in a way that heating fluid medium would enter reactor at 120ºC and leave it at 80ºC. Therefore, minimum 45939.77 kg hot oil must be stored at 120ºC for 12 hours to continue the operation at nights. To reach this aim, maximum single loop flow rate of Therminol® 66 was set as 0.088 kg per second while minimum single loop flow rate was 0.001 kg per second.

Figure 4.4 represents the mass in hot tank, total pressure drops and temperature of heating medium with respect to months in a year. As indicated in Figure 4.4, within these design specifications, intended amount of hot oil was collected at hot fluid storage tank for every 12 h with 10 % safe factor and total pressure drop altered in the acceptable range for this operation. The diameter and height of thermal fluid storage tanks were also calculated as 7.99 m and 3 m, respectively. Also, to minimize the heat loss occurring due to temperature change in night period at Imperial Valley, the tank surface could be coated

with commercial solid/solid phase change material; i.e. X120 product of PCM company. This application would decrease the operating cost of heaters inside the hot fluid storage tank which had set point at 120°C or eliminate these heaters which would reduce fixed cost of plant.

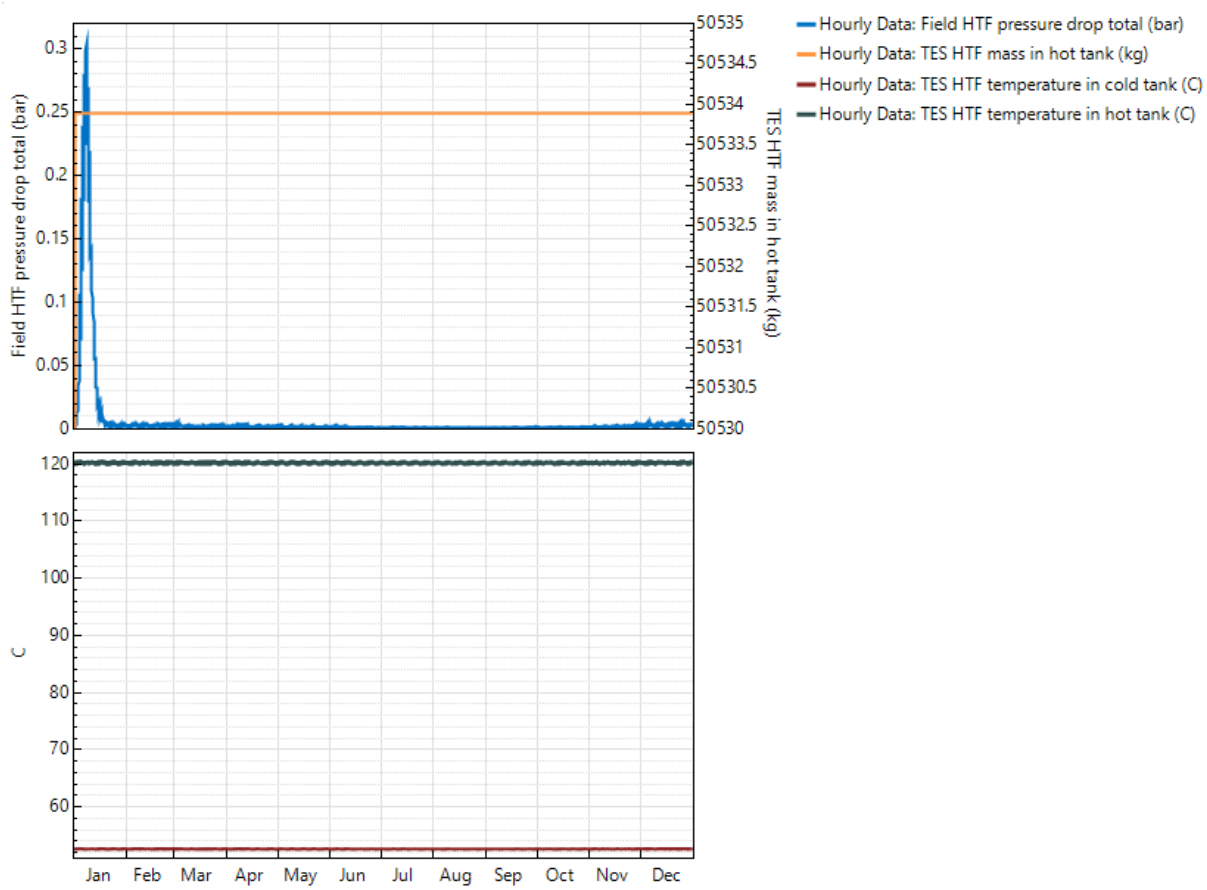

Figure 4.4. NREL System Advisor Model results of parabolic sun collectors

In proposed solution, the direct conversion of 6 wt.% *Nannochloropsis Oculata* into biofuels or biochemicals would be performed at 80°C and 1 atm for 24 h in structured tubular reactor which had coated surface with our catalyst formulation of 10% Ni-30% Al_2O_3-70% SiO_2-H_2SO_4.

Catalytic plate reactor (CPR) is one of the reactor types at which reactions are employed at catalyst coated surface. CPRs have metal plates with channels or grooves coated with catalysts. These channels or grooves can be arranged with respect to reaction behavior; exothermic or endothermic. Generally, CPRs have advantages compared to traditional reactors in a way that heat transfer rates are great and intraparticle diffusion resistance and pressure drop are at minimum (Doble and Kruthiventi 2007). There were various studies in the literature regarding catalytic plate reactor (Lakhete and Janardhanan 2014, Mundhwa et al. 2017, Mundhwa and Thurgood 2017, Zanfir and Gavriilidis 2001).

Lakhete and Janardhanan (2014) studied the modelling of methane steam reforming coupled with methane oxidation in catalytic plate reactor while Zanfir and Gavriilidis (2001) modelled catalytic ethane dehydrogenation in CPR serving great heat exchange performance. That's why, as seen in the literature, catalyst coated reactors are common whereas main challenge is to decide how to coat catalyst on substrate. There are several techniques to coat the surface of the tubes inside the reactor. These methods depend on the coating medium state: liquid or gas phase. In liquid phase coating, washcoating, electrochemical, electrophoretic deposition (EPD), spray coating, and electroless plating are the common methods to coat the surface. Chemical vapor deposition (CVD) is the method for vapor phase coating. Washcoating, in other words dip coating is the most used method in the deposition of catalyst on substrate. In this method, sols, colloids, and suspensions which includes catalyst, or its precursor could be used. Washcoating steps are given in Figure 4.5.

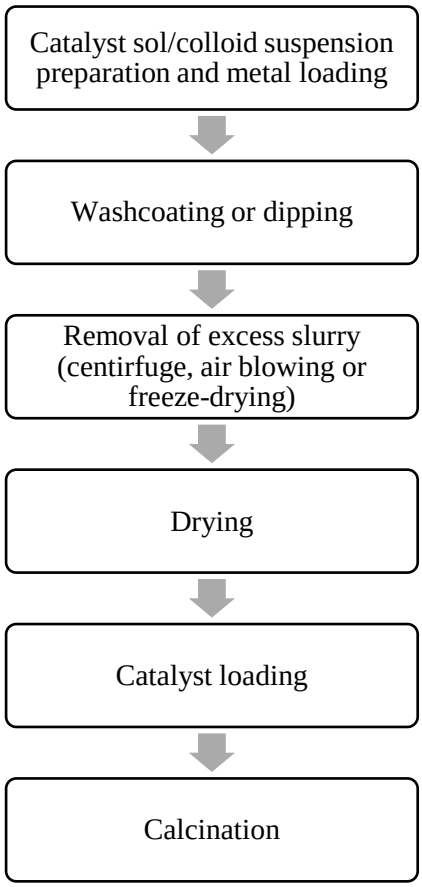

Figure 4.5. Typical steps observed in washcoating
(Source: adapted from Laguna et al. (2016))

In washcoating, the stabilization of suspension is very significant to coat the metallic surface; thus, particle size and pH must be controlled. It was recommended in

the studies that working with particle size below 10 μm was more convenient in washcoating; especially particle sizes higher than 6 μm could create problem as rapid settlement whereas reduction in size was also limited because smaller sizes could generate several problems that flocculation in suspension could be observed or thick dense layer could create mass transfer limitations (Nijhuis et al. 2001). Moreover, isoelectric point of catalyst is also significant parameter to make more stable coating in washcoating method. As known, in acidic medium, the charge of the particles is positive, and anion diffuse layer surrounds these particles to compensate the charge due to electroneutrality principle. For basic medium, vice versa is valid. Between these, at isoelectric point of the catalyst, the particles are not charged; thus, pH value must be set to a value at which repulsion of the particles are maximum to eliminate the agglomeration of the particles and improve the stability of the coating (Laguna et al. 2016). Also, another effective parameter is the viscosity of sol or suspension. To arrange rheological properties, generally binders as silica/alumina or surfactants as polyvinyl alcohol are used to make viscosity values between 10 and 20 cP and increase the coating adherence. Even if the usage of these kind of additives can increase the adherence, they can serve negative impact that they can interact with the active phase of catalyst which would be resulted in the loss of activity. That's why, these additives must be used at minimum value. In washcoating, immersion and emersion speeds which depends on the viscosity of suspension or sol, are also important. Surface tension of the suspension has to be enough to reach the channels because the suspension inlet through channels of substrates (e.g. ceramic or metallic monolith) occurs via capillarity so small surface contact angle of suspension and metallic surface is necessary to make suspension enter through the channels of substrate (Laguna et al. 2016). Also, it was reported that the coating quality, i.e. adhesion improved in substrates having smaller channel size when compared to substrates having larger size channels (Almeida et al. 2010). EPD is the other technique for charged particles deposition of stable colloidal suspension onto conductive metallic or ceramic substrate which acts as one of the oppositely charged electrode (Amrollahi et al. 2016). Particle accumulation and the layer formation on electrode occurs by electrophoretic migration (Laguna et al. 2016). Electrodes as substrate and counter electrode, suspension, and AC or DC power supply, in which DC power supply is more common, are the main parts in any EPD cell (Amrollahi et al. 2016). The thickness and adherence in EPD technique are dependent on the parameters of: current voltage, distance between electrodes, process time and properties of colloidal suspension (as particle size, dielectric constant, viscosity,

concentration of solids in suspension, zeta potential, conductivity etc.) (Laguna et al. 2016). Electrochemical deposition, also called as electrodeposition or electroplating, was another method to coat catalyst on substrate. In this method, coating is achieved by utilizing electric current. The substrate has negatively charges which acts like cathode and it is immersed into metal ionic solution. Metallic form is produced by reduction of metallic cation after reaching to cathode. The properties coating is dependent of the deposition conditions. Kim et al. (2009) studied the production of Co-Ni-P catalysts via electrodeposition. The authors investigated the effects of cathodic current density and process time on its surface morphology and its catalytic characteristics for hydrogen generation from $NaBH_4$ solution. To sound more rational, the studies of Akhtar et al. (2018), Szczygieł and Kołodziej (2005) investigated the coating of alumina supported nickel catalysts on substrate, could be significant. Akhtar et al. (2018) studied the electrodeposition of pure Ni and Ni-Al_2O_3 nanocomposites on steel surface. The authors investigated the corrosion resistance of steels electrochemically in the medium of NaCl solution and found that corrosion resistance was higher for Ni-Al_2O_3 deposition on steel surface when compared to pure nickel loading. Also, wear resistance of the composite coating was enhanced due to the embedded Al_2O_3 particles into coating. Szczygieł and Kołodziej (2005) also studied the corrosion resistance of Ni/Al_2O_3 coating deposited electrochemically. The authors found similar outcomes that corrosion resistance of Ni/Al_2O_3 was better than pure nickel coating. Electroless plating is the other technique for catalyst coating. In this method, there is no usage of electric current and the deposition of metal is performed with using a redox reaction. Muir et al. (2014) prepared Co-B catalyst supported on Ni foam by electroless plating method, which is required only one plating step for use in $NaBH_4$ hydrolysis. The authors mentioned that electroless plating method achieved higher loading efficiency than traditional multi step methods like wash coating or electroplating. Also, the prepared catalyst yielded higher activity results compared to other methods owing to the increment in Boron content and nanosheet like morphology. Spraying of the colloidal suspension is performed in spray coating. Since the shear rate is higher in spray, the viscosity of suspension is different than dip coating (Laguna et al. 2016). One of the spray coating methods is the plasma spraying in which sprayed particles are melted with the help of arc discharge produced high temperature, ~1500 K plasma. Rönkkönen et al. (2011) prepared thermal plasma-sprayed nickel catalyst for hot-gas clean up. The authors found that high adhesion on metal substrate was obtained via plasma spraying of the gibbsite and boehmite based composite powders with

hydrotalcite. Also, these coating powders could be used in the preparation of plasma sprayed metal substrate supported nickel catalyst which showed high thermal stability and mechanical strength. Schrijnemakers et al. (2009) studied mullite coating on ceramic substrate via plasma spraying method. The authors found that silica suspensions were stable at basic medium while alumina was stable at acidic pH values. Also, addition of ammonium polymethacrylate made 50 wt. % alumina and silica suspension stabilized on substrate at pH value of 10. Wu et al. (2001) deposited alumina-titania coating and alumina composite coating on 0Cr20Al7Y ferrite stainless steel (0 wt. % Cr, 20 wt. % Al, 17 % Y and 63 wt. %Fe) with NiCrAl bonding material via plasma spraying and washcoating technique. Within plasma spraying, homogenous ceramic coating with good thermal stability, high surface area, and strong adhesion on substrate were obtained.

As mentioned, there were several catalyst coating methods; whereas as known, sol-gel method was used to produce the proposed catalyst, alumina-silicate supported nickel catalyst due to the reasons of that the properties of catalyst as surface textures, porosity, variety of compositions could be tailored via sol-gel route. Therefore, sol-gel and hybrid sol-gel/suspension of dip coats could be good option to coat the surface of monoliths or tubes inside the reactor even if the coating process is no longer sol-gel method whereas hybrid of sol containing solid particles and suspension (Renken and Kiwi-Minsker 2010). For instance, Giornelli et al. (2007) prepared VOx/TiO_2 and Co/SiO_2 coating on metal plates to study oxidative dehydrogenation of propane and Fischer-Tropsch synthesis of clean fuels. For this aim, etching was initially carried out to the surface of metal as stainless steel or aluminum to increase surface roughness and -OH group concentrations for getting better primer adhesion. Then, multi-step coating was performed. The initial step was the aluminum coating including dipping of the metal plates in sol-gel medium during hydrolysis and condensation; then, drying and calcination were applied to the metal plates. Titanium oxide primer was transferred on plates and in-situ growth of porous TiO_2 layers happened. Ultimately, the metal plates were coated in $V(OiPr)_3$ in ethanol and then, calcined at 450^oC. Moreover, Truyen et al. (2006) made study regarding the coating of sol-gel catalysts which were metal nanoparticles as Rh, Ni, Pt on alumina and alumina-ceria supports, on stainless steel substrate via dip coating technique. After coating applied, the substrate initially dried at room temperature and then, calcined between 500-800^oC for 2 hours. The thickness of the coated layer was 3 μm and powders were added into sols to obtain thicker layer on substrate. The authors found that homogeneity and film quality gave optimum results when sols were

thixotropic, and the coatings yielded good thermal stability and high surface area compared to other methods.

All in all, for proposed solution, optimum catalyst coating on substrate must be developed in the future. In proposed study, either the catalyst could be coated on the tubes of tubular reactor or catalysts could be deposited on ceramic or metallic monolith via one of the given methods (e.g. hybrid sol-gel/suspension washcoating). The tubular structure reactor had 1 shell and 1000 tubes of which had 0.04 m diameter. The length of the reactor was calculated as 20 m. To reach intended capacity with 91.5 % microalgae conversion, approximately 255.4 kg catalyst was necessary for microalgae inlet of 1064.5 liter per hour. Minimum dry film thickness with calculated catalyst amount was calculated as 194.4 μm if the tubes of the reactor was coated with formulated catalyst. Figure 4.6 illustrates the schematic view of coated tube with our catalyst formulation.

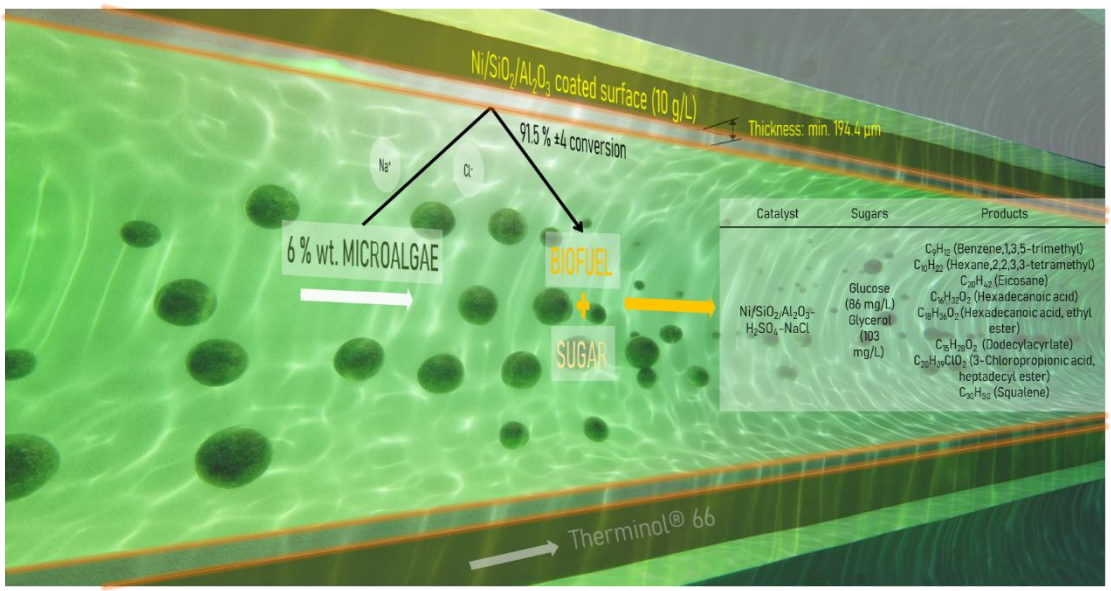

Figure 4.6. The schematic view of 10% Ni-70% SiO_2- 30% Al_2O_3-H_2SO_4 coated tube inside tubular rector

Alternatively, ceramic or metallic monoliths could be coated in a way that these monoliths could be like hot-plug. The tubes would be divided into 20 segments (each of segment would be 1 meter), and the monoliths having 1-meter length, 4-centimeter diameter would be prepared with proper coating method. When any segment or all segments lost their activity, new one could be replaced easily without damaging the tubes of the reactor. Figure 4.7 illustrates the conceptual view of 10% Ni-30% Al_2O_3-70% SiO_2-H_2SO_4 catalyst coated monolith.

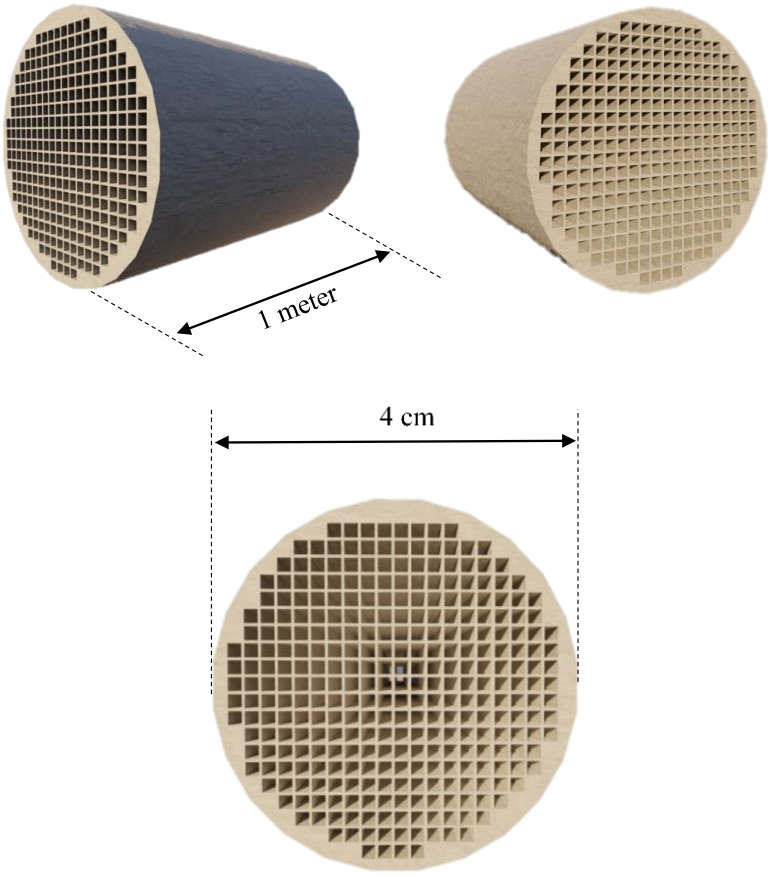

Figure 4.7. Conceptual illustration of 10 % Ni- 70% SiO_2- 30 % Al_2O_3- H_2SO_4 catalyst coated monolith

As an alternative to catalyst coated hot-plug monolith in tubular structured reactor or directly coated tubular reactor, continuous stirred reactor (CSTR) could be replaced in way that agitator of CSTR was coated with 10% Ni-30% Al_2O_3-70% SiO_2-H_2SO_4 catalyst. Figure 4.8 showed the conceptual view of CSTR for direct conversion of 6 wt. % *Nannochloropsis Oculata* into biofuels and biochemicals. The volume of the CSTR would be ~26 m^3 with 4-meter diameter and 2-meter length so the capacity of the operation could easily be increased by increasing CSTR number.

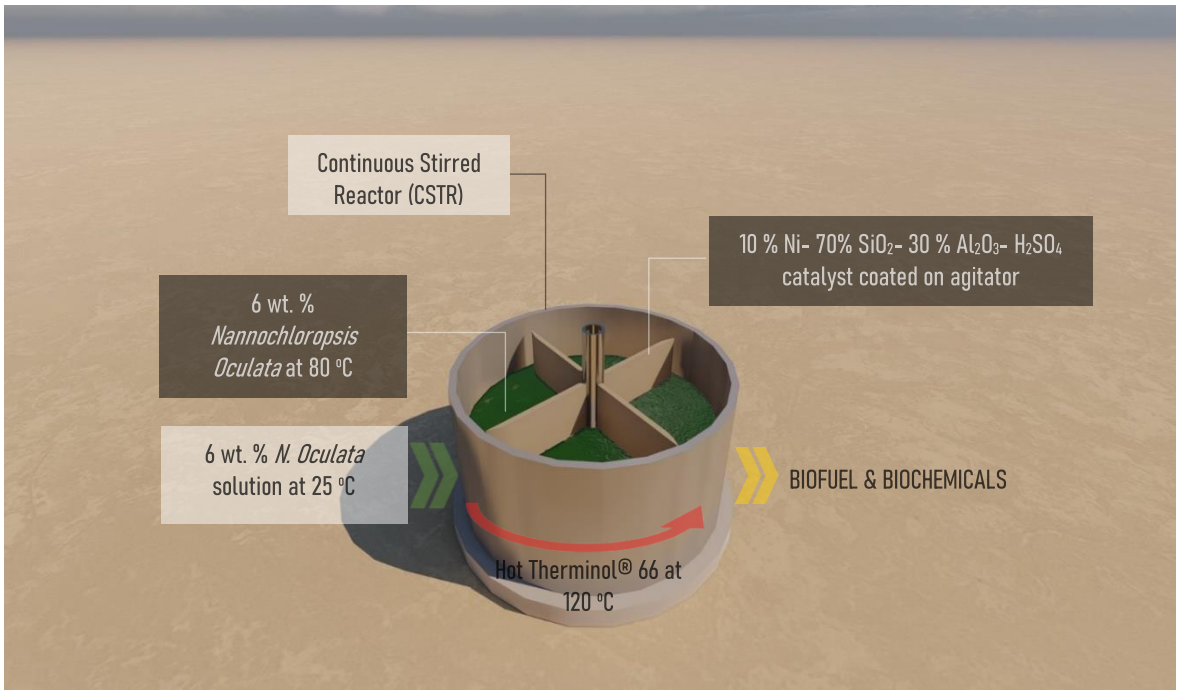

Figure 4.8. Conceptual view of CSTR in direct conversion of 6 wt. % *Nannochloropsis Oculata*

Moreover, since the exit stream of the tubular reactors would contain a mixture of seawater and soluble/insoluble compounds, liquid-liquid extraction technology could be used to separate biofuels and biochemicals from seawater and this could be followed by reforming and/or fermentation steps to upgrade biofuels and biochemicals to transport fuels or commodity chemicals in downstream processes in a refinery.

CHAPTER 5

CONCLUSION

This study dealt with the conversion of microalgae in growth medium and/or its lipids into biofuels and biochemicals over heterogeneous catalysts. Initially, direct conversion of 6 wt. % *Nannochloropsis Oculata* into biofuels and biochemicals without harvesting and dewatering was studied at 80^{o}C and 1 atm over alumina-silicate supported nickel catalyst. For this aim, 10% Ni -30% Al_2O_3-70% SiO_2 catalyst was prepared via single step sol-gel method by using the acids of hydrochloric acid, sulfuric acid, and nitric acid. The study showed that 10% Ni -30% Al_2O_3-70% SiO_2 catalyst prepared with sulfuric acid yielded ~74 % conversion of *N. Oculata* in seawater at 80^{o}C and 1 atm. Also, microalgae conversion was reached to 91.5% from 74% by treating this catalyst with 35 g NaCl per kg water. This high conversion was assigned to the presence of nickel, total acidity which was 25.1 μmol/g, and acidic strength obtained in the range of 130-380 ^{o} C. Moreover, a new industrial application model was proposed for direct conversion of 6 wt. % *N. Oculata* without harvesting and dewatering over alumina-silicate supported nickel catalyst. Initially, Therminol ® 66 which was used to heat microalgae solution inside the reactor, was primarily heated to 120^{o}C via 108 parabolic sun collectors. In reactor section, either tubes of tubular structured reactor which had 20-meter length and 1000 tubes each of which had 4 cm diameter, could be coated with the catalyst formulation by using conventional coating techniques as washcoating, electrophoretic deposition or 1-meter pluggable coated monoliths could be prepared. Also, in direct conversion of 6 wt. % *N. Oculata*, continuous stirred reactor having ~26 m^3 volume with 4-meter diameter and 2-meter length was used as the other option in a way that agitator of the reactor was coated with prepared alumina-silicate nickel catalyst.

Also, transesterification of *Spirulina sp.* and *N. Oculata* microalgal lipids into fatty acid ethyl ester biodiesel was studied over 60 % CaO on alumina catalyst prepared by single step sol-gel method, at 50 ^{o}C and 1 atm. It was found that 90-99 % *Spirulina sp.* and *N. Oculata* algal lipids conversion was obtained over 60 % CaO on alumina catalyst under ethanol: lipid ratios of 24 and 48 in 30 min. at 50^{o}C and 1 atm. However, there were no conversion obtained in the presence of commercial CaO, Al_2O_3, Ca $(OH)_2$,

and $CaCO_3$ catalysts under the same reaction conditions. Even if the basicity of the pure catalysts as CaO and Al_2O_3 was higher, basic strength of 60% CaO on alumina catalyst was weaker compared to these catalysts. On the other hand, glycerolysis of triacylglycerol was observed in series with reverse of triacylglycerol transesterification at relatively high ethanol: lipid molar ratios and the reaction time of 60 minutes.

REFERENCES

Akhtar, Khalida, Zia Ullah Khan, Muhammad Gul, Naila Zubair, and Syed Sajjad Ali Shah. 2018. "Electrodeposition and characterization of Ni-Al_2O_3 nanocomposite coatings on steel." Journal of Materials Engineering and Performance 27 (6):2827-2837.

Al-Dhabi, Naif Abdullah, and Mariadhas Valan Arasu. 2016. "Quantification of phytochemicals from commercial *Spirulina* products and their antioxidant activities." Evidence-Based Complementary and Alternative Medicine 2016:7631864.

Alamu, O. J., M. A. Waheed, and S. O. Jekayinfa. 2008. "Effect of ethanol–palm kernel oil ratio on alkali-catalyzed biodiesel yield." Fuel 87 (8):1529-1533.

Almeida, L. C., F. J. Echave, O. Sanz, M. A. Centeno, J. A. Odriozola, and M. Montes. 2010. "Washcoating of metallic monoliths and microchannel reactors." In *Studies in Surface Science and Catalysis*, edited by E. M. Gaigneaux, M. Devillers, S. Hermans, P. A. Jacobs, J. A. Martens and P. Ruiz, 25-33. Elsevier.

Amrollahi, Pouya, Jerzy S. Krasinski, Ranji Vaidyanathan, Lobat Tayebi, and Daryoosh Vashaee. 2016. "Electrophoretic deposition (EPD): Fundamentals and applications from nano- to microscale structures." In *Handbook of Nanoelectrochemistry: Electrochemical Synthesis Methods, Properties, and Characterization Techniques*, edited by Mahmood Aliofkhazraei and Abdel Salam Hamdy Makhlouf, 561-591. Cham: Springer International Publishing.

Antia, N. J., T. Bisalputra, J. Y. Cheng, and J. P. Kalley. 1975. "Pigment and cytological evidence for reclassification of *Nannochloris Oculata* and *Monaliantus Salina* in the eustigmatophyceae." Journal of Phycology 11 (3):339-343.

Arnold, Alexandre A., Bertrand Genard, Francesca Zito, Réjean Tremblay, Dror E. Warschawski, and Isabelle Marcotte. 2015. "Identification of lipid and saccharide constituents of whole microalgal cells by 13C solid-state NMR." Biochimica et Biophysica Acta (BBA) - Biomembranes 1848 (1, Part B):369-377.

Ballivet, D., D. Barthomeuf, and P. Pichat. 1972. "Acidic sites on silica-alumina catalysts with reduced aluminium content. Infra-red and thermogravimetric studies." Journal of the Chemical Society, Faraday Transactions 1: Physical Chemistry in Condensed Phases 68 (0):1712-1719.

Bart, Jan C. J., Natale Palmeri, and Stefano Cavallaro. 2010. "Biodiesel science and technology : from soil to oil."

Batan, Liaw Y., Gregory D. Graff, and Thomas H. Bradley. 2016. "Techno-economic and Monte Carlo probabilistic analysis of microalgae biofuel production system." Bioresource Technology 219:45-52.

Benbenek, Stanislaw, Elżbieta Fedoryńska, and Piotr Winiarek. 1993. "Investigation of the acidity of Ni/Al_2O_3 and $Ni/SiO_2{-}Al_2O_3$ catalysts." Reaction Kinetics and Catalysis Letters 51 (1):189-195.

Bourne, Kenneth H., F. R. Cannings, and R. C. Pitkethly. 1970. "Structure and properties of acid sites in a mixed-oxide system. I. Synthesis and infrared characterization." The Journal of Physical Chemistry 74 (10):2197-2205.

Brunner, E., H. Pfeifer, A. Auroux, J. Lercher, A. Jentys, A. Brait, E. Garrone, and F. Fajula. 2008. *Acidity and basicity*. Leipzig: Springer- Verlag Berlin Heidelberg.

Chambon, Flora, Franck Rataboul, Catherine Pinel, Amandine Cabiac, Emmanuelle Guillon, and Nadine Essayem. 2011. "Cellulose hydrothermal conversion promoted by heterogeneous Brønsted and Lewis acids: Remarkable efficiency of solid Lewis acids to produce lactic acid." Applied Catalysis B: Environmental 105 (1):171-181.

Chen, Huihui, Dong Zhou, Gang Luo, Shicheng Zhang, and Jianmin Chen. 2015. "Macroalgae for biofuels production: Progress and perspectives." Renewable and Sustainable Energy Reviews 47:427-437.

Chisti, Yusuf. 2007. "Biodiesel from microalgae." Biotechnology Advances 25 (3):294-306.

Chisti, Yusuf. 2008. "Biodiesel from microalgae beats bioethanol." Trends in Biotechnology 26 (3):126-131.

Choi, Sun- A., Joo-Young Jung, Kyochan Kim, Jin-Suk Lee, Jong-Hee Kwon, Seung Wook Kim, Ji-Won Yang, and Ji-Yeon Park. 2014. "Acid-catalyzed hot-water extraction of docosahexaenoic acid (DHA)-rich lipids from *Aurantiochytrium* sp. KRS101." Bioresource Technology 161:469-472.

Chu, Yueying, Zhiwu Yu, Anmin Zheng, Hanjun Fang, Hailu Zhang, Shing-Jong Huang, Shang-Bin Liu, and Feng Deng. 2011. "Acidic strengths of Brønsted and Lewis acid sites in solid acids scaled by 31P NMR chemical shifts of adsorbed trimethylphosphine." The Journal of Physical Chemistry C 115 (15):7660-7667.

Cullity, B. D. 1978. *Elements of x-ray diffraction*. Reading, MA: Addison-Wesley Publishing Company, Inc.

Doble, Mukesh, and Anil Kumar Kruthiventi. 2007. "Green chemistry and engineering."

Duan, Peigao, and Phillip E. Savage. 2011. "Hydrothermal liquefaction of a microalga with heterogeneous catalysts." Industrial & Engineering Chemistry Research 50 (1):52-61.

Durmaz, Yaşar. 2007. "Vitamin E (α-tocopherol) production by the marine microalgae *Nannochloropsis oculata* (*Eustigmatophyceae*) in nitrogen limitation." Aquaculture 272 (1):717-722.

EU. 2009. "Directive 2009/28/EC of the European Parliament and of the Council of 23 April 2009 on the promotion of the use of energy from renewable sources " Official Journal of the European Union (EU):16-62.

ExxonMobil. 2018. "Advanced biofuels and algae research." Exxon Mobil Corporation.

Fasaei, F., J. H. Bitter, P. M. Slegers, and A. J. B. van Boxtel. 2018. "Techno-economic evaluation of microalgae harvesting and dewatering systems." Algal Research 31:347-362.

Feng, Libang, Hui Li, Yongfeng Song, and Yulong Wang. 2010. "Formation process of a strong water-repellent alumina surface by the sol–gel method." Applied Surface Science 256 (10):3191-3196.

Giornelli, T., A. Löfberg, L. Guillou, S. Paul, V. Le Courtois, and E. Bordes-Richard. 2007. "Catalytic wall reactor: Catalytic coatings of stainless steel by VOx/TiO_2 and Co/SiO_2 catalysts." Catalysis Today 128 (3):201-207.

Grabowski, W., and Malinows.S. 1973. "Interpretation of isobutane transformations in presence of gels containing sodium by means of quantum chemistry methods." Bulletin De L Academie Polonaise Des Sciences-Serie Des Sciences Chimiques 21 (6):465-470.

Gruene, Philipp, Anuta G. Belova, Tuncel M. Yegulalp, Robert J. Farrauto, and Marco J. Castaldi. 2011. "Dispersed calcium oxide as a reversible and efficient CO_2−sorbent at intermediate temperatures." Industrial & Engineering Chemistry Research 50 (7):4042-4049.

Guldhe, Abhishek, Carla V. R. Moura, Poonam Singh, Ismail Rawat, Edmilson M. Moura, Yogesh Sharma, and Faizal Bux. 2017. "Conversion of microalgal lipids to biodiesel using chromium-aluminum mixed oxide as a heterogeneous solid acid catalyst." Renewable Energy 105:175-182.

Hájek, Martin, František Skopal, Aleš Vávra, and Jaroslav Kocík. 2017. "Transesterification of rapeseed oil by butanol and separation of butyl ester." Journal of Cleaner Production 155:28-33.

Harun, Razif, and Michael K. Danquah. 2011. "Influence of acid pre-treatment on microalgal biomass for bioethanol production." Process Biochemistry 46 (1):304-309.

Heimann, Kirsten, and Roger Huerlimann. 2015. "Chapter 3 - microalgal classification: Major classes and genera of commercial microalgal species." In *Handbook of Marine Microalgae*, edited by Se-Kwon Kim, 25-41. Boston: Academic Press.

Ho, Shih-Hsin, Po-Jen Li, Chen-Chun Liu, and Jo-Shu Chang. 2013. "Bioprocess development on microalgae-based CO_2 fixation and bioethanol production using *Scenedesmus obliquus* CNW-N." Bioresource Technology 145:142-149.

Hongsiri, Wijittra, Bart Danon, and Wiebren de Jong. 2015. "The effects of combined catalysis of oxalic acid and seawater on the kinetics of xylose and arabinose dehydration to furfural." International Journal of Energy and Environmental Engineering 6 (1):21-30.

Hossain, A. B. M. Sharif, Aishah Salleh, Amru Nasrulhaq Boyce, chowdhury Partha, and Mohd Husri. 2008. "Biodiesel fuel production from algae as renewable energy." American Journal of Biochemistry and Biotechnology.

Huang, Yao-Bing, and Yao Fu. 2013. "Hydrolysis of cellulose to glucose by solid acid catalysts." Green Chemistry 15 (5):1095-1111.

JCPDS-ICDD. 2000. "PDF-2 Database." International Centre for Diffraction Data, Pennsylvania.

Kesic, Zeljka, Lukić Ivana, Miodrag Zdujić, Ljiljana Mojovic, and Dejan Skala. 2016. "Calcium oxide based catalysts for biodiesel production: A review." Chemical Industry and Chemical Engineering Quarterly 22:10-10.

Kim, Deog-Ryung, Keun-Woo Cho, Yun-Il Choi, and Chan-Jin Park. 2009. "Fabrication of porous Co–Ni–P catalysts by electrodeposition and their catalytic characteristics for the generation of hydrogen from an alkaline $NaBH_4$ solution." International Journal of Hydrogen Energy 34 (6):2622-2630.

Kobayashi, Hirokazu, Tasuku Komanoya , Kenji Hara, and Atsushi Fukuoka. 2010. "Water-tolerant mesoporous-carbon-supported ruthenium catalysts for the hydrolysis of cellulose to glucose." ChemSusChem 3 (4):440-443.

Kótai, László, János Szépvölgyi, János Bozi, István Gács, Szabolcs Bálin, Agnes Gomory, Andras Angyal, Janos Balogh, Li Zhibin, Moutong Chen, Chen Wang, and Baiquan Chen. 2011. "An integrated waste-free biomass utilization system for an increased productivity of biofuel and bioenergy." In.

Kumar, Dipesh, Bhaskar Singh, Ayan Banerjee, and Sandeep Chatterjee. 2018. "Cement wastes as transesterification catalysts for the production of biodiesel from Karanja oil." Journal of Cleaner Production 183:26-34.

Kumar, Manish, and Kalyan Gayen. 2011. "Developments in biobutanol production: New insights." Applied Energy 88 (6):1999-2012.

Laguna, O. H., M. I. Domínguez, M. A. Centeno, and J. A. Odriozola. 2016. "Chapter 4 - Catalysts on metallic surfaces: Monoliths and microreactors." In *New Materials for Catalytic Applications*, edited by Vasile I. Parvulescu and Erhard Kemnitz, 81-120. Amsterdam: Elsevier.

Lakhete, Prashil, and Vinod M. Janardhanan. 2014. "Modeling process intensified catalytic plate reactor for synthesis gas production." Chemical Engineering Science 110:13-19.

Lam, Man Kee, and Keat Teong Lee. 2011. "Mixed methanol–ethanol technology to produce greener biodiesel from waste cooking oil: A breakthrough for $SO_4^{2-}/SnO^{2-}SiO_2$ catalyst." Fuel Processing Technology 92 (8):1639-1645.

Leadbeater, Nicholas E., T. Michael Barnard, and Lauren M. Stencel. 2008. "Batch and continuous-flow preparation of biodiesel derived from butanol and facilitated by microwave heating." Energy & Fuels 22 (3):2005-2008.

Lee, Inmok, Lawrence A. Johnson, and Earl G. Hammond. 1995. "Use of branched-chain esters to reduce the crystallization temperature of biodiesel." Journal of the American Oil Chemists' Society 72 (10):1155-1160.

Leggieri, Patrick A., Michael Senra, and Lindsay Soh. 2018. "Cloud point and crystallization in fatty acid ethyl ester biodiesel mixtures with and without additives." Fuel 222:243-249.

Li, Eugena, Zhi Ping Xu, and Victor Rudolph. 2009. "MgCoAl–LDH derived heterogeneous catalysts for the ethanol transesterification of canola oil to biodiesel." Applied Catalysis B: Environmental 88 (1):42-49.

Li, Xiufeng, Han Xu, and Qingyu Wu. 2007. "Large-scale biodiesel production from microalga *Chlorella protothecoides* through heterotrophic cultivation in bioreactors." Biotechnology and Bioengineering 98 (4):764-771.

Liu, Xuejun, Xianglan Piao, Yujun Wang, and Shenlin Zhu. 2008. "Liquid–liquid equilibrium for systems of (fatty acid ethyl esters + ethanol + soybean oil and fatty acid ethyl esters + ethanol + glycerol)." Journal of Chemical & Engineering Data 53 (2):359-362.

Machado, Alex Barreto, Yurany Camacho Ardila, Leonardo Hadlich de Oliveira, Martín Aznar, and Maria Regina Wolf Maciel. 2011. "Liquid−liquid equilibrium study in ternary castor oil biodiesel + ethanol + glycerol and quaternary castor oil biodiesel + ethanol + glycerol + NaOH systems at (298.2 and 333.2) K." Journal of Chemical & Engineering Data 56 (5):2196-2201.

Marczewski, Marek, Agnieszka Jakubiak, Hanna Marczewska, Anna Frydrych, Małgorzata Gontarz, and Anna Śnieguła. 2004. "Acidity of sulfated oxides: Al_2O_3, TiO_2 and SiO_2. Application of test reactions." Physical Chemistry Chemical Physics 6 (9):2513-2522.

Meher, L. C., D. Vidya Sagar, and S. N. Naik. 2006. "Technical aspects of biodiesel production by transesterification—a review." Renewable and Sustainable Energy Reviews 10 (3):248-268.

Miao, Xiaoling, and Qingyu Wu. 2006. "Biodiesel production from heterotrophic microalgal oil." Bioresource Technology 97 (6):841-846.

Mohammad, Zangouei, Abdolsamad Moghaddam, and Arasteh Mehdi. 2010. "The influence of nickel loading on reducibility of NiO/Al_2O_3 catalysts synthesized by sol-gel method." Chemical Engineering Research Bulletin 14.

Muir, Sean S., Zhigang Chen, Barry J. Wood, Lianzhou Wang, G. Q. Lu, and Xiangdong Yao. 2014. "New electroless plating method for preparation of highly active Co–B catalysts for $NaBH_4$ hydrolysis." International Journal of Hydrogen Energy 39 (1):414-425.

Mundhwa, Mayur, Rajesh D. Parmar, and Christopher P. Thurgood. 2017. "A comparative parametric study of a catalytic plate methane reformer coated with segmented and continuous layers of combustion catalyst for hydrogen production." Journal of Power Sources 344:85-102.

Mundhwa, Mayur, and Christopher P. Thurgood. 2017. "Numerical study of methane steam reforming and methane combustion over the segmented and continuously coated layers of catalysts in a plate reactor." Fuel Processing Technology 158:57-72.

Nijhuis, T. Alexander, Annemarie E. W. Beers, Theo Vergunst, Ingrid Hoek, Freek Kapteijn, and Jacob A. Moulijn. 2001. "Preparation of monolithic catalysts." Catalysis Reviews 43 (4):345-380.

Nimcevic, Dragan, Rupert Puntigam, Manfred Wörgetter, and J. Richard Gapes. 2000. "Preparation of rapeseed oil esters of lower aliphatic alcohols." Journal of the American Oil Chemists' Society 77 (3):275-280.

Ozdogru, Bertan. 2017. "Biofuels production using canola oil over heterogeneous catalysts." Izmir Institute of Technology.

Park, Charnho, Ja Hyun Lee, Xiaoguang Yang, Hah Young Yoo, Ju Hun Lee, Soo Kweon Lee, and Seung Wook Kim. 2016. "Enhancement of hydrolysis of *Chlorella vulgaris* by hydrochloric acid." Bioprocess and Biosystems Engineering 39 (6):1015-1021.

Philipp, Rosemarie, and Kaoru Fujimoto. 1992. "FTIR spectroscopic study of carbon dioxide adsorption/desorption on magnesia/calcium oxide catalysts." The Journal of Physical Chemistry 96 (22):9035-9038.

Prabandono, Kurniadhi, and Sarmidi Amin. 2015. "Chapter 10 - Biofuel production from microalgae." In *Handbook of Marine Microalgae*, edited by Se-Kwon Kim, 145-158. Boston: Academic Press.

Renken, Albert, and Lioubov Kiwi-Minsker. 2010. "Chapter 2 - Microstructured catalytic reactors." In *Advances in Catalysis*, edited by Bruce C. Gates and Helmut Knözinger, 47-122. Academic Press.

Rittmann, Bruce E. 2008. "Opportunities for renewable bioenergy using microorganisms." Biotechnology and Bioengineering 100 (2):203-212.

Rönkkönen, Hanne, Kristina Klemkaitė, Alexander Khinsky, Arūnas Baltušnikas, Pekka Simell, Matti Reinikainen, Outi Krause, and Marita Niemelä. 2011. "Thermal plasma-sprayed nickel catalysts in the clean-up of biomass gasification gas." Fuel 90 (3):1076-1089.

Santillan-Jimenez, Eduardo, Tonya Morgan, Joseph Lacny, Susanta Mohapatra, and Mark Crocker. 2013. "Catalytic deoxygenation of triglycerides and fatty acids to hydrocarbons over carbon-supported nickel." Fuel 103:1010-1017.

Schenk, Peer M., Skye R. Thomas-Hall, Evan Stephens, Ute C. Marx, Jan H. Mussgnug, Clemens Posten, Olaf Kruse, and Ben Hankamer. 2008. "Second generation biofuels: High-efficiency microalgae for biodiesel production." BioEnergy Research 1 (1):20-43.

Schrijnemakers, A., S. André, G. Lumay, N. Vandewalle, F. Boschini, R. Cloots, and B. Vertruyen. 2009. "Mullite coatings on ceramic substrates: Stabilisation of Al_2O_3–SiO_2 suspensions for spray drying of composite granules suitable for reactive plasma spraying." Journal of the European Ceramic Society 29 (11):2169-2175.

Shimizu, Ken-ichi, Hirotake Furukawa, Nobusuke Kobayashi, Yoshinori Itaya, and Atsushi Satsuma. 2009. "Effects of Brønsted and Lewis acidities on activity and selectivity of heteropolyacid-based catalysts for hydrolysis of cellobiose and cellulose." Green Chemistry 11 (10):1627-1632.

Shrotri, Abhijit, Akshat Tanksale, Jorge Norberto Beltramini, Hanmant Gurav, and Satyanarayana V. Chilukuri. 2012. "Conversion of cellulose to polyols over promoted nickel catalysts." Catalysis Science & Technology 2 (9):1852-1858.

Stanislaus, A., M. Absi-Halabi, and K. Al-Dolama. 1989. "Effect of nickel on the surface acidity of γ-alumina and alumina-supported nickel—molybdenum hydrotreating catalysts." Applied Catalysis 50 (1):237-245.

Szczepanska, S. 1975. "Studies on sorptive and catalytic properties of alumina-silica gels containing sodium ions .1. Adsorption of NH_3 and dehydration of methanol." Bulletin De L Academie Polonaise Des Sciences-Serie Des Sciences Chimiques 23 (8):649-654.

Szczygieł, Bogdan, and Małgorzata Kołodziej. 2005. "Composite Ni/Al_2O_3 coatings and their corrosion resistance." Electrochimica Acta 50 (20):4188-4195.

Tagusagawa, Caio, Atsushi Takagaki, Ai Iguchi, Kazuhiro Takanabe, Junko N. Kondo, Kohki Ebitani, Shigenobu Hayashi, Takashi Tatsumi, and Kazunari Domen. 2010. "Highly active mesoporous Nb–W oxide solid-acid catalyst." Angewandte Chemie International Edition 49 (6):1128-1132.

Tamele, M. W. 1950. "Chemistry of the surface and the activity of alumina-silica cracking catalyst." Discussions of the Faraday Society 8 (0):270-279.

Tanabe, Kozo. 1989. *New solid acids and bases : Their catalytic properties*. Amsterdam: Elsevier.

Teo, Siow Hwa, Aminul Islam, Talal Yusaf, and Yun Hin Taufiq-Yap. 2014. "Transesterification of *Nannochloropsis oculata* microalga's oil to biodiesel using calcium methoxide catalyst." Energy 78:63-71.

Thomas, Charles L. 1949. "Chemistry of cracking catalysts." Industrial & Engineering Chemistry 41 (11):2564-2573.

Thomas, J. M., and W. J. Thomas. 2015. "Principles and practice of heterogeneous catalysis."

Truyen, Dimitri, Matthieu Courty, Pierre Alphonse, and Florence Ansart. 2006. "Catalytic coatings on stainless steel prepared by sol–gel route." Thin Solid Films 495 (1):257-261.

Tsukahara, Kenichiro, and Shigeki Sawayama. 2005. "Liquid fuel production using microalgae." Journal of the Japan Petroleum Institute 48 (5):251-259.

Umdu, Emin Selahattin. 2008. "Methyl ester production from vegetable oils on heterogeneous basic catalysts." Izmir Institute of Technology.

Umdu, Emin Selahattin. 2012. "Hydrogen production from biomass on structured catalysts." Izmir Institute of Technology.

Umdu, Emin Selahattin, Mert Tuncer, and Erol Seker. 2009. "Transesterification of Nannochloropsis oculata microalga's lipid to biodiesel on Al_2O_3 supported CaO and MgO catalysts." Bioresource Technology 100 (11):2828-2831.

Viswanathan, V. N., and L. M. Yeddanapalli. 1974. "Surface properties of impregnated mixed oxide catalysts." Zeitschrift für anorganische und allgemeine Chemie 407 (1):98-108.

Volkman, John K., Malcolm R. Brown, Graeme A. Dunstan, and S. W. Jeffrey. 1993. "The biochemical composition of marine microalgae from the class *Eustigmatophyceae*." Journal of Phycology 29 (1):69-78.

Ward, John W., and Rowland C. Hansford. 1969. "The nature of active sites on zeolites: IX. Sodium hydrogen zeolite." Journal of Catalysis 13 (4):364-372.

Wright, J. D., and Nico A. J. M. Sommerdijk. 2001. "Sol-gel materials : Chemistry and applications."

Wu, Xiaodong, Duan Weng, Luhua Xu, and Hengde Li. 2001. "Structure and performance of γ-alumina washcoat deposited by plasma spraying." Surface and Coatings Technology 145 (1):226-232.

Xu, Yufu, Xiaojing Zheng, Huiqiang Yu, and Xianguo Hu. 2014. "Hydrothermal liquefaction of *Chlorella pyrenoidosa* for bio-oil production over Ce/HZSM-5." Bioresource Technology 156:1-5.

Yalman, Emir. 2012. "Biodiesel production from safflower using heterogeneous CaO based catalysts." Izmir Institute of Technology.

Yusoff, Mohamad Firdaus Mohamad, Xuebing Xu, and Zheng Guo. 2014. "Comparison of fatty acid methyl and ethyl esters as biodiesel base stock: A review on

processing and production requirements." Journal of the American Oil Chemists' Society 91 (4):525-531.

Zachariadis, Theodoros, and Nikos Kouvaritakis. 2003. "Long-term outlook of energy use and CO_2 emissions from transport in Central and Eastern Europe." Energy Policy 31 (8):759-773.

Zaki, Mohamed I., Helmut Knözinger, Bernd Tesche, and Gamal A. H. Mekhemer. 2006. "Influence of phosphonation and phosphation on surface acid–base and morphological properties of CaO as investigated by in situ FTIR spectroscopy and electron microscopy." Journal of Colloid and Interface Science 303 (1):9-17.

Zanfir, M., and A. Gavriilidis. 2001. "Modelling of a catalytic plate reactor for dehydrogenation–combustion coupling." Chemical Engineering Science 56 (8):2671-2683.

APPENDIX A

ACIDITY MEASUREMENTS OF THE CATALYSTS

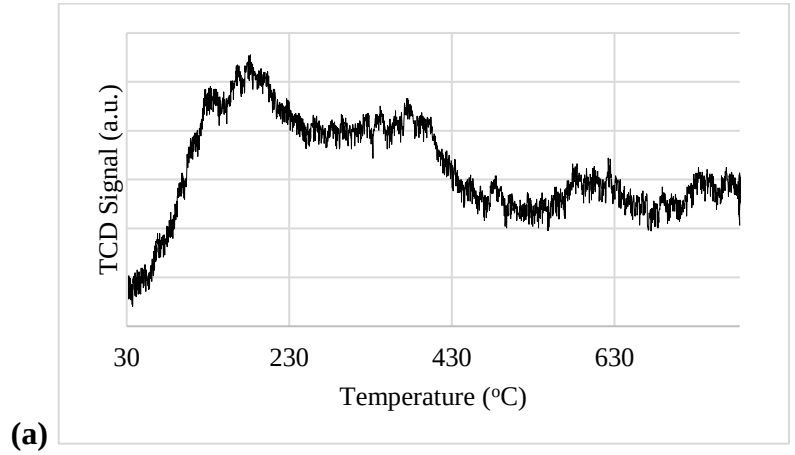

(a)

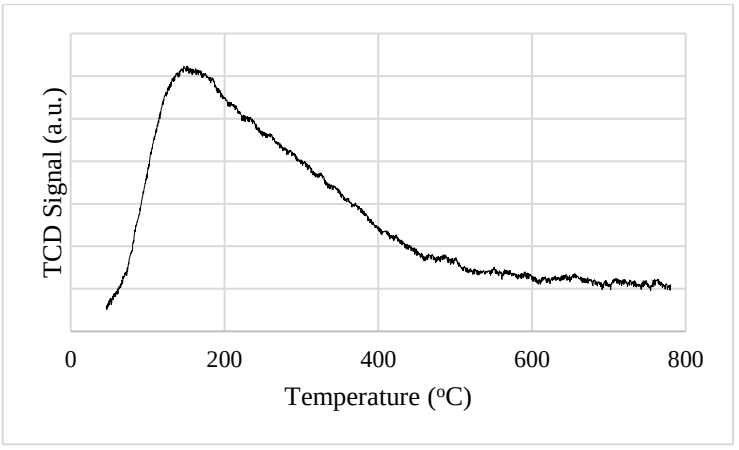

(b)

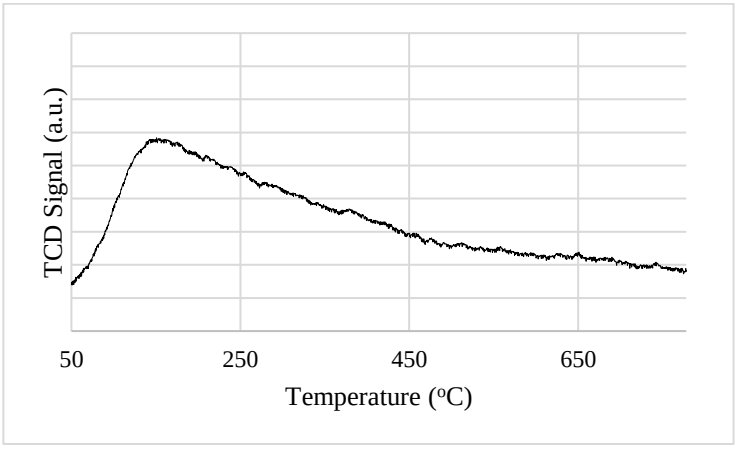

(c)

Figure A.1. NH_3-TPD Profiles of (a) 10% Ni-30% Al_2O_3-70% SiO_2-H_2SO_4 (b) 10% Ni-30% Al_2O_3-70% SiO_2-HNO_3 (c) 10% Ni-30% Al_2O_3-70% SiO_2-HCl

APPENDIX B

CHEMICAL STRUCTURE OF CATALYSTS

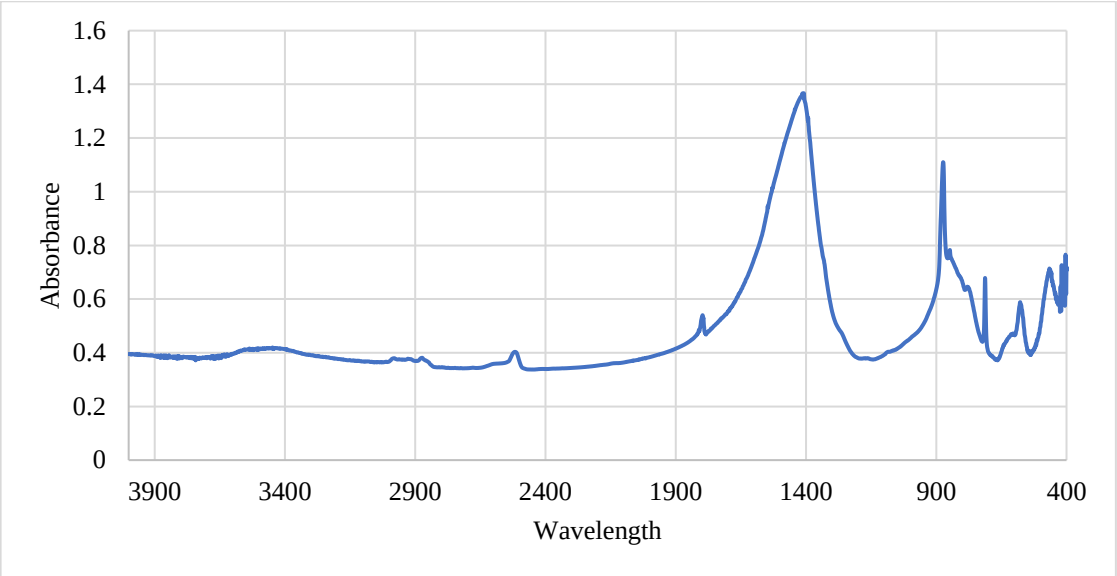

Figure B.1. FTIR spectrum of 60 wt. % CaO/Al_2O_3 catalyst after CO_2 adsorption

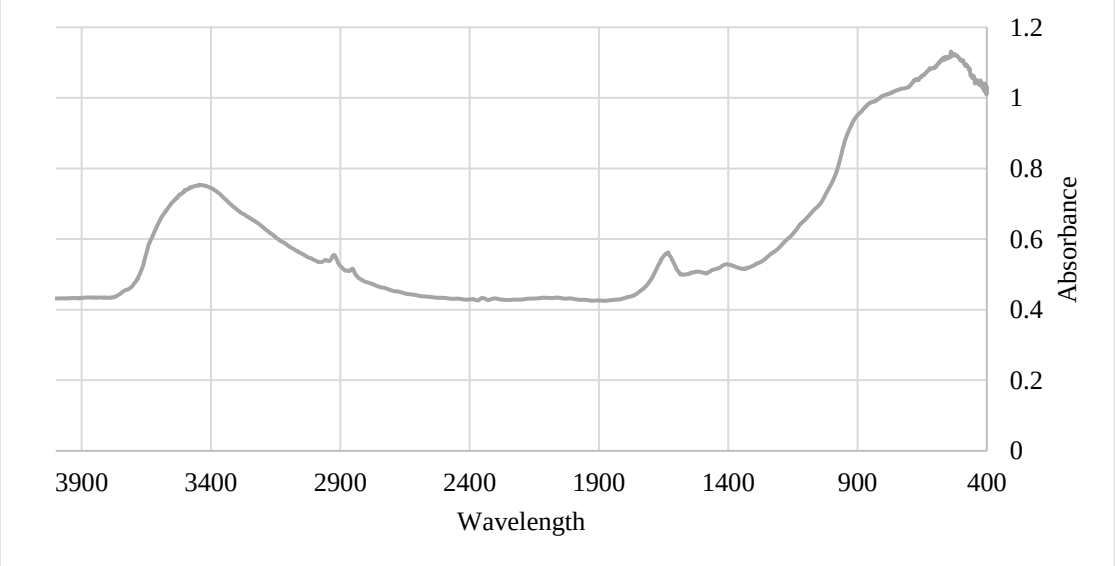

Figure B.2. FTIR spectrum of pure alumina after CO_2 adsorption

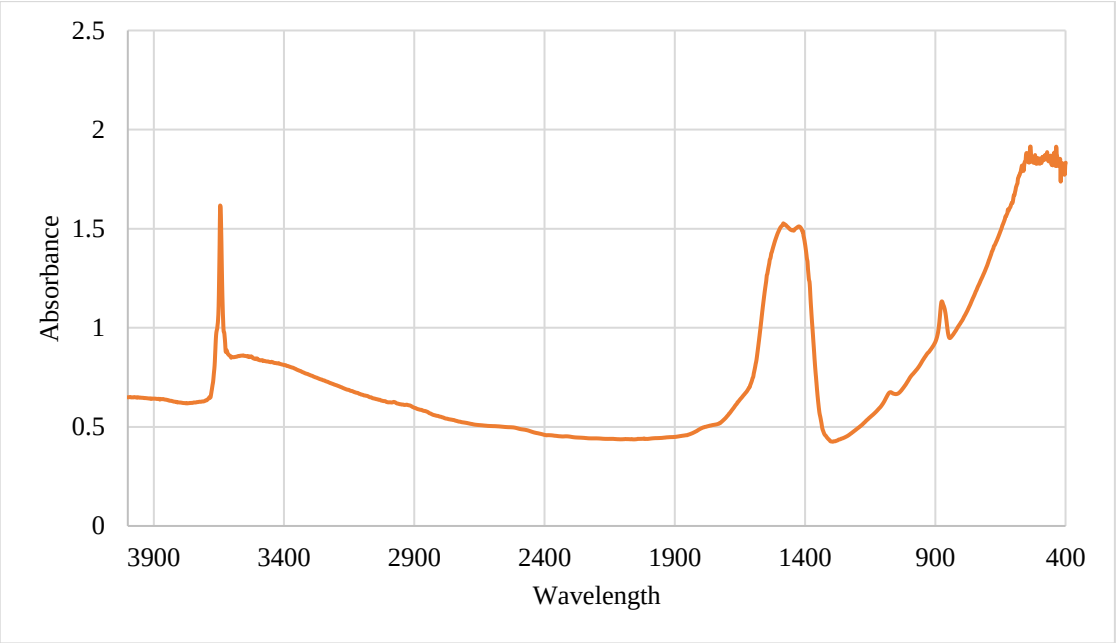

Figure B.3. FTIR spectrum of commercial CaO after CO_2 adsorption